TECHNISCHE UNIVERSITÄT MÜNCHEN

Lehrstuhl für Experimentelle Genetik

Multifunctionality in the enzyme family of 17beta-hydroxysteroid dehydrogenases

Ferdinand Haller

Vollständiger Abdruck der von der Fakultät Wissenschaftszentrum Weihenstephan für Ernährung, Landnutzung und Umwelt der Technischen Universität München zur Erlangung des akademischen Grades eines

Doktors der Naturwissenschaften

genehmigten Dissertation.

Vorsitzender	Univ.-Prof. Dr. M. Klingenspor
Prüfer der Dissertation	1. apl. Prof. Dr. J. Adamski
	2. Univ.-Prof. Dr. J.J. Hauner
	3. Univ.-Prof. Dr. J. Buchner

Die Dissertation wurde am 15.11.2010 bei der Technischen Universität München eingereicht und durch die Fakultät Wissenschaftszentrum Weihenstephan für Ernährung, Landnuttzung und Umwelt am 06.05.2011 angenommen.

Contents

Abstract

Protein multifunctionality is an important aspect of protein evolution that allows species to survive in a changing environment. A growing number of enzymes are described that accept more than a single substrate, sometimes even substrates from different classes of molecules. Within the group of 17beta-hydroxysteroid dehydrogenases several enzymes are known for their multifunctionality. This substrate promiscuity was investigated in three representatives of this enzyme family.

17beta-Hydroxysteroid dehydrogenase type 1 (17beta-HSD1) catalyzes the reduction of estrone to estradiol, the latter being important for sex-specific differentiation. The evolutionarily closely related photoreceptor-associated retinol dehydrogenase (prRDH) is part of the visual pigment recycling system within the eye. The role of an enzyme specific amino acid (methionine in prRDH and glycine in 17beta-HSD1) was investigated using mutagenesis, steady-state kinetics, and tissue expression analysis. It was shown that these enzyme specific amino acids are responsible for steroid / retinoid discrimination in human and zebrafish enzymes. Furthermore, an up to now not described multifunctionality towards retinoids was discovered in 17beta-HSD1. The implications of this discovery with respect to drug development were investigated with IC_{50} measurements using an 17beta-HSD1 specific inhibitor.

The actual substrate preference of the enzyme 17beta-HSD12 has been debated for some time. Initially discovered as ketoacyl reductase, later studies found that the enzyme also catalyzes the conversion of estrogens. 17beta-HSD12 proteins from several vertebrate and invertebrate species were investigated using yeast complementation assays and enzymatic activity assays. Together with results from a co-immunoprecipitation a role in fatty acid synthesis is suggested for this enzyme with the steroid converting ability being a stepping stone for the development of the endocrine system seen in today's vertebrates.

Surprisingly, a new multifunctionality was also found in rodent 17beta-HSD3. Although substrate promiscuity seems to be quite common in rodent 17beta-HSDs, it was not expected to find a catalytic activity towards retinoids. This multifunctionality was not detected in the human enzyme. Several mutagenesis experiments were conducted to find residues responsible for the observed substrate spectrum. Although the specificity could not be pinpointed to one residue, this discovery underlines the substantial differences in the endocrine system of rodents and humans.

In a more global approach to investigate hormone metabolism, an online-SPE coupled LC-MS/MS method for the analysis of steroids was developed, validated and adapted for high throughput routine use. Using this method two minor studies with murine and human samples were measured and evaluated. To gain possible insights into the interplay of different hormonal pathways it was attempted to adapt the method developed for

steroids to the analysis of thyroid hormones and retinoids.

This work contributes to a better understanding of the disease relevant enzyme family of 17beta-hydroxysteroid dehydrogenases and gives insights into the evolution of substrate specificities within this group. Furthermore, the development of a method for high-through-put steroid analysis is the starting point for a deeper exploration of steroid metabolism.

Zusammenfassung

Die Multifunktionalität von Proteinen ist ein wichtiger Aspekt der Proteinevolution, der es einer Spezies erlaubt in einer sich verändernden Umgebung zu überleben. In den letzten Jahren wurden immer mehr Enzyme entdeckt die mehr als ein Substrat akzeptieren. In manchen Fällen setzen diese Enzyme sogar Substrate aus verschiedenen Klassen von Molekülen um. Innerhalb der Gruppe der 17beta-Hydroxysteroiddehydrogenasen sind mehrere multifunktionelle Enzyme bekannt. In der vorliegenden Arbeit wurde die Proteinmultifunktionalität von drei Vertretern dieser Enzymfamilie untersucht.

17beta-Hydroxysteroiddehydrogenase Typ 1 (17beta- HSD1) katalysiert die Reduktion von Estron zu Estradiol, einem Steroid das in der geschlechtsspezifischen Differenzierung von Zellen eine wichtige Rolle spielt. Die evolutionär nahe verwandte Photorezeptorspezifische Retinoldehydrogenase (prRDH) ist Teil des Regenerationssystems der visuellen Pigmente im Auge. Die Rolle einer enzymspezifischen Aminosäure (ein Methionin in der prRDH und ein Glycin in der 17beta-HSD1) wurde mit Hilfe von Mutagenese, Michaelis-Menten Kinetiken und der Analyse der gewebsspezifischen Genexpression untersucht. Es konnte gezeigt werden, dass diese enzymspezifischen Aminosäuren für die Unterscheidung von Steroiden und Retinoiden in menschlichen und Zebrafischenzymen verantwortlich sind. Zusätzlich wurde eine bisher noch nicht beschriebene Multifunktionalität gegenüber Retinoiden in der 17beta-HSD1 entdeckt. Die Auswirkungen dieser Entdeckung auf die Entwicklung neuer Medikamente wurde über IC_{50} Messungen mit einem 17beta-HSD1 spezifischen Inhibitor untersucht.

Darüber welches das bevorzugte Substrat des Enzyms 17beta-HSD12 ist wird seit einiger Zeit diskutiert. Ursprünglich wurde es als Ketoacylreduktase beschrieben. Neuere Veröffentlichungen zeigten, dass das Enzym auch den Umsatz von Estrogenen katalysiert. Die 17beta-HSD12 Enzyme mehrerer Vertebraten und Invertebraten wurde unter Verwendung von Hefekomplementationsexperimenten und enzymatischen Aktivitätstests untersucht. In der Zusammenschau dieser Ergebnisse, mit denen einer Co-Immunopräzipitation wird eine Rolle dieses Enzyms in der Fettsäuresynthese vorgeschlagen. Die Fähigkeit zum Umsatz von Steroiden scheint dagegen ein Zwischenschritt in der Entwicklung des endokrinen Systems heutiger Vertebraten zu sein.

Überraschenderweise wurde eine neue katalytische Aktivität der Nagetier 17beta-HSD3 entdeckt. Obwohl die Akzeptanz verschiedener Substrate in den 17beta-HSDs von Nagetieren verbreitet ist war es ungewöhnlich eine Multifunktionalität gegenüber Retinoiden zu entdecken. Diese Multifunktionalität wurde dabei nicht vom menschlichen Enzym geteilt. Es wurden Mutageneseexperimente durchgeführt die das Ziel hatten die Aminosäurereste zu finden die für das beobachtete Substratspektrum verantwortlich sind. Die Substratspezifität konnte dabei nicht auf einen Aminosäuerest festgemacht werden. Trotzdem konnte diese Entdeckung weitere Erkenntnisse zu den beträchtlichen

Unterschieden im endokrinen System von Nagetieren und Menschen liefern.

Um eine etwas weiter gefasste Betrachtung des Hormonstoffwechsels zu erreichen, wurde eine online-SPE gekoppelte Hochdurchstz-LC-MS/MS Methode für die Steroidanalytik entwickelt, validiert und für die Routineanalytik angepasst. Mit dieser Methode wurden zwei kleinere Studien mit murinen und menschlichen Plasmaproben gemessen und ausgewertet. Um Einblicke in das Zusammenspiel verschiedener Hormonstoffwechselwege zu gewinnen, wurde versucht die für Steroide entwickelte Methode auf die Analyse von Thyroidhormonen und Retinoiden auszudehnen.

Diese Arbeit liefert einen Beitrag zum besseren Verständnis der in vielen Krankheiten relevanten Enzymfamilie der 17beta-Hydroxysteroiddehydrogenasen. Sie liefert Einblicke in die Evolution von Substratspezifitäten in dieser Gruppe. Zusätzlich könnte die hier beschriebene Entwicklung einer Hochdurchsatz Methode für die Steroidanalytik der Ausgangspunkt für eine tiefergehende Untersuchung des Steroidstoffwechsels sein.

Abbreviations

ADH	alcohol dehydrogenase
BLAST	basic local alignment search tool
bp	base pair
BSA	bovine serum albumine
cDNA	complementary DNA
cds	coding sequence
CoA	coenzyme A
CV	coefficient of variation
DMEM	Dulbecco's modified eagle medium
EDTA	ethylenediaminetetraacetic acid
ER	endoplasmic reticulum
FBS	fetal bovine serum
GC	gas chromatography
GC-MS	gas chromatography coupled to mass spectrometry
HPLC	high performance liquid chromatography
HSD	hydroxysteroid dehydrogenase
LC-MS/MS	liquid chromatography coupled to tandem mass spectrometry
LOD	limit of detection
LOQ	limit of quantitation
MRM	multiple reaction monitoring
m/z	mass to charge ratio
PCR	polymerase chain reaction
PDB	protein database
prRDH	photoreceptor associated retinol dehydrogenase
PTM	post translational modification
RAR	retinoic acid receptor
RDH	retinol dehydrogenase
rpm	revolutions per minute
RT-PCR	reverse transcriptase PCR
RXR	retinoid X receptor
SDR	short chain dehydrogenase/reductase
SPE	solid phase extraction
UV	ultra violet
VLCFA	very long chain fatty acids

1. Introduction

Even 150 years after its inception, Darwin's theory of evolution is one of the most successful scientific theories ever to be proposed (for a short introduction on the impact of Darwin's work see [1]). His findings did not only revolutionize science, but also greatly influenced Western culture as it introduced a more naturalistic view of the world. While earlier researchers based their analyses on the assumption that life and its development follow a predetermined plan, Darwin challenged this notion and replaced it with his concept of natural selection. Another concept inherent in Darwin's theory of evolution is the idea of common descent. Although this part of his theory seems to be easy to grasp by today's standards, at its time it was revolutionary.

Following major progresses in molecular biology and biochemistry, the principle of common ancestry has been extended to the molecular level. Instead of grouping species, in biochemistry proteins are clustered according to their sequence homologies. These relationships can be visualized in phylogenetic trees, which in turn enable us to identify homologs of protein sequences deposited in databases. A better understanding of evolutionary contexts may therefore allow us to better understand complex biochemical systems as for example molecular effects of hormones in organisms.

The endocrine system relies on the coaction of a variety of receptors and enzymes to mediate signals between different cells. While the receptors are relatively restricted in their specificity, the enzymes have recently been shown to accept a larger variety of substrates. This kind of "promiscuity" is suggested to be an evolutionary remnant and stems from earlier metabolic functions of these enzymes. The origins of these proteins may lie in more basal metabolic pathways like fatty acid or isoprenoid conversion.

Despite their new functionalities some of these enzymes may still retain their original role in the organism. Therefore, a deeper insight into evolutionary interrelations is important in the development of drugs. An inhibition of a multifunctional enzyme could have unpredictable effects on the entire organism, as not only the targeted metabolic pathway is affected but also other seemingly unrelated pathways are disturbed.

Even in our post-genomic age such an old theory as evolution still retains its importance. Moreover, in today's perspective we may still be puzzled that the relatively "primitive" means that were at Darwin's disposal sufficed to create such a long lasting theory. Modern methods have further enhanced our understanding of evolution and will do so even more in the future. This will in turn further our knowledge of biology itself, as Theodosius Dobzhansky's sentence still holds true: "Nothing in Biology Makes Sense Except in the Light of Evolution".

1.1. Protein promiscuity drives the evolution of enzymes

Many articles written for textbooks still describe concepts like the lock and key model, assuming that an enzyme is specific for only a single substrate. In recent decades this view has been proven to be insufficient to describe enzyme specificity. Indeed a plethora of enzymes has been shown to accept and convert several substrates, a fact for which the term 'enzyme promiscuity' (less often also called substrate ambiguity or moonlighting activity) has been coined [2]. But what are the origins of this observed promiscuity? According to Jensen [3] enzymes lacked in specificity in primitive cells. The biochemical pathways were flexible but higher complexity was prevented by the lack in specificity. During the development to higher life-forms the enzymes gained in specificity but still retained some degree of multifunctionality. This remaining promiscuity may be important during evolution to enable a protein to rapidly be adapted to changing environmental conditions [4, 5, 6]. A prominent example in this context is the rapid development of resistance to antibiotics in bacteria [7, 8]. On a molecular level this process corresponds to selection of enzymes that convert (and thereby detoxify) the antibiotic. A superfamily of enzymes, the short-chain dehydrogenases/reductases, are an example of promiscuous enzymes. Members of this group have not only been found in microorganisms but also in higher vertebrates like humans.

1.2. The role of short-chain dehydrogenases/reductases in metabolism

Members of the protein superfamily of short chain dehydrogenases/reductases (SDRs) constitute a group of oxidoreductases that have been identified in all three domains of life. Among the more than 21000 members identified so far more than 70 are found in humans [9]. While the sequence identity between SDRs is relatively low (15 -30 %), three-dimensional structures, especially of the N-terminal part, are strongly conserved. The N-terminus contains the Rossmann-fold, a structural element that forms the cofactor binding region of SDRs. Additionally, several sequence motifs are typical for these enzymes, such as the cofactor binding motif TGxxxGxG and the active center motif YxxxK.

SDR enzymes have been shown to catalyze oxidations and reductions of a wide variety of substrates including sugars, steroids, retinoids, fatty acids, and xenobiotics [10]. Several members of this protein superfamily are not restricted to one substrate but exhibit a considerable multifunctionality. Examples are SDR enzymes from the subgroup of sterol/retinoid metabolizing enzymes that convert a variety of retinoids as well as androgens. Another example are the multifunctional 17beta-HSDs, like for instance 17beta-HSD4 [11, 12, 13]. This enzyme does not only catalyze the conversion of estrogens but also those of acyl-CoA-conjugates and bile acids.

1.3. Characteristics of retinol dehydrogenases

Retinoids are derivatives of vitamin A and constitute an important class of signaling molecules (see Figure 1.1). Hormonal retinoids, especially all-trans and 9-cis retinoic acid act by binding to nuclear receptors like the retinoic acid receptors (RAR) and retinoid X receptors (RXR) [14, 15]. Receptor binding then activates downstream target gene transcription. Additionally, retinoids fulfill another important physiological function: they act as the light sensitive molecules in the visual process [16].

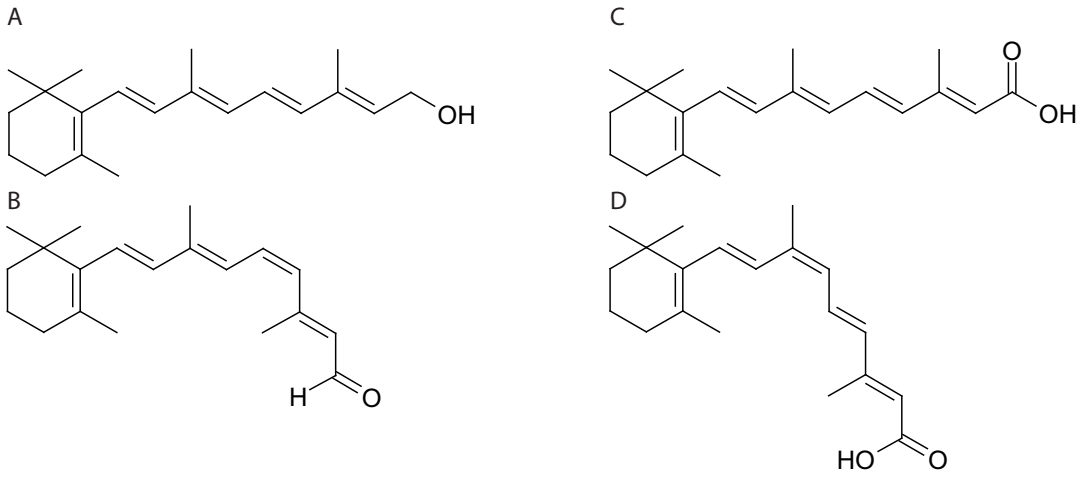

Figure 1.1.: Physiologically important retinoids.
(A) all-trans retinol (vitamin A1) is an essential fat-soluble vitamin that is involved in a variety of physiological processes including among other functions vision, reproduction, and development; (B) 11-cis retinal is an essential part of the light-sensitive molecule rhodopsin (it consists of the protein part opsin and 11-cis retinal that is bound to the protein as a Schiff base); (C) all-trans retinoic acid is of particular importance in developmental processes by binding to the retinoic acid receptor (RAR); (D) 9-cis retinoic acid binds to the retinoid X receptor which also play a role in development.

As some retinoids are cytotoxic, while others have a strong morphogenic potential, the concentrations of these molecules have to be tightly regulated. The retinol dehydrogenases (RDHs) fulfill this physiological task by catalyzing the inter-conversion of retin-alcohols, -aldehydes and -acids (for a review on RDHs see [17]).

The RDHs can be grouped into two different classes: the classical cytosolic alcohol dehydrogenases (ADHs) [18, 19] belonging to the medium chain dehydrogenases/reductases (MDRs) and SDR type RDHs. However, the physiological importance of the retinoid converting abilities observed in ADHs is still disputed. In contrast, SDR type RDHs have been shown to fulfill important roles in retinoid metabolism.

Of the various RDHs the photoreceptor-associated retinol dehydrogenase (prRDH) has a special physiological role as it is involved in the regeneration of visual pigments after photoactivation of rhodopsin [20]. This enzyme catalyzes the first step of the visual cycle: all-trans retinal that is released from rhodopsin is reduced to all-trans retinol. In subsequent steps all-trans retinol is esterified, transported to the retinal

pigment epithelium and isomerized to 11-cis retinol. After an oxidation step, an 11-cis retinal molecule is bound to opsin to regenerate rhodopsin. The rate-limiting step of this process, namely the reduction of the active aldehyde all-trans retinal, is catalyzed by prRDH [21]. Interestingly, these *in vitro* results did not exactly match analyses of prRDH knock-out mice. Despite their lack of the enzyme these mice were still able to see. Even multiple knock-outs of retinol dehydrogenases (double knock-outs of prRDH and RDH12 as well as triple knock-outs of prRDH, RDH12, and RDH5) did not impair vision in the mice. Nevertheless, the importance of prRDH is highlighted by the fact that prRDH knock-out mice were susceptible to retinal degeneration as the knock-out caused accumulation of cytotoxic all-trans retinal and its derivatives [22, 23, 24].

Close relationships between several RDHs and 17beta-HSDs have been observed [25, 26]. Not only amino acid sequences or protein folds are conserved but also substrate specificities are often similar. These overlapping substrate specificities may complicate the proper naming of the enzymes as their catalytic capabilities do not necessarily reflect their *in vivo* functions [27].

1.4. 17beta-Hydroxysteroid dehydrogenases and their role in steroid metabolism and other pathways

Initially 17beta-hydroxysteroid dehydrogenases have been annotated due to their functionality. Members of this group catalyze oxido-reductive reactions at position 17 of the steroid backbone, producing keto- or hydroxysteroids [28, 29]. The identity of the functional group in this position governs the steroid's binding efficiency to their receptors. While steroids bearing a hydroxy group in position 17 have a high affinity to their receptors, the affinity of 17-ketosteroids is rather low [30]. Up to now, 14 different types of 17beta-HSDs have been identified, either due to functional analyses or due to sequence similarities. Despite their annotation as 17beta-HSDs some of these enzymes may have substrate specificities apart from steroids, some of which may even constitute the main functionality of the given enzyme *in vivo*. For example 17beta-HSD7 has initially been described as an enzyme involved in estrogen metabolism. In depth functional analyses revealed that this enzyme was part of the cholesterol biosynthetic process [31]. Recently discovered 17beta-HSDs, like 17beta-HSD13 got their name solely on the basis of sequence similarity before functional tests were conducted.

This approach may be problematic as 17beta-HSDs do not form a gene family but rather emerged by convergent evolution without having a common ancestor. This diversity also explains the substantial differences between expression patterns, subcellular localization patterns, and substrate specificities that have been found for 17beta-HSDs. As most members of the 17beta-HSD group are SDR enzymes (with the exception of 17beta-HSD5 which is an aldo-keto reductase), they accept a broad spectrum of substrates. Apart from steroids several 17beta-HSDs have been shown to catalyze reaction of substrates as diverse as acyl-CoAs (17betaHSDs type 4, 8, 10 and 12), or bile acids (17betaHSDs type 4 and 10), or retinoids (17betaHSDs type 6 and 9) [27].

17beta-HSD type	synonyms	substrate	additional substrates
17beta-HSD1	EDHB17	estrogens	all-trans retinoids, androgens
17beta-HSD2	E2DH	androgens, estrogens	-
17beta-HSD3		androgens	-
17beta-HSD4	MFP2	β-oxidation of VLCFA, bile acids	estrogens
17beta-HSD5	AKR1C3	androgens	prostaglandins
17beta-HSD6	HSE	androgens, retinoids	-
17beta-HSD7		cholesterol synthesis intermediates	estrogens
17beta-HSD8	HsKAR, Ke6	β-ketoacyl thioester	estrogens, androgens
17beta-HSD9		retinoids	estrogens, androgens
17beta-HSD10	HADH2, SCHAD, ABAD, ERAB, MHBD	3-ketoacyl-CoA SCFA	androgens, bile acids
17beta-HSD11	DHRS8, retSDR2	androgens, estrogens	-
17beta-HSD12	KAR	3-ketoacyl-CoA LCFA	estrogens
17beta-HSD13	SCDR9	unknown	unknown
17beta-HSD14	DHRS10, retSDR3	androgens, estrogens	-

Table 1.1.: Overview of 17beta-HSDs and their respective substrates.
The substrates listed are probably incomplete. Furthermore, knowledge of substrate specificities does not need to infer *in vivo* functions. Retinoids as substrate for 17beta-HSD1 were discovered in the course of this work (see Chapter 3.1).

In vivo many 17beta-HSDs seem to prefer one direction of reaction, either oxidation or reduction (some 17beta-HSDs could also be bi-directional) [32, 33]. Hence, there are obviously two different types of 17beta-HSDs: those that activate, and those that inactivate steroids. To catalyze these reactions, the enzymes need different cofactors. While, for example 17beta-HSD1 prefers NADP(H) as cofactor, 17beta-HSD2 shows higher activity when a NAD(H) cofactor is used.

1.5. 17beta-HSD1 and its role in estrogen metabolism

Human 17beta-HSD type 1 was the first member of the 17beta-HSD family to be identified. The enzyme's ability to catalyze the reduction of estrone to estradiol by using the the cofactor NADPH has been known for many years (see Figure 1.2). While this constitutes the main action of this enzyme in humans, the rodent homologs (of *Rattus norvegicus* and *Mus musculus*) also catalyze the reduction of androstenedione to testosterone [34] (the human enzyme additionally catalyzes this reaction but the activity is negligibly small). The amino acids responsible for the discrimination between the androgen and estrogen substrates have been identified in a study with rat / human chimeric enzymes [34]. A homolog of 17beta-HSD1 has also been characterized in the zebrafish *Danio rerio*. Concomitantly, two homologous photoreceptor-associated retinol dehydrogenases were identified, due to their high sequence homology with 17beta-HSD1 [35].

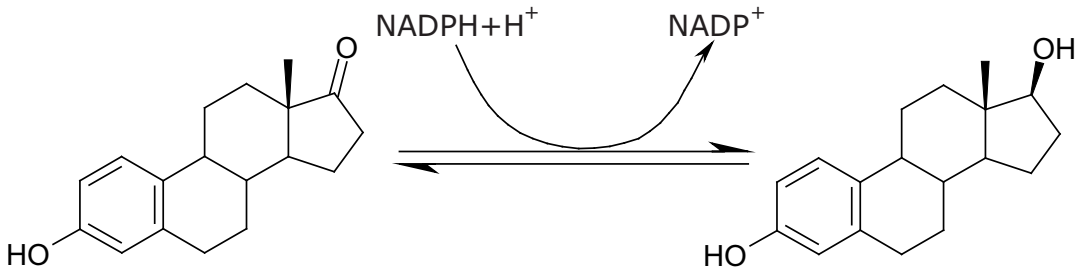

Figure 1.2.: Reduction of estrone to estradiol catalyzed by 17beta-HSD1.
The keto group at position 17 of the steroid backbone is converted to a hydroxy group while consuming the cofactor NADPH.

The 17beta-HSD1 enzyme has been shown to be mainly expressed in reproductive tissues like placenta and ovary [36, 37, 38]. Additionally, low expression levels have been found in breast tissue, uterus, testis, brain, and adipose tissue [39, 40]. As estrogen metabolism has been observed in nearly all these tissues, and given the high estrone reducing potential of this enzyme, it is safe to assume that 17beta-HSD1 is the most important enzyme to provide an organism with active estrogens, i.e. estradiol.

Intracellular concentrations of estrogens have a major impact on regulatory processes within the cell. Estradiol, the most potent estrogen, has pro-proliferative effects in

different tissues and therefore was associated with the tumorigenesis of estrogen-related cancers [41]. For instance, an increase of estradiol concentrations in breast cancer cells has been shown in postmenopausal patients. These results together with the observation that 17beta-HSD1 mRNA levels are elevated in breast carcinomas, suggest an important role for this enzyme in the progression of breast cancer. Furthermore, patients with tumors that express high levels of 17beta-HSD1 have a significantly shortened disease-free and overall survival [42].

The three-dimensional structure of 17beta-HSD1 is one of the few structures solved in the superfamily of SDR enzymes [43, 44]. Studies on this structure provided insights into the mode of substrate binding in this enzyme. Furthermore, it allowed for the proposal of a reaction mechanism, which in turn may be important in the design of potential inhibitors. Indeed a wide variety of compounds have been shown to selectively inhibit 17beta-HSD1 [45, 46, 47, 48]. The inhibition of 17beta-HSD1 may proof useful in the treatment of estrogen related cancers.

1.6. 17beta-HSD3 and its role in androgen metabolism

17beta-HSD3 is an enzyme that is mainly expressed in the Leydig cells of the testicular tissue. In accordance with this localized expression it is thought to be the most important enzyme to generate active androgens by reducing Δ4-androstenedione to testosterone (see Figure 1.3) [49]. Although the aldo-keto-reductase 17beta-HSD5 has also been shown to catalyze this reaction, 17beta-HSD3 seems to play the key role in androgen metabolism. Its significance is further corroborated by the effects that are observed when the enzyme is mutated. A lack of 17beta-HSD3 activity (e.g. caused by mutations in this enzyme) in humans leads to a disease called pseudohermaphroditism [49]. Males affected by this disorder retain a male genetic composition while showing female external genitalia. Furthermore, it has been shown that this enzyme is overexpressed in prostate cancer tissue making it a potential drug target [50].

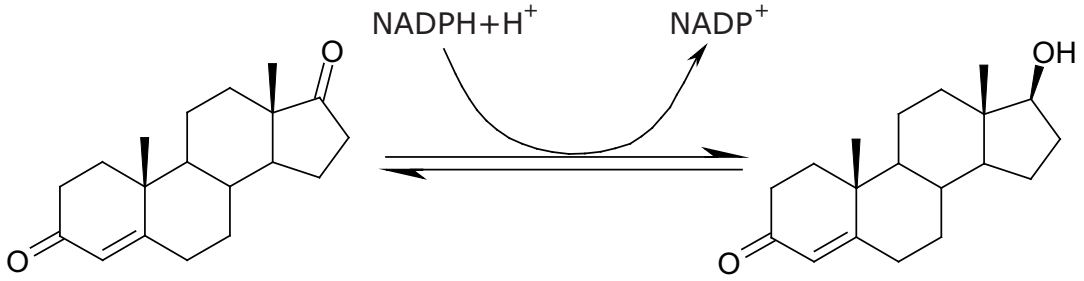

Figure 1.3.: Reduction of Δ4-androstenedione to testosterone catalyzed by 17beta-HSD3.
The keto group at position 17 of the steroid backbone is converted to a hydroxy group while consuming the cofactor NADPH.

17beta-HSD3 enzymes have been investigated in several different organisms including humans, mice, rats and zebrafish [49, 51, 52]. The enzymes from these species not only show a high degree of sequence conservation among each other but also to the group of 17beta-HSDs type 12. This close evolutionary relationship is reflected in their common subcellular localization in the endoplasmic reticulum [51]. Another possible remnant derived from the common ancestry with 17beta-HSD12 is the acceptance of estrone as substrate (although with low reaction rates) that was described by Geissler et al. [49]. Later publications have shown that 17beta-HSD3 catalyzes the conversion of a variety of other androgens, establishing substrate promiscuity for this enzyme [51].

Despite the aforementioned similarities several differences between steroid metabolism in different model organisms seem to exist. This becomes evident when tissue distributions of 17beta-HSD3 enzymes are compared. In mice expression is relatively widespread: apart from testis, 17beta-HSD3 can be found in kidney, liver, brain, muscle, heart, spleen, uterus, and ovary [53]. In rats a more restricted expression can be observed as the enzyme can only be detected in testis, ovary, and bone marrow. Expression in testis, brain, bone marrow, and fat tissue was reported for the human enzyme [54]. Interestingly, 17beta-HSD3 is also expressed in platelets, where it has been shown to be down-regulated in essential thrombocythemia [55]. The molecular basis for the disease and the reasons why steroidogenic enzymes are expressed in platelets is still unknown, making 17beta-HSD3 an enzyme that is still worthwhile to be studied.

1.7. 17beta-HSD12 and its dual role in fatty acid and steroid metabolism

Initially 17beta-HSD12 was described as keto-acyl reductase, catalyzing the conversion of 3-keto-acyl-CoAs to 3-hydroxy-acyl-CoAs [56]. The enzyme seems to be part of the microsomal very long chain fatty acid (VLCFA) elongation process, which is composed of four distinct enzymatic reactions (see also Figure 1.4): 1) the condensation of malonyl-CoA to CoA-conjugated fatty acid substrates, 2) the reduction of 3-ketoacyl-CoA intermediates (the reaction catalyzed by 17beta-HSD12), 3) the dehydration of 3-hydroxyacl-CoA, and 4) the reduction of enoyl-CoA to a saturated fatty acid (for a detailed review of the elongation process see [57]). This elongation process has been studied in detail in yeast, in which a homolog of 17beta-HSD12, the YBR159 protein (YBR159p), has already been identified [58]. Although being a non-essential protein, YBR159p is an important component of the elongase complex, as ΔYBR159 mutants produce less very long chain fatty acids. This lack in VLCFAs in turn leads to a slow growth phenotype of YBR159 knock-out mutants, which is further aggravated at elevated temperatures. Indeed human 17beta-HSD12 was investigated due to its homology to YBR159p. Furthermore, several facts like its ER localization and its ubiquitous expression corroborated the enzyme's role in VLCFA elongation [56].

In accordance with its annotation as 17beta-HSD (which was solely based upon sequence similarity) other research groups investigated this enzyme's role in steroid

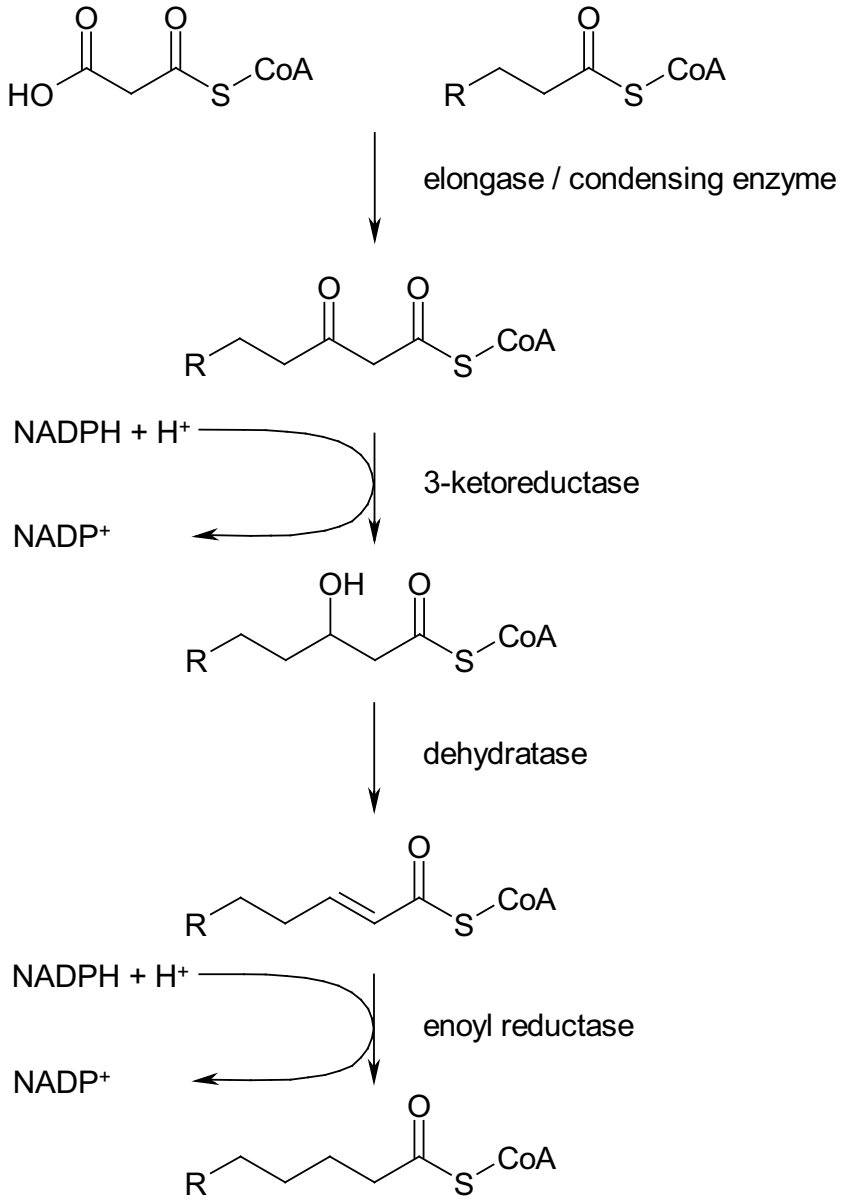

Figure 1.4.: Mechanism of very long chain fatty acid elongation in the endoplasmic reticulum.
Elongases (e.g. Elo2p and Elo3p in yeast or Ssc1, Cig30, ELOVL3, LCE, and TER in humans) catalyze the condensation of CoA-activated long chain fatty acids with malonyl-CoA. After reduction by a 3-ketoacyl reductase (YBR159p in yeast or presumably 17beta-HSD12 in humans) the product is further processed in a dehydration reaction (catalyzed by a dehydratase that is neither known in yeast nor in humans). In the final step another reduction that is catalyzed by an enoyl reductase (Tsc13p in yeast or TER in humans) completes the cycle. Very long chain fatty acids are generated from long chain fatty acids by several passages through this elongation cycle.

metabolism. Recent results showed that this enzyme accepts estrone as substrate, which led the authors of the report to assume that 17beta-HSD12 has a prominent role in estrogen metabolism [59]. This assumption was in part based on the close homology of 17beta-HSD12 to the androgen specific enzyme 17beta-HSD3 which has been discovered in an earlier study [35]. In subsequent reports homologs of 17beta-HSD12 were characterized in monkeys [60], mice [61] and *C.elegans* [62], all showing conversion of steroid substrates. Furthermore, an upregulation of 17beta-HSD12 was detected in breast cancer [63]. Yet, there is still no conclusive evidence that this enzyme has a steroidogenic role *in vivo*.

In contrast, a more recent study showed that there is no correlation between expression of 17beta-HSD12 and breast cancer [64]. Another report, describing that 17beta-HSD12 has no effect on estrogens in several cell lines, casts further doubt on the importance of this enzyme in steroid metabolism [65]. Entchev et al. suggested that the C.elegans homolog of 17beta-HSD12, LET-767, does not participate in steroid/sterol metabolism [66] but takes part in fatty acid metabolism. Although these more recent reports indicate that 17beta-HSD12 is a ketoacyl-reductase, conclusive proof in terms of activity measurements with acyl-CoAs is still missing.

1.8. Mass spectrometry based metabolomics

1.8.1. What is metabolomics?

Generally metabolomics is defined as the quantitative measurement of the entirety of low molecular weight molecules (below 3000 m/z) present in cells, tissues or body fluids in a particular physiological or developmental state of an organism. As metabolomics data provide information about the endpoint of physiological alterations (e.g. gene knockouts or drug treatments) it is considered to be the 'omics' technology that is closest to the phenotype (see Figure 1.5).

Within all 'omics' technologies metabolomics represents a unique challenge. Unlike in genomics or transcriptomics there is no sequence information to work with (in proteomics amino acid sequences are known but the situation is more complicated due to the introduction of post-translational modifications). Furthermore, while in genomics and transcriptomics the analyzed nucleic acids can be amplified, in metabolomics (and in proteomics) there are no comparable methods. This restriction makes sensitivity a major issue in metabolome analyses [67]. Further challenges are the tremendous diversity in chemical and physical properties of the analytes and the broad concentration range in which they are present within an organism [68]. On the one hand there are compounds like glucose that is hydrophilic and quite abundant in the body and on the other hand there are hydrophobic intermediates of fatty acid synthesis that are only present in low concentrations.

A further challenge in generating metabolomics data is the sampling step as there are spatial (e.g. tissue vs. blood) and temporal (e.g. circadian and seasonal rhythms) fluctuations of metabolite concentrations. In this respect it is also important to consider

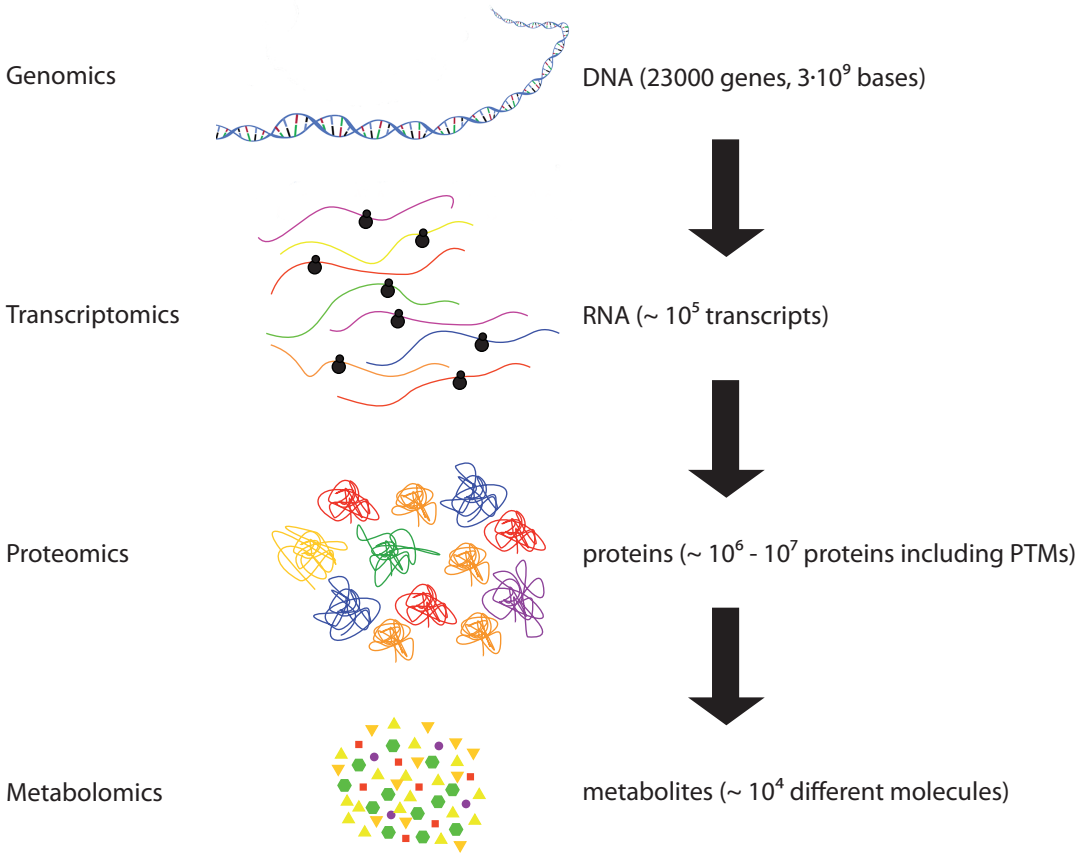

Figure 1.5.: Overview of different 'omics' technologies and their respective target molecules.
All numbers given in this figure represent estimates for human organisms. Each 'omics' technology represents a unique challenge. Although a metabolomics approach has the advantage of a low number of different molecules (roughly 10^4), this molecules have very different properties and no sequence information is available to put them in a physiological context.

the stability of metabolites as some of them may be very labile.

The aforementioned set of challenges and problems explains why there is no single method to quantitatively measure 1000s of metabolites [67]. To cope with this complexity two different metabolomics approaches are used: metabolic fingerprinting and metabolic profiling. In metabolomic fingerprinting the focus is not on identifying each detected metabolite but to detect differences between different physiological states (e.g. healthy vs. disease) by comparing metabolite patterns (fingerprints). In metabolic profiling approaches (also known as targeted metabolomics) the focus is on one or sometimes several groups of known metabolites for which concentrations are determined. As metabolic profiling is not a global approach it is often not considered to be a true 'omics' approach, but as this kind of analyses have been applied for decades, their scientific merit is without question. An example of early metabolic profiling dates back to the 1960s when Horning and Sjövall already used GC to measure bile acids, sterols and steroids in urine and serum [69, 70].

1.8.2. The steroid metabolome

As morphogenic signaling molecules steroids play an important role in a plethora of physiological processes. Therefore, analyses of steroid concentrations allow for the diagnosis of endocrine diseases and hormonal imbalances. Nowadays, the determination of steroid patterns enables physicians to diagnose diseases like hyperaldosteronism, adrenal insufficiency, congenital adrenal hyperplasia, Cushing's syndrome, and disorders of gonadal function. Recently the term 'sterome' was introduced for these analyses [71].

But steroid profiling is not only applicable to human related issues. Due to high concentrations of anthropogenic steroids and endocrine disrupting chemicals in rivers and lakes, animal metabolomes become interesting in ecotoxological investigations [72, 73]. Steroid analyses may help to better understand how these contaminants may affect reproductive development in fish.

Furthermore, systematic generation of mouse mutants has led to a need for comprehensive phenotyping. As these mouse models may bear defects that affect steroid synthesis or homeostasis, knowledge of the mouse steroid metabolome could help to identify these mutants and connect phenotypes to their molecular cause. Up to 1984 no information concerning mouse steroid profiles had been published, but in this year the first report appeared regarding the GC/MS urine metabolic profile of the mouse [74]. A closer look at the steroid profile in mouse shows several differences to humans. For example, corticosterone (and not cortisol like in humans) is the active corticosteroid in mice. Hence, 11-dehydrocorticosterone is the functional analog of cortisone in mice. Despite these differences detailed analyses of steroid profiles in mutant mice may lead to a better understanding of endocrine disorders in humans.

1.8.2.1. Liquid chromatography coupled to tandem mass spectrometry and its use in steroid metabolomics

In routine steroid analyses, particularly in clinics, immunoassays have been the standard technique for years. These assays combine simplicity and sensitivity while delivering results relatively fast. However, this method also has several disadvantages especially concerning assay specificity. So it is known that antibodies may cross-react with structurally similar compounds within the matrix. Furthermore, every analyte that needs to be measured requires a different antibody and in consequence another assay has to be performed. Gas chromatography coupled to mass spectrometry (GC-MS) has been the only alternative to immunoassays for a long time. Although having superior assay specificity compared to immunoassays the time consuming sample preparation has precluded a use in routine analytics.

Advancements in the coupling of liquid chromatography to mass spectrometry (tandem mass spectrometry in particular) have led to its increased use in the analysis of human serum metabolites. LC-MS/MS combines high sensitivity and analytical specificity without having the disadvantages of GC-MS. Measurements can be performed in a fast and robust way while multiple reaction monitoring (MRM) multiplexing allows for the simultaneous analysis of a large set of molecules. Further automation is possible by using online solid phase extraction (SPE) that dramatically shortens the hands-on time for sample preparation.

1.8.2.2. Future developments

Metabolomics promises to become a valuable diagnostic and prognostic tool for a large variety of metabolic diseases and disorders. Biomarkers discovered by metabolomic studies are much closer to the phenotype than other 'omics' biomarkers. Furthermore, the ever growing understanding of metabolic pathways may help us to find cross-roads between these pathways to place the biomarker in a complex metabolic network. Hence, these metabolite markers may not only provide a diagnostic tool but open new avenues of research for drug discovery and therapeutic intervention.

In the last decades we have seen a steady progress of mass spectrometry concerning sensitivity as well as mass accuracy. Additionally, inventions of new ionization techniques opened up new possibilities to apply mass spectrometry to biological samples. Therefore, developments in mass spectrometry systems will not only allow us to analyze molecules for which today's instrumentation is not sensitive enough but the application of new ionization principles may enable us to do analyses we have not thought about yet. But mass spectrometry is not the only part of the metabolomics methods that will see improvements. Developments in chromatography will enable us the separation of ever more complex sample matrices. For example the increased use of multidimensional separations (e.g. combining reversed-phase with ion exchange chromatography) will be useful in the analysis of very complex samples. Furthermore, the use of columns with increased surface areas (either very small particle sizes like in UHPLC or using monolithic columns) will provide better separations while decreasing the analysis time.

Another area in which metabolomic analyses may become important is evolutionary studies. Today, sequence alignments and phylogenetic trees are the main tools of researchers in this field. But profiles of secondary metabolites (especially in plants) have been shown to be unique to different species. Metabolite profiles are, at least up to now, much more easily accessible than entire genomes. Furthermore, these profiles contain functional information about interactions between the investigated organism and its environment. Therefore, metabolomics has the potential to become a tool to identify and classify organisms and thereby further our understanding of evolution.

1.9. Aims of this study

Protein promiscuity represents a major driving force in the evolution of new protein functions. From today's perspective this promiscuity is also a promising avenue for the development of new drugs. This work aimed at the characterization of promiscuity in proteins involved in steroid metabolism.

A potential multifunctionality of the well characterized enzyme 17beta-hydroxysteroid dehydrogenase type 1 was intended to be investigated. Furthermore, the role of conserved amino acids was to be determined. Steady-state kinetics as well as IC_{50} values of wild type and mutant enzymes should be measured and the results were to be put into perspective by *in silico* molecular docking and analysis of expression patterns.

Metabolic characterization of 17beta-HSD12 was aimed to clarify if this enzyme has a role in fatty acid or steroid metabolism. Phylogenetic analyses of vertebrate and invertebrate homologs established several candidate genes of organisms from different evolutionary backgrounds. These candidates needed to be characterized using yeast complementation assays, co-immunoprecipitation, and enzymatic assays.

A newly discovered promiscuity of rodent 17beta-HSD3 was the starting point for an in-depth analysis of this enzyme's substrate spectrum. Enzymatic assays of different mutants were intended to clarify the role of this up to now uncharacterized multifunctionality in rodents and to get new insights into steroid/retinoid metabolism in these important model organisms.

While the aforementioned projects focused on single enzymes, a different avenue was taken as steroid metabolism was to be characterized using a global approach. A method for the high-through-put mass spectrometric analysis of steroids had to be developed to gain insights into steroid metabolism from a systemic perspective.

2. Methods, Material and Equipment

2.1. Methods

2.1.1. Methods using DNA

2.1.1.1. Isolation of plasmids from bacteria

For plasmid preparations in small scale (mini-prep) 4 mL of an overnight culture was used. The isolation was performed with the NucleoSpin Plasmid Kit (Machery-Nagel) according to the manufacturer's protocol. To isolate larger quantities of plasmids (midi-prep) 50 mL of an overnight culture was utilized. In this case the Nucleobond AX Kit (Machery-Nagel) was employed. Plasmid elution was generally achieved by addition of Ampuwa water in order to prevent negative influences on subsequent enzymatic reactions (e.g. restriction digestions). Mini-preps were eluted in 30 μL and midi-preps in 120 μL.

2.1.1.2. Determination of DNA concentration

Concentration as well as quality of DNA was monitored by UV-spectrometry. At $\lambda = 260\,nm$ DNA quantity and at $\lambda = 280\,nm$ the quality of DNA preparations was determined. The concentration of DNA was calculated according to the following formula:

$$\mathrm{c(ng/\mu L)} = OD_{260nm} \cdot \ 50\ \mathrm{ng/\mu L}$$

2.1.1.3. Separation of DNA by agarose gel electrophoresis

For gel electrophoresis of large DNA fragments ($>$ 2000 kb) 1 % (w/v) agarose was dissolved in 1x TBE by heating the solution in a microwave oven. For smaller DNA fragments 2 % (w/v) gels were used. To visualize the DNA, gels were supplemented with ethidium bromide (0.5 μg/mL) which allows for detection of nucleic acids at $\lambda = 254\,nm$. The DNA solution was mixed with 6x loading dye before application to the gel and the DNA fragments were subsequently separated in a constant electric field. To determine the size of DNA fragments markers III and VIII (MBI Fermentas) were used.

2.1.2. Polymerase-chain-reaction (PCR) based methods

In the course of this work PCRs were used for several purposes: to amplify inserts for cloning, for site directed mutagenesis, to obtain genes by RT-PCR and to screen colonies

for inserts. For these diverse applications different polymerases were used. To amplify templates for cloning a high fidelity Pfu-Polymerase was used, whereas screenings were conducted with Taq-Polymerase. The composition of these reactions is depicted in Table 2.1.

For the amplification of inserts for cloning the following program was used: 1 cycle 5' at 95 °C; 35 cycles 45" at 95 °C, 45" at 55 °C and 1'30" at 72 °C finishing with 1 cycle 10' at 72 °C. To screen for colonies this program was changed to: 1 cycle 10' at 95 °C; 35 cycles 35" at 95 °C, 35" at 55 °C and 1'15" at 72 °C. All reactions were carried out in a RoboCycler (Stratagene). The corresponding primers are listed in appendix B.

PCR-Products that were subsequently used for cloning, were purified with the Wizard SV Gel and PCR Cleanup Kit (Promega), according to the manufacturer's protocol.

	Pfu-Polymerase	Taq-Polymerase
Water	33 μL	12.3 μL
10x Buffer (see 2.2.1.10)	5 μL	2 μL
dNTPs (2 mM)	5 μL	2 μL
Primer 1 (10 μM)	2.5 μL	1 μL
Primer 2 (10 μM)	2.5 μL	1 μL
Template	1 μL	1 μL
Polymerase	1 μL (2.5 U)	0.3 μL
Total volume	50 μL	20 μL

Table 2.1.: Composition of PCRs

2.1.2.1. RT-PCR

To clone genes for which no cDNA clones were commercially available as templates, it was necessary to perform a RT-PCR (reverse transcriptase polymerase chain reaction). Isolated RNA was reverse transcribed into cDNA using the RevertAid First Strand cDNA Synthesis Kit (MBI Fermentas). Resulting cDNA was used as template for a subsequent PCR reaction.

2.1.2.2. Quantitative RT-PCR for Expression Analysis

Sequence specific primers for quantitative RT-PCR were designed using Primer3 (see http://frodo.wi.mit.edu). Primers were designed to generate PCR products that span an exon-exon border to exclude any influence of genomic DNA on the results. Primers were tested for specificity in preliminary experiments using a dilution series of cDNA isolated from cells in which the gene of interest was expressed.

To evaluate the expression of genes in different tissues a cDNA-panel of 48 human tissues (TissueScan Human Major Tissue qPCR Array HMRT102, Origene, USA) was used. The manufacturer normalized all tissue samples to equal levels of GAPDH and

verified the absence of genomic DNA. PCR was performed in a real-time 7900HT qPCR-system (Applied Biosystems) using Power SybrGreen Master Mix with ROX as reference (Applied Biosystems). Results were recorded and analyzed using the SDS 2.2 software (Applied Biosystems). Results were evaluated using the $\Delta\Delta$Ct method, normalized to the GAPDH housekeeping gene and the lowest expression. Specific amplification of PCR products was proven by complete sequencing (data not shown).

2.1.2.3. PCR based mutagenesis

Two different methods were used to generate site-directed mutations. For the first method two complementary primers were designed that harbored the desired mutation in their middle. The mutation site was flanked by 15 nucleotides upstream and downstream of this core. PCR reactions were performed generating two products that overlap in this region. Corresponding fragments were joined by fusion PCR using a second set of primers to get the full-length mutated product.

In another approach similar primers were designed but the entire plasmid was amplified during the PCR. Template strands were then digested with DpnI to remove all plasmids devoid of the mutation.

2.1.2.4. Colony screen

The colonies designated for screening were inoculated in 150 μL LB-Medium and incubated at 37 °C for 2 h. From this culture 1 μL was employed in a screening-PCR with Taq-Polymerase (composition see Table 2.1). Screening with primers binding in the vector identified potential positive clones. A rescreen using one primer binding in the vector in combination with a primer binding in the insert was used to verify successful cloning. Candidates that were positive in both screens were sequenced to check for errors in the insert sequence.

2.1.2.5. Sequencing

To verify the fidelity of cloned inserts the corresponding plasmids were sequenced. To this end the Sanger dideoxy method was used. A typical sequencing reaction was set up as seen in Table 2.2.

The corresponding PCR program was: 1 cycle 1' at 95°C and 35 cycles 35" at 95°C, 45" at 53°C, 4' at 60°C. Clean-up of the sequencing reaction was performed with the Montage SEQ_{96} Sequencing Reaction Cleanup Kit (Millipore) according to the manufacturer's protocol. The detection of the different fragments generated by the dideoxy method was done by an ABI 3730 Sequencer (Applied Biosystems).

	Sequencing reaction setup
Primer (10 μM)	1 μL
Template (150 - 300 ng/ μL)	1 - 2 μL
Water	0 - 1 μL
5x Buffer (Qiagen)	1 μL
BigDye 3.1 (Qiagen)	1 μL
Total volume	5 μL

Table 2.2.: Composition of sequencing reaction

2.1.3. Molecular Cloning

2.1.3.1. Restriction digestion

For restriction digestions 1 μg of DNA (either PCR-product of desired insert or target vector) was mixed with 1 μL of the appropriate enzyme(s) (20 U/μL) in the matching buffer (according to manufacturer's protocol). The digest was adjusted to a total volume of 20 μL with water and incubated at 37 °C for 2 h to 16 h. The digest was stopped either by heat inactivation or by purification with the Wizard SV Gel and PCR Cleanup Kit (Promega).

2.1.3.2. Ligation

For ligation reactions 150 ng of digested vector was mixed with a 5-10 times molar excess of digested insert (or PCR product in the case of blunt cloning). This mixture was heated to 80 °C for 10 minutes and then chilled on ice for another 5 minutes. T4-DNA-Ligase (MBI Fermentas) and ligase-buffer were added and the total volume was adjusted to 20 μL with water. The reaction was incubated for 3 h up to 16 h at room temperature.

2.1.3.3. Gateway cloning

For the generation of several constructs the Gateway cloning system (Invitrogen) was used. Primers containing attB recombination sites at their 5' ends were designed and used for PCR amplification (see chapter 2.1.2). To generate the entry construct the PCR product was recombined into pDONR201 using the Gateway BP Clonase Enzyme Mix (Invitrogen) according to the manufacturer's protocols. The entry clone was sequenced and subsequently subjected to a second recombination reaction with the Gateway LR Clonase Enzyme Mix (Invitrogen). The resulting destination clone was then used for downstream experiments.

2.1.4. Working with *E.coli*

2.1.4.1. Cultivation of *E.coli*

Liquid cultures of recombinant *E.coli* were cultivated in LB-medium containing either 50 μg/mL ampicillin or 50 μg/mL kanamycin. During incubation the bacteria were agitated (200 rpm) at a temperature of 37 °C. For cultivation on plates, the agar was also supplemented with 50 μg/mL ampicillin (or 50 μg/mL kanamycin). For long term storage of *E.coli*-cultures glycerol stocks were prepared as follows: 800 μL of an overnight culture was mixed with 800 μL of autoclaved 80 % glycerol. Glycerol stocks were frozen at -80 °C for further use.

2.1.4.2. Transformation of *E.coli*

For transformations 5 μL of a ligation reaction was added to 50 μL of chemocompetent *E.coli* DH5α or TOP10 cells. The mixture was incubated on ice for 20 minutes and heat-shocked at 42 °C for 45 seconds. Then 400 μL of LB-Medium was added and the cells were incubated at 37 °C and 900 rpm for 1 h. 100 - 200 μL of transformed *E.coli* were plated on agar plates complemented with 50 μg/mL of the appropriate antibiotic. After an overnight-incubation the resulting colonies were screened for the desired insert (see 2.1.2.4).

2.1.5. Working with yeasts

2.1.5.1. Cultivation of yeasts

For the cultivation of yeasts three different kinds of media were used: YDPA medium (a complete medium suitable to grow untransformed yeasts), a selection medium (to grow transformed yeast and to select against untransformed yeasts) and a complementation medium (to investigate the effects of complementation). Yeast cells either were plated on the appropriate media using glass beads or inoculated in 5 mL of liquid medium. Subsequently yeasts were grown at 30 °C (37 °C for complementation) in humidified incubators. For long term storage 500 μL of sterile 50 % glycerol was mixed with 500 μL of an overnight yeast culture and frozen at -80 °C.

2.1.5.2. Transformation of yeasts

Competent yeast cells have to be prepared fresh for each transformation. Appropriate yeast strains had to be plated on YPDA agar plates and grown for 3 - 5 days at 30 °C. A single colony was inoculated in 50 mL of YPDA medium and incubated at 30 °C with continuous shaking (200 rpm) until the culture reached its stationary phase (OD600 = 1,5). Yeast cells were diluted to an OD_{600} of 0.2 - 0.3 and incubated until they reached an OD_{600} of 0.4 - 0.5. Cells were harvested by centrifugation (5 min, 1000 g, 4 °C) and the pellet was washed with 25 mL sterile water. After another centrifugation step (5 min, 1000 g, 4 °C) the pellet was resuspended in 500 μL 1.1x TE/1.1x LiAc. These competent yeast cells were then used for transformation. 100 μL of competent yeast

cells were mixed with 0.1 - 0.5 μg plasmid DNA, 100 μg denatured herring testes carrier DNA and 600 μL PEG/LiAc solution. After an incubation of 30 min at 30 °C 70 μL of DMSO was added and the cells were heat shocked for 15 min at 42 °C. The cells were chilled on ice for 2 - 5 min, followed by another centrifugation step at 14000 rpm for 15 s. The pellet was resuspended in 1 mL YPDA and the resulting yeast suspension was incubated at 30 °C for 90 min. Yeasts were harvested by centrifugation (14000 rpm for 15 s) and the pellet was resuspended in 1x TE. 100 μL yeast suspension was spread on selection plates (glucose rich minimal medium lacking uracil) and plates were incubated upside down at 30 °C until small colonies formed.

2.1.5.3. Yeast complementation assay

From the selection plates one colony was picked for each plasmid, resuspended in 50 μL of sterile water and cells were counted and adjusted to 10^6 cells/mL. After a serial dilution (1:1; 1:10; 1:100; 1:1000) 5 μL suspension was applied to complementation plates (-Ura medium containing 2 % galactose and 1 % raffinose but no glucose). As YBR159 knock-outs are temperature sensitive, complementation plates were incubated at 37 °C. After 2 to 3 days plates were photographed for documentation.

2.1.6. Working with mammalian cells

2.1.6.1. Cultivation of mammalian cells

HEK293 cells were cultivated in DMEM (GibcoBRL), which was supplemented with 10 % FBS, 100 U/mL penicillin and 100 μg/mL streptomycin. When the cells reached a confluence of 90 - 100 %, they were split 1:6 using trypsine-EDTA (GibcoBRL). The cells were incubated at 37 °C with 5 % CO_2 in humidified atmosphere.

2.1.6.2. Transfection with FuGENE6

Cells were transfected at a confluence of approximately 50 %. For each cell culture flask (T-75, Nunc) 800 μL serum-free medium was mixed with 24 μL of FuGENE6-reagent (Roche) and incubated at room temperature for 5 minutes. After this incubation 8 μg of plasmid DNA was added to the mixture and incubated for 15 minutes at room temperature. The resulting DNA-FuGENE-complex was pipetted on the cells, which were then incubated for 24 h at 37 °C before they were harvested.

2.1.6.3. Harvesting of cells

Cells were harvested 48 h after transfection. To this end, the cells were treated with trypsine-EDTA (2 mL) and resuspended in DMEM (8 mL). Cells were centrifuged at 1100 rpm for 5 minutes, the medium was removed and the cells were resuspended in 5 mL PBS (to wash the cells). 20 μL of cell suspension was used for quantification of total protein (see 2.1.7.1) and cells were aliquoted in batches that correspond to 600 μg

total protein. Cells were centrifuged once again and after removal of the supernatant cell aliquots were frozen at -80 °C until further use.

2.1.7. Protein Chemistry

2.1.7.1. Determination of total protein concentration

For the determination of total protein concentrations 20 μL of resuspended cells were lysed by sonication and the suspension was mixed with Bradford reagent (BioRad) according to the manufacturer's instructions. After 5 minutes of incubation at room temperature total protein content was measured at a wavelength of 595 nm. A dilution series of bovine serum albumin was used as standard.

2.1.7.2. SDS-PAGE

For SDS-PAGE (sodium dodecylsulfate poly acrylamide gel electrophoresis) frozen cell aliquots were used (for preparation see 2.1.6.3). The aliquots were thawed and cells were lysed by sonication. The suspension was mixed with 5x Laemmli, heated for 5 minutes at 95 °C and subsequently separated on a polyacrylamide gel. The corresponding resolving and stacking gels were prepared as described in Table 2.3. Separation of proteins was achieved by the application of a constant electric field. Following separation, the gel was either subjected to Western blotting (see 2.1.7.3) or stained with Coomassie.

Staining was attained by immersion in Coomassie staining solution (see 2.2.1.10) for 30 minutes and subsequent destaining with 10 % acetic acid (over night).

Reagent	Resolving Gel (10 %)	Stacking Gel (4 %)
AA/bis-AA (30/0.8), 30 %	3.3 mL	0.67 mL
Gel buffer	3 mL	0.67 mL
H_2O	1 mL	3.67 mL
Glycerol (50 %)	2.5 mL	0 mL
TEMED	10 μL	10 μL
APS	50 μL	40 μL

Table 2.3.: Composition of SDS gels

2.1.7.3. Western Blot

To selectively detect tagged proteins semi-dry western blotting was performed. To this end, membranes were moistened (with methanol for PVDF membranes or water for nitrocellulose membranes). The gel, membrane and four pieces of filter paper were equilibrated in blotting buffer (see 2.2.1.10) for 5 minutes. The blot was set up as follows: two pieces of filter paper were put onto the anode, followed by the membrane, the gel and another two pieces of filter paper. The cathode was put on top and transfer of proteins to the membrane was achieved by the application of 20 V for 30 minutes. To

saturate unspecific binding sites, the membrane was blocked 30 minutes with 5 % milk powder dissolved in PBS or Odyssey Blocking Buffer (Licor). The membrane was washed with PBS three times for 10 minutes. Primary antibodies were diluted in a solution of 0.5 % milk powder in PBS and incubated with the membrane over night at 4 °C. The following day the membrane was washed again with PBS and incubated with the appropriate secondary antibody for 2 hours at room temperature. After a final washing step with PBS detection was performed with the Western Lightning Chemiluminiscence ECL-Kit (Perkin Elmer) according to the manufacturer's protocol or using an Odyssey Infrared Imager (Licor).

2.1.7.4. Co-immunoprecipitation

In the first co-immunoprecipitation experiments a protocol using protein A sepharose was used. Later the experiment was performed using an anti-Myc immunoprecipitation kit (Sigma). The proteins used in co-immunoprecipitation were expressed separately in HEK293 cells (bait constructs with a C-terminal Myc-tag and prey constructs with a C-terminal Flag-tag).

Cells were transfected as described above (see Chapter 2.1.6.2) but were harvested by scraping with a rubber policeman (for this a lab made solubilization buffer was used). Cells were lysed by short bursts of sonication (10 s sonication / 10 s on ice; 5 cycles) and cell debris was pelleted by centrifuging for 10 min at 500 g. 200 μL supernatants of 'bait' and 'prey' lysates were mixed in an eppendorf tube. 40 μL protein A sepharose and 5 μL anti-c-Myc antibody (undiluted; Cell Signalling) were added to the samples. After an incubation over night at 4 °C, protein A sepharose was washed 5 times with IP-buffer. 40 μL Laemmli were added to the sepharose beads and the tube was heated to 95 °C for 10 minutes. Samples were applied to a SDS gel (see Chapter 2.1.7.2) and interactions were detected on Western blots (see Chapter 2.1.7.3) treated with anti-FLAG antibodies. Immunoprecipitations using the anti-Myc immunoprecipitation kit were done accoring to the manufacturer's protocol.

2.1.7.5. Enzymatic assays with steroids

For activity assays with steroids tritiated substrates were used. The reactions had the following composition:

190 μL activity assay buffer (see 2.2.1.10)

50 μL cell suspension (in activity assay buffer)

0.5 μL tritiated substrate (final concentrations: 11 nM androstenedione [1,2,6,7-^{3}H(N)], 13 nM estrone [2,4,6,7-^{3}H(N)])

10 μL non-radioactive steroid diluted for kinetics measurements

250 μL corresponding cofactor (dissolved in activity assay buffer)

Reactions were initiated by addition of the appropriate cofactor (NAD(P)H for reduction; $NAD(P)^+$ for oxidation). After varying incubation times (2 minutes to 2 h) at 37 °C the reactions were stopped by addition of 100 μL stop solution (see 2.2.1.10).

The incubation was followed by solid phase extraction using Strata RP18-cartridges (Phenomenex). Cartridges were prepared by washing with 2 x 1 mL methanol and equilibrated with 2 x 1 mL water. Samples were then directly applied to the cartridges, reaction tubes were washed with 600 μL of water, which was also applied to the cartridge. Elution of samples was achieved by addition of 2 x 200 μL methanol.

2.1.7.6. Enzymatic assays with retinoids

The composition of activity assays with retinoids was essentially similar to that of steroids:

190 μL activity assay buffer (see 2.2.1.10)

50 μL cell suspension (in activity assay buffer)

10 μL all-trans retinal in appropriate dilution (for kinetics measurements)

250 μL corresponding cofactor (dissolved in activity assay buffer)

While the initiation, incubation and termination were performed as for radioactive substrates, the clean-up procedure was slightly different. Briefly, Strata C18E SPE-columns (Phenomenex) were washed with 1 mL acetonitrile and equilibrated with 2 x 1 mL acetonitrile:water (40:60). After applying the sample to the column, it was washed with 2 x 1 mL acetonitrile:water (40:60) and eluted with 2 x 200 μL methanol:acetonitrile (5:95).

2.1.7.7. Enzyme kinetics

All measurements for the calculation of enzyme kinetics were done in triplicate. Kinetic parameters were calculated using the Enzyme Kinetics 1.3 add-on for SigmaPlot (Systat Software Inc.). As enzyme kinetics were done using cell lysates in this work a normalization factor was calculated from quantitative Western Blots and kinetic parameters were corrected by this factor.

2.1.7.8. Inhibitor assays

The composition of inhibitor assays was very similar to that of the respective enzymatic assays (see Chapters 2.1.7.5 and 2.1.7.6). The alteration was that 185 μL instead of 190 μL reaction buffer was used. Additionally 5 μL of the inhibitor was added for final concentrations ranging from 10^{-3} to 10^{-12} M. The substrate concentration used was the same as the K_m determined for the respective enzyme. All other parameters were set to match those of the according kinetics measurement.

2.1.8. Analytical Chemistry

2.1.8.1. HPLC

Steroids were separated on a Phenomenex RP18 column (125 mm x 4 mm; particle size 5 μm). The elution was achieved using an isocratic separation with a solvent composition of 57 % water and 43 % acetonitrile and a flow rate of 1 mL/min. Under these conditions steroids were base line separated with retention times of 8 minutes for androstenedione and 5.9 minutes for testosterone (E1 7.5 min; E2 5.5 min). After separation, the eluate was mixed 1:1 with scintillation liquid and radioactive substances were detected using a radioactivity monitor. Chromatograms were analyzed using the 32Karat Software (Beckman Coulter). The conversion of substrates was calculated by comparing the integrated peak areas in corresponding chromatograms.

Retinoids were analyzed by HPLC with UV-VIS detection (Perkin Elmer Series 200 Micropumps, autosampler, UV/VIS-detector). Retinoids were separated on a Synergi Fusion RP-18 column (4.6 x 150 mm; 4 μm; Phenomenex) using a mobile phase consisting of acetonitrile:water (92:8). Elution was monitored at a wavelength of 345 nm. Quantification was attained by comparison of peak areas with those of a series of external retinal and retinol standards.

2.1.8.2. LC-MS/MS: setting up the mass spectrometer

For the determination of ion optics parameters the steroids to be analyzed were diluted to concentrations of 10 μg/L (in some cases this concentration proved to be too high necessitating a further dilution of according analytes). Analytes were directly infused into the mass spectrometer using a syringe pump. Optimization of parameters and determination of mass transitions for multiple reaction monitoring (MRM) were performed using the quantitative optimization tool (for parameters see table 3.5).

Mass transitions and ion optics parameters were inserted into a flow injection analysis (FIA) method. The FIA method was then used to optimize the source parameters using a solution of analytes diluted ten times compared to those used for ion optics optimization. Parameters were then chosen to give the highest sensitivity for the analyte that was hardest to ionize. Optimized source parameters are shown in table 3.6.

2.1.8.3. LC-MS/MS: setup of online-SPE/HPLC

In order to separate the steroids before mass transition, online-solid phase extraction (SPE) coupled to chromatography was used (the HPLC system consisted of 1 controller CBM-20A, 1 pump LC20-AB, 1 pump LC20-AD, a column oven CTO-20A, and an autosampler SIL-20A with an integrated 6-way switching valve). After application to the online SPE column (Oasis HLB, 20 x 2.1 mm, 20 μm particle size) a valve was switched and analytes were eluted in backflush onto the analytical column (Restek Biphenyl 50 x 2.1 mm, 3 μm particle size). After separation the steroids were detected in the mass spectrometer. Setup of the online-SPE system is depicted in Fig. 3.13 and a summary

of the final HPLC program is given in table 2.4 for human plasma samples and in table 2.5 for mouse plasma samples.

Time	Module	Event	Parameter
0.01	Controller	Start	-
0.01	Pumps	Pump B Flow	3
0.01	Pumps	Total A Flow	0.5
0.01	Pumps	Pump AB Conc	42
1.00	Oven	Right Valve	0
1.00	Pumps	Pump AB Conc	42
1.10	Pumps	Pump B Flow	3
1.50	Pumps	Pump B Flow	0.2
2.80	Pumps	Pump AB Conc	49
3.30	Pumps	Pump AB Conc	67
3.30	Oven	Right Valve	1
3.35	Pumps	Pump AB Conc	100
3.81	Pumps	Pump AB Conc	100
3.90	Pumps	Pump AB Conc	42
3.91	Pumps	Pump B Flow	0.2
4.30	Pumps	Pump B Flow	3
4.50	Pumps	Pump AB Conc	42
4.51	Controller	Stop	-

Table 2.4.: Description of the HPLC Program used for human plasma samples

2.1.8.4. Sample pre-treatment for analysis of plasma samples

Plasma contains a complex mixture of proteins that have to be removed before it can be analyzed by LC-MS/MS. Therefore, a mixture of $ZnSO_4$ and methanol was used to precipitate the proteins. 100 μL plasma (50 μL for mouse plasma) were mixed with 200 μL precipitation agent (100 μL for mouse plasma) containing the internal standards. Samples were vortexed for 1 minute and incubated in an over-head-tumbler at 4 °C for 30 minutes. Samples were then centrifuged at 14000 rpm at 4 °C for 10 minutes and supernatants were transferred to measurement vials.

2.1.8.5. Preparation of steroid depleted plasma

Plasma of different donors was pooled, mixed with 5 % (w/v) Norit A (charcoal) and briefly vortexed. This suspension was rotated over night at 4 °C using an overhead tumbler. After 15 min centrifugation at 4500 rpm 4 °C the supernatant was transferred to a new tube and again mixed with 5 % (w/v) Norit A. Following another incubation at 4 °C for 3 h the suspension was centrifuged and the supernatant was passed through a 0.22 μm sterile filter. Aliquots of 200 μL were prepared and stored at -80 °C. Later mass

Time	Module	Event	Parameter
0.01	Controller	Start	-
0.01	Pumps	Pump B Flow	3
0.01	Pumps	Total A Flow	0.5
0.01	Pumps	Pump AB Conc	47
1.00	Oven	Right Valve	0
1.00	Pumps	Pump AB Conc	47
1.10	Pumps	Pump B Flow	3
1.50	Pumps	Pump B Flow	0.2
2.50	Pumps	Pump AB Conc	55
2.55	Pumps	Pump AB Conc	80
2.60	Pumps	Pump AB Conc	100
2.90	Oven	Right Valve	1
2.91	Pumps	Pump AB Conc	100
3.00	Pumps	Pump AB Conc	47
3.01	Pumps	Pump B Flow	0.2
3.30	Pumps	Pump B Flow	3
3.50	Pumps	Pump AB Conc	47
3.51	Controller	Stop	-

Table 2.5.: Description of the HPLC Program used for mouse plasma samples

spectrometric analyses showed that plasma prepared by this method was not totally free of steroids but the steroid levels were sufficiently reduced to concentrations near the detection limit (the plasma is therefore not 'steroid free' but 'steroid depleted').

2.1.8.6. Development of a LC-MS/MS method for the analysis of acyl-CoA conjugated fatty acids

For the analysis of coenzyme A conjugated fatty acids a slightly different approach was needed. The method described by Magnes *et al.* [75] was used with several modifications. To 200 μL of 3-ketopalmitoyl-CoA containing solutions (either standard solutions or cell lysates with overexpressed enzymes) 400 μL of acetonitrile was added and vortexed. This mixture was centrifuged and the supernatant was transferred to a glass vial for measurement.

The hardware configuration used for analysis included the same components as for steroid analysis but additionally a second LC20-AB pump was used (setup: 1 x CBM-20A; 1 x LC20-AD; 1 x CTO-20A; 1x SIL-20A; 2 x LC20-AB). The solvents used were A) 10 % acetonitrile, 0.1 % formic acid; B) 100 % acetonitrile, 0.1 % formic acid; C) 60 % acetonitrile, 15 mM ammonium hydroxide; D) 10 % acetonitrile, 100 mM ammonium hydroxide; E) 100 % acetonitrile, 100 mM ammonium hydroxide. The corresponding HPLC program is shown in Table 2.6.

For mass spectrometric detection positive ESI mode was used. The mass spectrom-

Time	Module	Event	Parameter
0.01	Controller	Start	-
0.01	Pumps	Total B Flow	0.2
0.01	Pumps	Pump B B Conc	1
0.01	Pumps	Total A Flow	1
0.01	Pumps	Pump A B Conc	0
0.01	Pumps	Pump C Flow	0
0.8	Pumps	Total A Flow	1
0.8	Pumps	Pump A B Conc	0
0.9	Pumps	Total A Flow	1.5
0.9	Pumps	Pump A B Conc	40
3.5	Pumps	Pump A B Conc	40
3.6	Pumps	Pump A B Conc	0
6	Oven	Right Valve	0
6	Pumps	Total A Flow	1.5
6	Pumps	Pump C Flow	0
6.1	Pumps	Total A Flow	0
6.1	Pumps	Pump C Flow	0.2
7	Pumps	Pump B B Conc	1
7.7	Pumps	Pump B B Conc	45
13	Pumps	Pump B B Conc	95
14	Pumps	Pump B B Conc	95
14.4	Pumps	Pump C Flow	0.2
14.5	Pumps	Pump C Flow	1.5
15	Pumps	Pump B B Conc	1
15.4	Pumps	Pump C Flow	1.5
15.4	Pumps	Total A Flow	0
15.5	Oven	Right Valve	1
15.5	Pumps	Pump C Flow	0
15.5	Pumps	Total A Flow	1.5
17	Pumps	Pump B B Conc	1
17	Pumps	Total A Flow	1.5
17	Pumps	Pump C Flow	0
17.01	Controller	Stop	-

Table 2.6.: Description of the HPLC Program used for the analysis of CoA conjugated fatty acids

eter was set to detect the mass transition 1020.3 → 513.3 (DP=141, EP=10, CE=51, CXP=16).

2.1.9. Validation of analytical methods

To create an analytical method suitable for routine use, several validation parameters have to be determined: intra-day precision, inter-day precision, intermediate precision, selectivity, linearity, limit of detection, limit of quantification, and recovery.

2.1.9.1. Precision

To determine intra-day precision 10 independent samples were prepared in two sets of 5. Samples were measured and the coefficient of variation between the samples was determined. For determination of inter-day precision two sets of 5 samples were measured on two consecutive days. For intermediate precision two different experimentators each prepared a set of 5 samples.

2.1.9.2. Linearity

To determine the linearity of the developed methods a series of nine dilutions was prepared in triplicate. Regression curves were fitted using the algorithms of Analyst 1.5.1. The R values calculated by the software were used to evaluate the quality of the investigated regression.

2.1.9.3. Limits of detection and quantification

The limit of detection (LOD) and limit of quantification (LOQ) were determined by injecting six blank samples. LOD and LOQ were then calculated according to the following formula:

$LOD = x + 3s$ bzw. $LOQ = x + 10s$

With x being the mean of integrated peak areas and s being the variation of the peak areas.

2.1.9.4. Recovery

To determine recoveries of the analytes investigated, plasma and steroid-depleted plasma was spiked with two different concentrations of the steroids of interest. After measuring the steroid concentration in spiked plasma, recovery was calculated using the following formula:

$$recovery = \frac{S1 - S2}{S3}$$

S1 was the signal of untreated plasma spiked with different amounts of steroid standards, S2 was untreated plasma without spiking (an appropriate amount of solvent was

added instead), S3 was steroid-depleted plasma spiked with the same amount of steroid standards as used for S1. Five replicates were measured for each concentration.

2.2. Materials, Equipment

2.2.1. Materials

2.2.1.1. Chemicals and media

1,4-dithiothreitol	Biomol
3-ketopalmitoyl-CoA	S. Gobec (University of Ljubljana)
3,3',5-triiodo-L-thyronine	Sigma
acetonitrile (gradient grade)	Sigma
acetic acid	Fluka
acrylamide/bisacrylamide (30/0.8), 30%	Roth
agarose	Biozym
all-trans retinal	Sigma
all-trans retinoic acid	Sigma
all-trans retinol	Sigma
ammonium acetate	Fluka
ammonium peroxodisulfate (APS)	Merck
ampicillin	Fluka
ampuwa water	Fresenius
ascorbic acid	Merck
BACTO peptone	Difco
boric acid	neolab
bovine serum albumine (BSA)	Sigma
coenzyme A	Sigma
Coomassie blue G250	Biomol
D-galactose	Fluka
D-raffinose	Fluka
dichloromethane	Acros Organics
dimethyl sulfoxide	Sigma
dNTPs	MBI Fermentas
dodecyl-beta-D-maltoside	Calbiochem
Dulbecco's Modified Eagle Medium	GibcoBRL
DMEM:F12 (1:1)	GibcoBRL
ethanol	Merck
ethidium bromide	Sigma
ethylenediaminetetraacetate (EDTA)	Biomol
fetal bovine serum (FBS)	GibcoBRL
formic acid	Fluka
FuGENE6 transfection reagent	Roche

glucose	Sigma
kanamycine	Sigma
L-thyroxine	Sigma
lithium acetate	Sigma
loading dye (6x)	Fermentas
methanol (gradient grade)	Merck
Minimal SD Agar Base	Clontech
NADPH	Fluka
Norit A	Serva
PEG 3350	BD Biosciences
penicillin/streptomycin	GibcoBRL
sodium chloride	Merck
sodium dihydrogenphosphate	Merck
sodium dodecylsulfate (SDS)	Merck
tert-buthylmethylether	Merck
TEMED	Sigma
trietyhlamine	Merck
tricine	Roth
Tris-HCl	Promega
Tween-20	Merck
-Ura drop out supplement	Clontech
yeast extract	Nordwald
YPD medium	BD Biosciences
zinc sulfate	Fluka

2.2.1.2. Enzymes

BamHI	New England Biolabs
BP Clonase II Enzyme Mix	Invitrogen
EcoRI	New England Biolabs
EcoRV	New England Biolabs
Endonuclease	Sigma
HindIII	New England Biolabs
LR Clonase II Enzyme Mix	Invitrogen
Lysozyme	Sigma
Pfu-Polymerase	Stratagene
RQ1 RNase-free DNase I	Promega
SacII	New England Biolabs
T4-Ligase	MBI Fermentas
Taq-Polymerase	lab-made
Trypsine	GibcoBRL
XhoI	New England Biolabs

2.2.1.3. Antibodies

mouse anti-Myc 9B11 MAB	Cell Signaling
mouse anti-FLAG M2 MAB	Sigma
mouse anti-beta actin AC-74 MAB	Sigma
goat anti mouse IRDye800CW	Licor

2.2.1.4. Steroids

For all radioactively labeled substrates the specific activity is given in parentheses. All radioactive substrates were diluted to 37 MBq/mL.

17OH-progesterone	Sigma
androstenedione	Sigma
$^{13}C_2$-testosterone	Cambridge Isotope Laboratories
corticosterone	Sigma
cortisol	Sigma
cortisone	Sigma
d4-cortisol	C/D/N
d8-corticosterone	C/D/N
d9-progesterone	C/D/N
estrone	Sigma
estradiol	Sigma
^{3}H-androstenedione (3,37 TBq/mmol)	NEN
^{3}H-estrone (3,7 TBq/mmol)	NEN
progesterone	Sigma
testosterone	Sigma

2.2.1.5. Kits

Anti-c-Myc Immunoprecipitation Kit	Sigma
BigDye Terminator v3.1 Cycle Sequencing Kit	Applied Biosystems
DyeEx Spin Kit	Qiagen
Montage SEQ96 Sequencing Reaction Cleanup Kit	Millipore
NucleoBond PC 100 Kit	Machery & Nagel
NucleoSpin Plasmid Kit	Machery & Nagel
Power SYBR Green PCR Master Mix	Applied Biosystems
RevertAid First Strand cDNA Synthesis Kit	MBI Fermentas
SV Total RNA Isolation Kit	Promega
TOPO TA cloning kit	Invitrogen
Western Lightning ECL Kit	Perkin Elmer
Wizard SV Gel and PCR Clean-Up System	Promega

2.2.1.6. Solid phase extraction cartridges

Strata C18E-columns	Phenomenex
Strata C8-columns	Phenomenex

2.2.1.7. Other material

Centricon centrifugal filter device	Millipore
Immobilon-FL PVDF membrane	Millipore
Nitrocellulose membrane	Amersham Biosciences
PVDF membrane	Pall
Ready Flow III scintillation liquid	Beckman Coulter

2.2.1.8. Vectors

NFLAG-pcDNA3	modified pcDNA3
pcDNA3	Invitrogen
pcDNA4/myc-His B	Invitrogen
pCTAP	C. Glöckner (HMGU/IHG)
pDONR201	Invitrogen
pENTR/U6	Invitrogen
pYES2.1	Invitrogen

2.2.1.9. Organisms

BY4741	*S.cerevisiae* (Invitrogen)
ΔYBR159w BY4741	S. Mörtl (HMGU/ISB)
DH5α	*E.coli* K12 (Live Technologies)
HEK293	human embryonic kidney 293 (DSMZ)
TOP10	*E.coli* (Invitrogen)

2.2.1.10. Buffers and solutions

All buffers and solutions were prepared with Millipore-water.

Buffer for activity assays

100 mM	Na_2HPO_4
1 mM	EDTA

Adjusted to pH 7.4 with 100 mM NaH_2PO_4.

Stop-solution for activity assays

500 mM	ascorbic acid
1 %	acetic acid

Dissolved in Methanol.

LB-Medium

1 %	BACTO Peptone
0.5 %	Yeast Extract
1 %	NaCl

Autoclaved LB-Medium was available for use.

PCR-buffer for GAC-Taq-Polymerase

100 mM	Tris-HCl, pH 9.0
500 mM	KCl
15 mM	$MgCl_2$

TE buffer

10 mM	Tris-HCl pH 8.0
1 mM	EDTA

10x TBE

108 g	Tris
55 g	boric acid
9.3 g	EDTA

Ad 1 L with H_2O.

Coomassie staining solution

200 mL	methanol
5 mL	acetic acid
295 mL	H_2O
500 mg	Coomassie Blue G250 (filtrate)

Blotting buffer

48 mM	Tris
33 mM	Tricin
1.3 mM	SDS (10 %)
20 %	methanol

Gel buffer

3 M	Tris-HCl pH 8.45
0.3 %	SDS

Anode buffer

200 mM	Tris-HCl pH 8.9

Cathode buffer

100 mM	Tris-HCl pH 8.9
100 mM	Tricin
0.1 %	SDS

5x Laemmli buffer

50 %	glycerol
4 %	SDS
0.1 %	Coomassie Blue G250 (filtrate)
200 mM	Tris-HCl pH 6.8

Solubilisation buffer

20 mM	Tris/HCl pH 7.5
150 mM	NaCl
0.5 %	dodecyl-β-D-maltoside
1 tablet	protease inhibitor mixture (Roche)

Total volume of 10 mL.

2.2.2. Equipment

2.2.2.1. Hardware

5973N MSD	Agilent Technologies
ABI 3730 sequencer	Applied Biosystems
ABI Prism 9700HT	Applied Biosystems
API 4000 Q trap	Applied Biosystems
CBM-20A	Shimadzu
CTO-20AC column oven	Shimadzu
DGU-20A3 degasser	Shimadzu
DGU-20A5 degasser	Shimadzu
dotLINK Data Handling System	Perkin Elmer
FCV-12AH switching valve	Shimadzu
HPLC-system Gold Basic	Beckman Coulter
HPLC radioactivity monitor LB506D	Berthold
LC-20AB liquid chromatograph	Shimadzu
LC-20AD liquid chromatograph	Shimadzu
Mini-PROTEAN III electrophoresis cell	BioRad
Odyssey Infrared Imaging System	Licor
RoboCycler 96	Stratagene
Series 200 Autosampler	Perkin Elmer
Series 200 Micropump	Perkin Elmer
Series 200 Mixer	Perkin Elmer
Series 200 UV/VIS detector	Perkin Elmer
Series 200 Vacuum Degasser	Perkin Elmer
SIL-20AC autosampler	Shimadzu
Trans-Blot SD - Semidry Transfer Cell	BioRad
UV-VIS-spectrometer	Beckman

2.2.2.2. HPLC columns

Allure Biphenyl 50 x 2.1 mm 3 μ	Restek
Fusion RP18 150 x 3 mm 4 μ	Phenomenex
Kinetex PFP 50 x 2.1 mm 2.6 μ	Phenomenex
Luna C18 150 x 4.6 mm 4 μ	Phenomenex
Oasis HLB 20 x 2 mm 20 μ	Waters
ZORBAX Extend-C18 100 x 2.1 mm 3.5 μ	Agilent

2.2.2.3. Software

32Karat Software	Beckman Coulter
Analyst 1.5.1	Applied Biosystems
Basic linear alignment search tool (BLAST)	www.ncbi.nlm.nih.gov
BioEdit	Ibis Therapeutics
MEGA4	Tamura *et al.* [76]
Primer3	http://frodo.wi.mit.edu/primer3
SDS 2.2	Applied Biosystems
SigmaPlot	SPSS
TotalChrom Workstation 6.3.1	Perkin Elmer
VectorNTI	InforMax

3. Results

In this work two different conceptional approaches were used to gain new insights into the metabolism of hormones.

The biochemical approach focused more on the enzymes and their function within the organism. In this context, Chapters 3.1, 3.2, and 3.3 describe an in-depth analysis of multifunctionality in different 17beta-hydroxysteroid dehydrogenases. This enzyme promiscuity may represent a cross-talk between different metabolic pathways.

A hormone profiling approach may be useful in finding new crossroads between pathways and could lead to the discovery of new multifunctionalities in metabolic enzymes. Therefore, the second approach that was pursued in this work focused on the establishment of new methods to characterize the steroid metabolome (described in Chapter 3.4). Furthermore, it was attempted to extend these methods by including additional hormones.

The analytical chemistry approach overlapped with the biochemical approach in several instances. The division between the two approaches is therefore not as strict as may be assumed from the outline of this section. Nevertheless, the separation was maintained to ensure the lucidity of the 'Results' part.

3.1. 17beta-HSD1: assignment of a new function to an 'old' enzyme

3.1.1. Evolutionary context suggests a new function

A high degree of evolutionary conservation between 17beta-hydroxysteroid dehydrogenase 1 (17beta-HSD1) and photoreceptor-associated (prRDH, also known as RDH8) has been known for some time. A closer investigation of the differences between these two enzymes in zebrafish (*Danio rerio*, abbreviated 'dr' in this work) and humans (*Homo sapiens*, abbreviated 'hs' in this work) implied that a glycine residue is important for 17beta-HSD1 function while a methionine has the same role in prRDH (Alignment see Figure 3.1). To investigate potential influences of these residues on substrate specificities of the respective enzymes, mutated enzymes were generated and compared to their wild type forms. Human and zebrafish wild type enzymes and the following mutants were cloned into a mammalian expression vector: hs17bHSD1-G145M, dr17bHSD1-G143M, hsprRDH-M144G, drprRDH1-M146G, and drprRDH2-M147G.

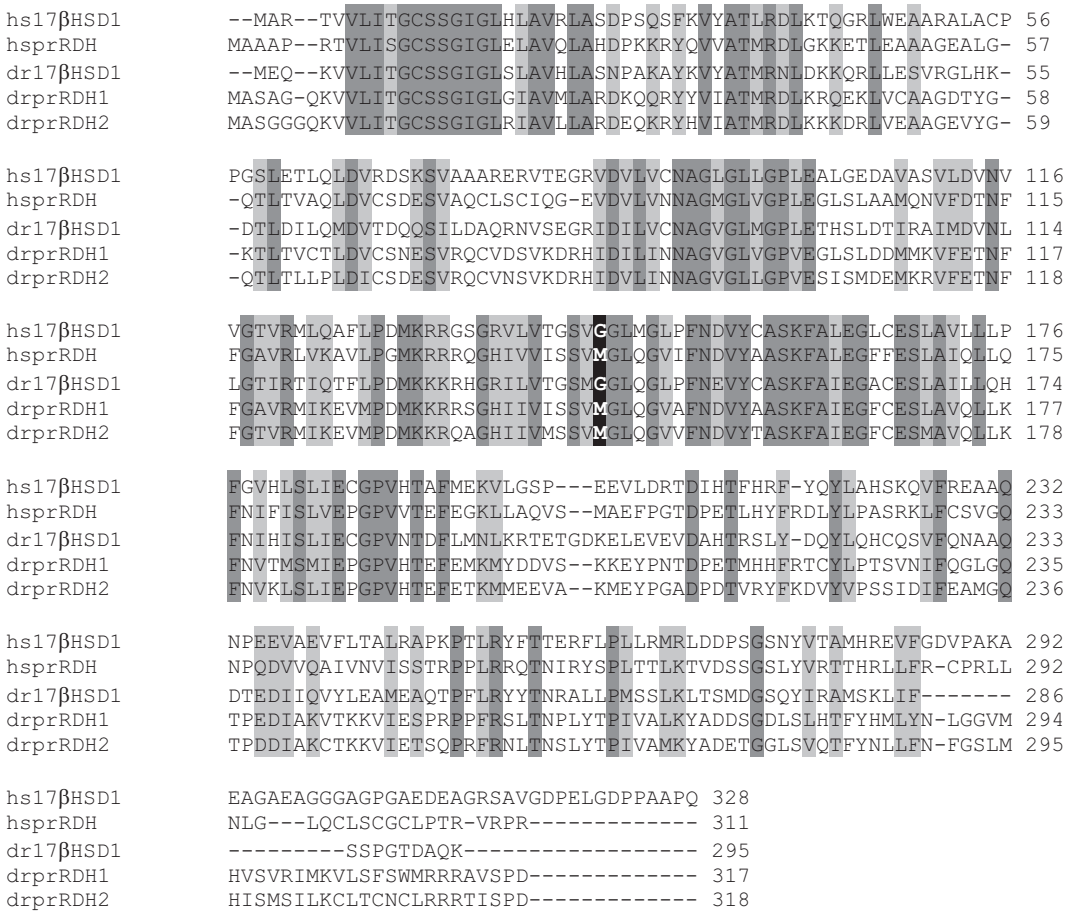

Figure 3.1.: Alignment of prRDH and 17beta-HSD1 sequences from human and zebrafish.
The conserved glycine in 17beta-HSD1 and methionine in prRDH is highlighted in white on black, residues identical in all sequences are shown in dark gray, those identical in each functional group are shown in light gray.

3.1.2. Molecular modelling experiments infer substrate-binding mechanisms in 17beta-HSD1 and prRDH

Based on the alignment shown in Figure 3.1 homology models of 17beta-HSD1 and prRDH were generated in collaboration with Edelmiro Moman (Saarland University, Saarbrücken). Modeling of hs17beta-HSD1 showed that estrone is bound to the enzyme by two H-bond networks composed of Ser143/Tyr156 and His222/Glu283 (see Figure 3.2A). This observation is in agreement with X-ray structure 1FDT that is deposited in PDB. When all-trans retinal was docked to 17beta-HSD1 only one H-bond network can be formed because the polar His222 and Glu283 residues cannot form H-bonds with the non-polar hexenyl ring (Figure 3.2B).

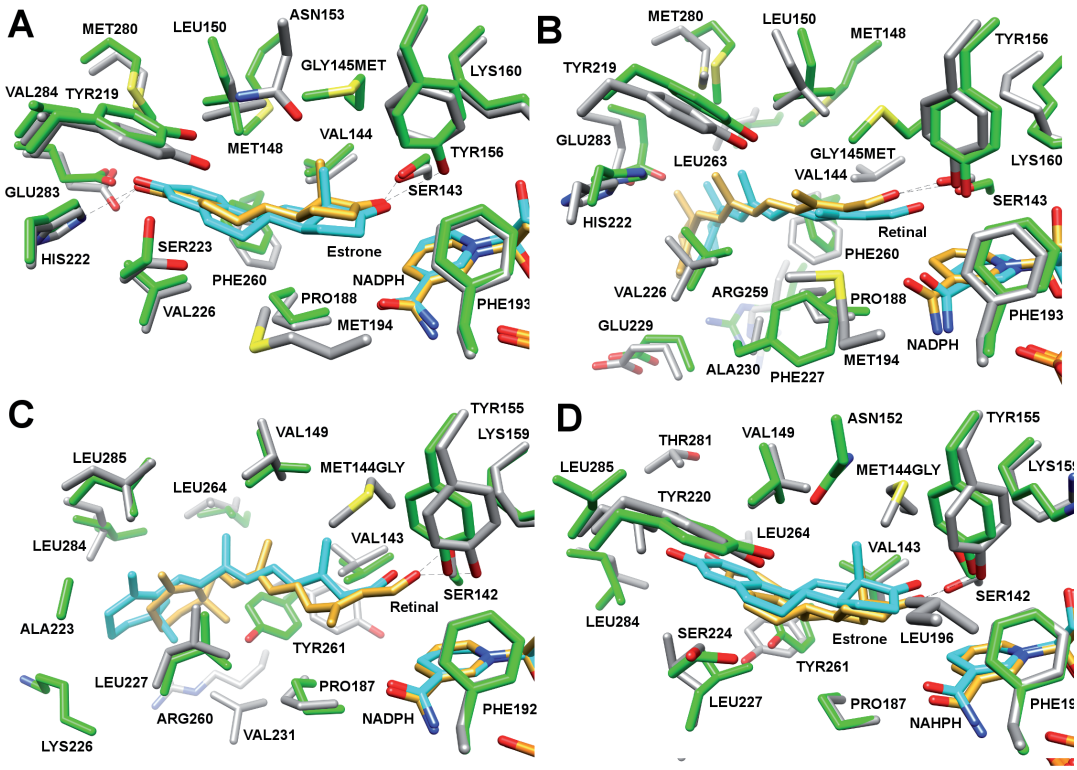

Figure 3.2.: Docking of estrone and all-trans retinal to the models of human 17beta-HSD1 and human prRDH.
Only residues closer than 4.5 Å to the ligand are shown. Amino acids of wild type enzymes are shown in silver with their ligands/cofactors in gold. Amino acids of mutant enzymes are shown in green with their ligands/cofactors in cyan. (A) Model of human 17beta-HSD1 superimposed with its mutants and estrone as substrate. (B) Model of human 17beta-HSD1 superimposed with its mutants and all-trans retinal as substrate. (C) Model of human prRDH superimposed with its mutants and all-trans retinal as substrate.(D) Model of human prRDH superimposed with its mutants and estrone as substrate.

In human prRDH the polar His222/Glu283 residues are replaced with Ala222/Leu283. In this enzyme the non-polar leucine forms van der Waals contacts with retinal's hexenyl

ring (Figure 3.2C) resulting in a reduced solvent exposure when compared to 17beta-HSD1. A very interesting observation during substrate docking experiments with prRDH was the formation of a clamp consisting of Leu227 (Val226 in 17beta-HSD1) and Met144 (Gly145 in 17beta-HSD1). These amino acids force retinal into a conformation in which the planarity of retinal's polyene chain is broken. Furthermore, residues surrounding Leu227 (e.g. Val231) seem to reduce the rotational degrees of freedom of Leu227 and therefore contribute to the clamp effect (Figure 3.2C).

By exchanging the glycine to methionine at position 145 in human 17beta-HSD1 the surrounding residues are impaired in their flexibility. For instance, the catalytical Tyr156 is forced into a different conformation when compared to the wild type. In prRDH the methionine is easily accommodated as the amino acid in its vicinity are smaller: Glu148/Val150 are less bulky than Met148/Leu150 in human 17beta-HSD1. An exchange of glycine 145 for methionine in human 17beta-HSD1 may therefore cause a disruption in the enzyme's substrate binding pocket that reduces the catalytical efficiency towards both substrates (Figure 3.2A).

In the zebrafish the substrate-binding site of 17beta-HSD1 shows a greater similarity to prRDH than in human 17beta-HSD1. The residues surrounding Gly145 are smaller in the zebrafish homolog. For example, Met148 is replaced by a glutamine in the zebrafish enzyme. Due to these slight differences zebrafish 17beta-HSD1 is much better suited to accommodate the Gly145Met mutation than its human homolog.

When the Met144Gly mutation is inserted into human prRDH the aforementioned leucine-methionine-clamp is lost. In wild type prRDH Met144 forms van der Waals interactions with retinal. When Met144 is exchanged with glycine these contacts are lost weakening binding to retinal. The binding of estrone to wild type prRDH is prevented by the leucine-methionine-clamp. Only the Met144Gly exchange enables the estrogen to bind in a productive pose that is similar to that observed in 17beta-HSD1 (Figure 3.2D).

When human prRDH was compared to its two zebrafish homologs only minor differences were apparent, with residue 227 of hsprRDH being the most notable distinction. In the human enzyme a leucine can be found in this position while the zebrafish enzymes harbor an isoleucine. This isoleucine allows for a more planar conformation of the conjugated π-system which would result in a looser clamp effect. A looser clamp could theoretically enable estrone to bind in more productive conformation, but Met145 (for drprRDH1 or Met147 for drprRDH2) still prevents the carbonyl of the ligand from lying above the hydronicotinamide methylene group. When the methionine is exchanged to glycine estrone can bind more readily, while the protein-ligand interactions between retinal and the enzyme are weakened.

3.1.3. Expression and quantification of 17beta-HSD1 and prRDH in HEK293 cells

All aforementioned constructs were transiently transfected into HEK293 cells. For a normalization of protein amounts quantitative Western Blotting was performed. The

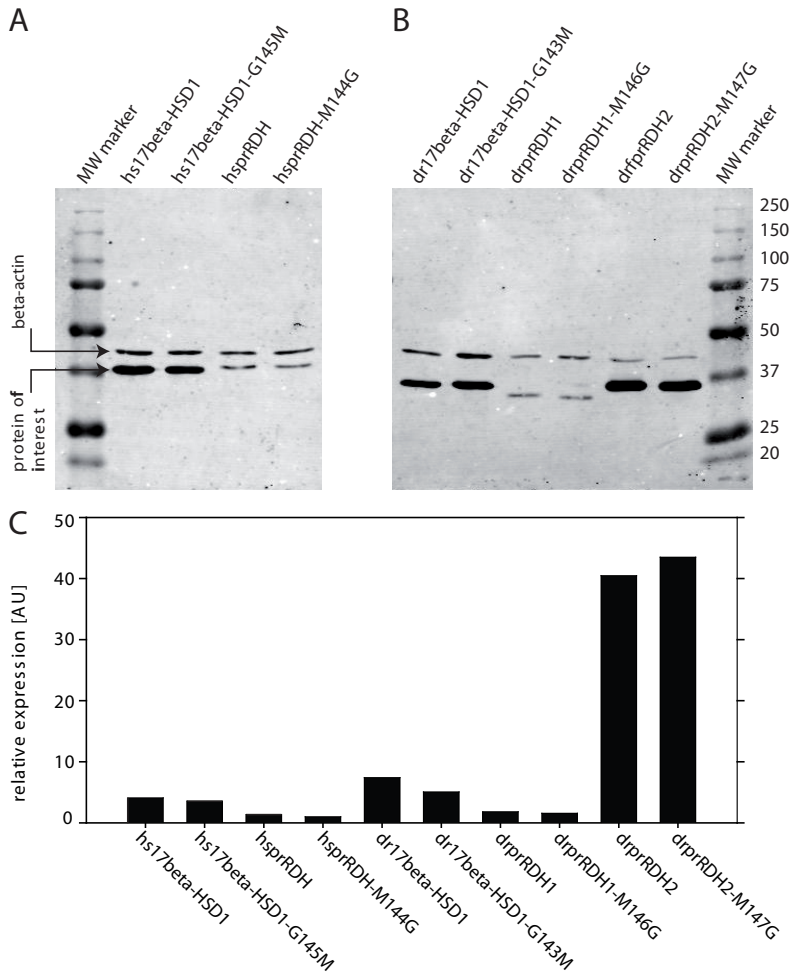

Figure 3.3.: Western blot and densitometric evaluation of protein expression levels of 17beta-HSDs 1 and prRDHs.
Immunoblotting of proteins expressed in transiently transfected HEK293 cells. The blot was developed using anti-Flag antibody targeted against the Flag-tag that was used to label the proteins. Anti-beta-actin antibody was used to normalize for the amount of loaded protein. (A), immunoblot of human 17beta-HSD1, prRDH and their respective mutants, (B), immunoblot of zebrafish 17beta-HSD1, prRDH1, prRDH2, and their respective mutants, (C), densitometric evaluation of both immunoblots.

blots shown in Figure 3.3 were evaluated densitometrically and expression levels of the respective proteins of interest were divided by the expression of beta-actin. While the expression greatly differed between the five different proteins (hs17beta-HSD1, hsprRDH, dr17beta-HSD1, drprRDH1, and drprRDH2), the expression level of each protein was very similar to those of their respective mutants. For most enzymes protein concentrations were similar, only for drprRDH2 and its mutant expression was significantly higher. The quantitative evaluation of the results allowed for the determination of a normalization factor that was then used to recalculate the V_{max} values derived from enzyme kinetics measurements (see third column of Tables 3.1 and 3.2).

3.1.4. Enzyme kinetics of 17beta-HSD1 and prRDH with different substrates

3.1.4.1. Catalysis of estrogen conversion by 17beta-HSD1 and prRDH

Transiently transfected HEK293 cells were used for activity measurements. Total protein concentrations ranging from 1 μg to 60 μg (150 μg were used for negative controls) were used in the assays. Incubation times were optimized to exclude an influence of background conversion by the cells. Substrate and product of the reactions were extracted by SPE and resolved by HPLC using a method that was developed in this work (data not shown). Results from HPLC runs were used to calculate kinetic parameters (for kinetics see Appendix D, for a summary see Table 3.1). Quantitative Western Blot were used for normalization.

Both human and zebrafish wild type 17beta-HSD1 enzymes showed low K_M values towards estrone indicating a high affinity to this substrate. The V_{max} values of human 17beta-HSD1 were a near 100-fold higher than for the zebrafish enzyme. Insertion of the Gly to Met mutation resulted in a dramatic decrease in V_{max}, nearly abolishing the activity of the enzyme. In zebrafish the enzyme seemed to be much more resistant to the insertion of this mutation as only the affinity to the substrate was reduced while V_{max} remained quite stable.

The investigated prRDHs from human and zebrafish were not capable of catalyzing the reduction of estrone. To confirm this observation incubation times up to 5 hours and total protein concentrations up to 150 μg were used in the assay. Consequently, it can be stated that the activity was well below 0.004 nmol/min/mg protein) and can therefore be assumed to be non-existent. Insertion of the Met to Gly point mutation resulted in a gain of function in all three prRDHs. However, the catalytical efficiency was poor for human prRDH and kinetics were non-saturable for both zebrafish paralogs. The values for K_M and V_{max} given in Table 3.1 are therefore only estimates.

3.1.4.2. All-trans retinal reduction by 17beta-HSD1 and prRDH

Upon investigating the reduction of all-trans retinal to all-trans retinol catalyzed by hs17beta-HSD1, we found an unexpectedly high catalytical efficiency (V_{max}/K_M) for this enzyme (see Table 3.2). Judging solely from kinetics data human 17beta-HSD1

Enzyme	K_M [μM]	V_{max} [nmol/min/mg total protein]	app.V_{max} [nmol/min/mg total protein]	V_{max}/K_M
hs17bHSD1	0.138 ± 0.028	75.2 ± 6.7	18.43	133.540
hs17bHSD1M	0.161 ± 0.019	0.037 ± 0.002	0.01	0.065
hsprRDH	ND	ND	ND	ND
hsprRDHM	9.6 ± 3.1	0.055 ± 0.006	0.06	0.006
dr17bHSD1	0.043 ± 0.008	1.451 ± 0.087	0.20	4.561
dr17bHSD1M	0.321 ± 0.015	1.351 ± 0.034	0.27	0.832
drprRDH1	ND	ND	ND	ND
drprRDH1M	30.7 ± 5.1 *	602.8 ± 53.7 *	388.10 *	12.642 *
drprRDH2	ND	ND	ND	ND
drprRDH2M	23.3 ± 1.3 *	17700 ± 597 *	407.02 *	17.469 *

Table 3.1.: Kinetic constants of human 17beta-HSD1 and prRDH as well as zebrafish 17beta-HSD1, prRDH1, and prRDH2 using estrone as substrate.
Kinetic constants for all enzymes were determined in presence of saturating NADPH (600 μM) in 50 mM sodium phosphate pH 7.3 with 1 mM EDTA at 37 °C (see Chapter 2.1.7.5). Kinetic constants were calculated by non-linear fitting using the Enzyme Kinetics 1.3 add-on for SigmaPlot (Systat Software Inc.); *kinetics were not saturable within substrate solubility range, theoretical value; ND, no activity detected (activity $<$ 0.004 nmol/min/mg protein)). Reactions with prRDHs and estrone were incubated for 5 hours with 150 μg of total protein.

Enzyme	K_M [μM]	V_{max} [nmol/min/mg total protein]	app.V_{max} [nmol/min/mg total protein]	V_{max}/K_M
hs17bHSD1	3.01 ± 0.38	48.6 ± 2.3	11.91	3.956
hs17bHSD1M	1.6 ± 0.3	5.6 ± 0.3	1.57	0.982
hsprRDH	1.26 ± 0.26	38.1 ± 2.2	28.25	22.417
hsprRDHM	2.3 ± 0.3	11.3 ± 0.5	11.30	4.913
dr17bHSD1	6.5 ± 1	1.611 ± 0.098	0.22	0.034
dr17bHSD1M	6.5 ± 1.7	12.4 ± 1.3	2.45	0.377
drprRDH1	3.1 ± 0.4	1.47 ± 0.06	0.81	0.261
drprRDH1M	1.7 ± 0.2	0.553 ± 0.02	0.36	0.209
drprRDH2	4.4 ± 0.5	195.2 ± 8.2	4.82	1.096
drprRDH2M	3.02 ± 0.76	44.85 ± 4.18	1.03	0.342

Table 3.2.: Kinetic constants of human 17beta-HSD1 and prRDH as well as zebrafish 17beta-HSD1, prRDH1, and prRDH2 using all-trans retinal as substrate.
Kinetic constants for all enzymes were determined in presence of saturating NADPH (600 μM) in 50 mM sodium phosphate pH 7.3 with 1 mM EDTA at 37 °C (see Chapter 2.1.7.6). Kinetic constants were calculated by non-linear fitting using the Enzyme Kinetics 1.3 add-on for SigmaPlot (Systat Software Inc.)

seems to be a more potent retinol dehydrogenase than both zebrafish RDHs. Even in comparison to human prRDH, the specialized retinol dehydrogenase is merely 5-fold more efficient than hs17beta-HSD1. In zebrafish the results were quite similar: the catalytic efficiency for zf17beta-HSD1 was only about 5 times lower compared to the eye-specific prRDH1. Replacement of glycine to methionine in human 17beta-HSD1 did not result in the expected improvement in catalytical efficiency but decreased the enzyme's potential to reduce all-trans retinal. In contrast, the same mutation caused a 10-fold increase in catalytical efficiency in zebrafish 17beta-HSD1.

Insertion of the point mutation into human prRDH resulted in a dramatically reduced reductive potential towards retinal. In hsprRDH-M144G K_M was nearly twice as high, while V_{max} decreased by a factor of 4. Mutating the methionine to glycine resulted in reduced catalysis of the reduction of retinal in both zebrafish paralogs of prRDH. M146G-drprRDH1 showed a 2-fold lower apparent V_{max} compared to the wild type enzyme. For drprRDH2 the effect was even more pronounced, apparent V_{max} decreased nearly by the factor of 5.

3.1.5. Expression of 17beta-HSD1 and prRDHs in human tissues

The remarkably high catalytical efficiency of human 17beta-HSD1 for the substrate all-trans retinal posed the question whether this observation had physiological significance. The mRNA expression of human 17beta-HSD1 and prRDH was analyzed by quantitative RT-PCR in 48 tissues (see Figure 3.4). As expected, expression of 17beta-HSD1 was highest in placenta, the organ from which this enzyme was first isolated. Relatively high expression of 17beta-HSD1 was also observed in ovary and testis. Furthermore, 17beta-HSD1 showed a relatively widespread (but low) expression in a variety of different tissues.

It was not surprising to find the highest expression levels of hsprRDH in the retina. Expression was also found in the intracranial artery and the vena cava as well as some other tissues. In general, prRDH expression was lower and much more localized when compared to 17beta-HSD1. Taking into account the observation that human 17beta-HSD1 catalyzes the conversion of all-trans retinal the expression of this enzyme in the retina was of special interest. In this organ 17beta-HSD1 mRNA levels are about 30 times lower than those of prRDH.

3.1.6. Inhibition of prRDH and 17beta-HSD1 enzymes by 2-phenethyl-D-homo-estrone

Inhibitors of 17beta-HSD1 have been developed for many years as treatments with these substances may be effective in fighting estrogen related cancers like breast cancer. The aforementioned kinetics data of 17beta-HSD1 and prRDH suggested a cross-talk between steroid and retinoid metabolism. Furthermore, 17beta-HSD1 showed a low but ubiquitous expression pattern, while prRDH was also expressed in several tissues. Therefore, inhibitors targeted against 17beta-HSD1 may not only be effective in cancer treatment but they could also have adverse effects. To determine the effects of inhibiting these en-

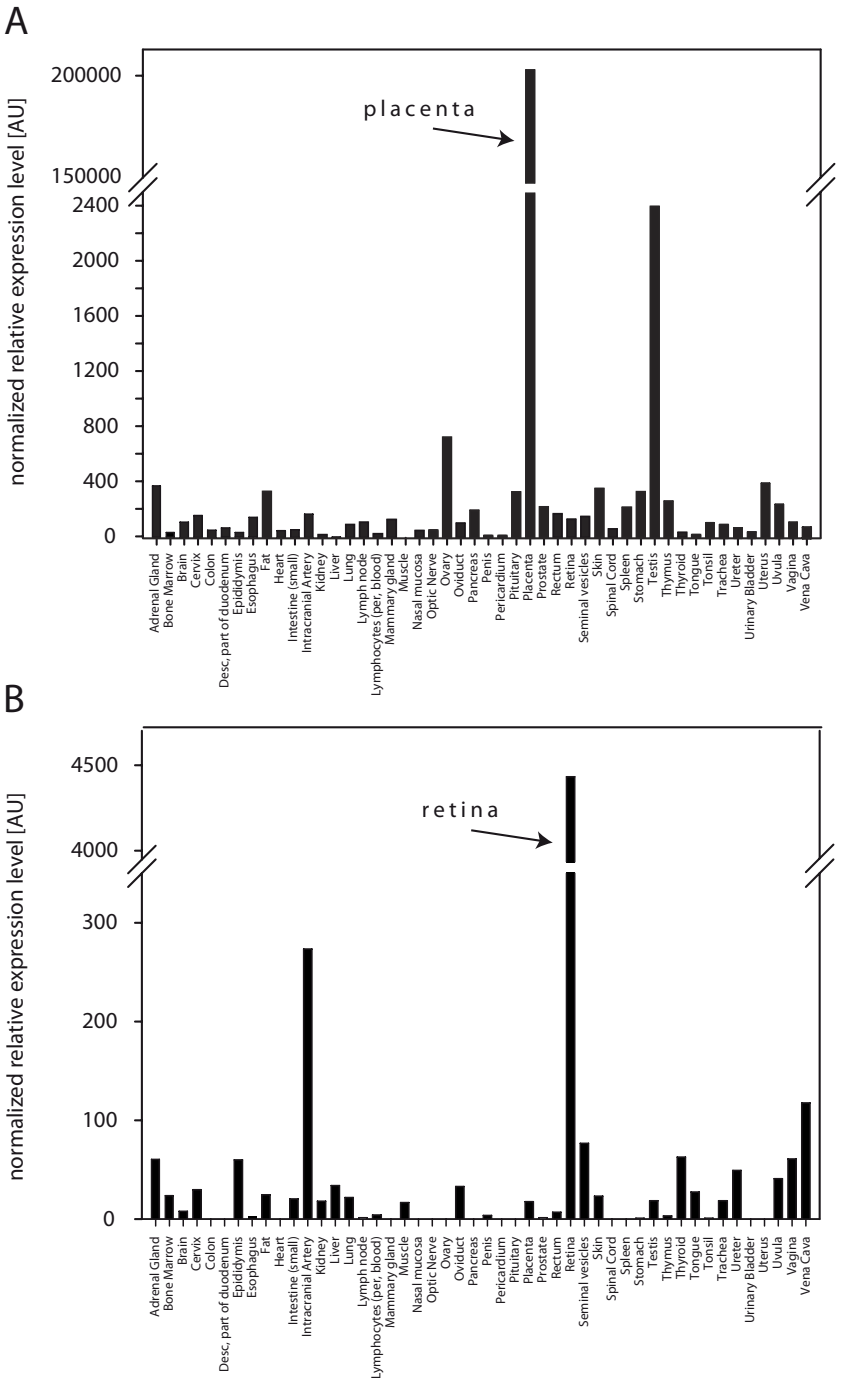

Figure 3.4.: Expression analysis of 17beta-HSD1 and prRDHs.
Real time qRT-PCR analysis of mRNA expression. Expression was normalized to the housekeeping gene GAPDH and the tissue with lowest detectable expression (prRDH expression in tonsil), (A), expression of human 17beta-HSD1 in 48 human tissues, (B), expression of human prRDH in 48 human tissues.

zymes IC_{50} values of a 17beta-HSD1 inhibitor, 2-phenethyl-D-homo-estrone, were measured.

Enzyme	K_M [μM]	IC_{50} [μM]	calculated Ki [μM]
hs17bHSD1	0.138 ± 0.028	0.015 ± 0.007	0.007
hs17bHSD1M	0.161 ± 0.019	0.012 ± 0.002	0.006
hsprRDH	ND	ND	ND
hsprRDHM	9.6 ± 3.1	5.3 ± 1.6	2.7
dr17bHSD1	0.043 ± 0.008	0.0057 ± 0.0013	0.003
dr17bHSD1M	0.321 ± 0.015	0.83 ± 0.29	0.4
drprRDH1	ND	ND	ND
drprRDH1M	30.7 ± 5.1	1.54 ± 0.62	0.8
drprRDH2	ND	ND	ND
drprRDH2M	23.3 ± 1.3	16.3 ± 5.3	8.2

Table 3.3.: Inhibition of the estrone to estradiol reduction by 2-phenetyl-D-homo-estrone. Human and zebrafish 17beta-HSD1 and prRDHs were assayed for their IC_{50} values after treatment with the inhibitor. The experimental setup was similar to that used for determining kinetic constants but here the substrate concentration was fixed, while the inhibitor concentration was varied (for a detailed description see Chapter 2.1.7.8). IC_{50} values were calculated by non-linear fitting using SigmaPlot. Ki values were calculated from K_M and IC_{50} values using the following formula: $K_i = \frac{IC_{50}}{1+\frac{[S]}{K_M}}$

The inhibitor used for this study showed a very efficient suppression of 17beta-HSD1 activity (see Table 3.4 and Table 3.3). Especially the conversion of estrone to estradiol was inhibited in human as well as zebrafish 17beta-HSD1. While in the human enzyme the Gly to Met mutation does not seem to have an influence on estrone conversion, the mutant of zebrafish 17beta-HSD1 showed a 100 times higher IC_{50}. When all-trans retinal was used as a substrate IC_{50} values were considerably higher indicating a weaker inhibition of the reaction. Interestingly, with this substrate the effects of the mutation were reversed: when comparing hs17beta-HSD1 with its mutant there is a 100 fold change in IC_{50} while for the zebrafish enzyme there is no difference between the mutant and the wild type. Generally, the differences between the different substrates are much more pronounced in the human enzyme than in the zebrafish. While the substrate related differences in IC_{50} values range between the factor 50 to 5000 for human wild type and mutant 17beta-HSD1, these values differ only by a factor of 2 to 300 for the zebrafish enzymes.

The investigated prRDHs were less susceptible to the inhibition by 2-phenethyl-D-homo-estrone. Using retinal as substrate, human prRDH showed a 20 times higher IC_{50} compared to human 17beta-HSD1. Similar results can be observed when comparing zebrafish prRDH1 and 17beta-HSD1. For zebrafish prRDH2 the difference is not as pronounced but still observable. The mutants of human prRDH and zebrafish prRDH1 showed a further increase in IC_{50} when compared to the wild type. Solely for prRDH2 a decrease in IC_{50} by a factor of 2 could be observed.

Enzyme	K_M [μM]	IC_{50} [μM]	calculated Ki [μM]
hs17bHSD1	3.01 ± 0.38	0.501 ± 0.053	0.3
hs17bHSD1M	1.6 ± 0.3	58.1 ± 11.3	29.1
hsprRDH	1.26 ± 0.26	10.4 ± 3.6	5.1
hsprRDHM	2.3 ± 0.3	38.9 ± 13.6	19.5
dr17bHSD1	6.5 ± 1	1.96 ± 0.95	1.0
dr17bHSD1M	6.5 ± 1.7	1.46 ± 0.8	0.7
drprRDH1	3.1 ± 0.4	23.5 ± 6.8	11.9
drprRDH1M	1.7 ± 0.2	45.5 ± 9.1	22.8
drprRDH2	4.4 ± 0.5	6.44 ± 1.87	3.2
drprRDH2M	3.02 ± 0.76	3.02 ± 1.39	1.5

Table 3.4.: Inhibition of the all-trans retinal to all-trans retinol reduction by 2-phenetyl-D-homo-estrone.
Human and zebrafish 17beta-HSD1 and prRDHs were assayed for their IC_{50} values after treatment with the inhibitor. The experimental setup was similar to that used for determining kinetic constants but here the substrate concentration was fixed, while the inhibitor concentration was varied (for a detailed description see Chapter 2.1.7.8). IC_{50} values were calculated by non-linear fitting using SigmaPlot. Ki values were calculated from K_M and IC_{50} values using the following formula: $K_i = \frac{IC_{50}}{1+\frac{[S]}{K_M}}$

When estrone was used as a substrate, only the mutant prRDHs could be assayed for their IC_{50} values as the wild type prRDHs do not convert estrone (see Chapter 3.1.4.1). All prRDH mutants showed higher IC_{50} values compared to both, 17beta-HSD1 wild type and mutant. For human prRDH and zebrafish prRDH1 IC_{50} values with estrone as substrate were lower than those using retinal as substrate. Only for prRDH2 the IC_{50} values for retinal were lower than the values measured for estrone.

3.2. Multifunctionality in 17beta-HSD12: the evolutionary origins

The official annotation of several sequences described in this section was not used as the results of the functional studies presented here suggest a different naming. Sequences to which a functionality could not be assigned are denominated with the suffix 'like' to indicate close sequence similarities with the other sequences described in this section.

3.2.1. Phylogenetic analysis of 17beta-HSD12 origins

To better assess the evolutionary relationships of the candidates with known enzymes a phylogenetic tree was calculated using a neighbor-joining algorithm. As plant 3beta-ketoacyl reductases are more distantly related to the set of other sequences the tree was rooted here. Several groups can be discerned from the presented tree. The 17beta-

HSD12 group contains sequences of partially characterized (e.g. human 17beta-HSD12) as well as a number of potential 17beta-HSD12 enzymes. But also from the more distantly related branches several of the candidate sequences were chosen for investigation. Judging solely from this tree one of the *Branchiostoma floridae* candidates seems to be the most closely related sequence with the *Strongylocentrotus purpuratus* sequence being a little more distant to the other 17beta-HSD12 enzymes. Additionally, a *Ciona intestinalis* homolog also groups with 17beta-HSDs type 12.

Two of the *Branchiostoma floridae* candidates and one of the *Ciona intestinalis* candidates did not readily group with other sequences. One of the *Branchiostoma floridae* candidates was found in the 17beta-HSD3 group, but this observation was only supported by a low bootstrap value. The other *Branchiostoma floridae* candidate was found in a separate group together with yeast YBR159w and *C.elegans* LET-767. The bootstrap values supporting this arrangement were only mediocre. The other *Ciona intestinalis* candidate was located in the HSDlike group.

3.2.2. Identification of 17beta-HSD12 homologs by yeast complementation assays

To investigate the involvement of different 17beta-HSD12 enzymes in fatty acid metabolism yeast complementation assays were performed (see Figure 3.6). Yeasts lacking YBR159w (the yeast homolog of 17beta-HSD12) were generated by Simone Mörtl (Institute of Radiation Biology, Helmholtz Center Munich). Candidate sequences were cloned into the yeast expression vector pYES2.1. Sequences of human 17beta-HSDs type 1, type 5, and type 7 were included as negative controls, while yeast YBR159w (gift of Tea Lanisnik-Rizner) was cloned as a positive control for the assay (for details see 2.1.5.3). Three yeast transformants from each transformation selection plate were plated on complementation plates (minimal media without fatty acids). The plates were incubated at 37 °C for 3 days and photographs were taken for documentation.

The strong growth of scYBR159w transformants was the reference to which all other complementation results were compared. As expected human 17beta-HSD12 as well as both zebrafish paralogs of 17beta-HSD12 showed clear complementation. For *Ciona intestinalis* two sequences were investigated, one of which was described as a 17beta-HSD3 in literature [77]. Interestingly, this sequence was the one that gave a signal in complementation, while for the other protein no growth was observable. Three potential 17beta-HSD12 candidates were identified in *Branchiostoma floridae*, but only one of these proteins complemented the ΔYBR159w phenotype. The one sequence taken from *Strongylocentrotus purpuratus* also enabled the knock-out yeast to grow, making it another possible candidate for a 17beta-HSD12 homolog. Of the four included negative controls the sequences of 17beta-HSDs type 5 and 7 as well as the empty vector did not give any signal. For 17beta-HSD1 weak growth was observable, but it was distinctly weaker than that observed for the other sequences.

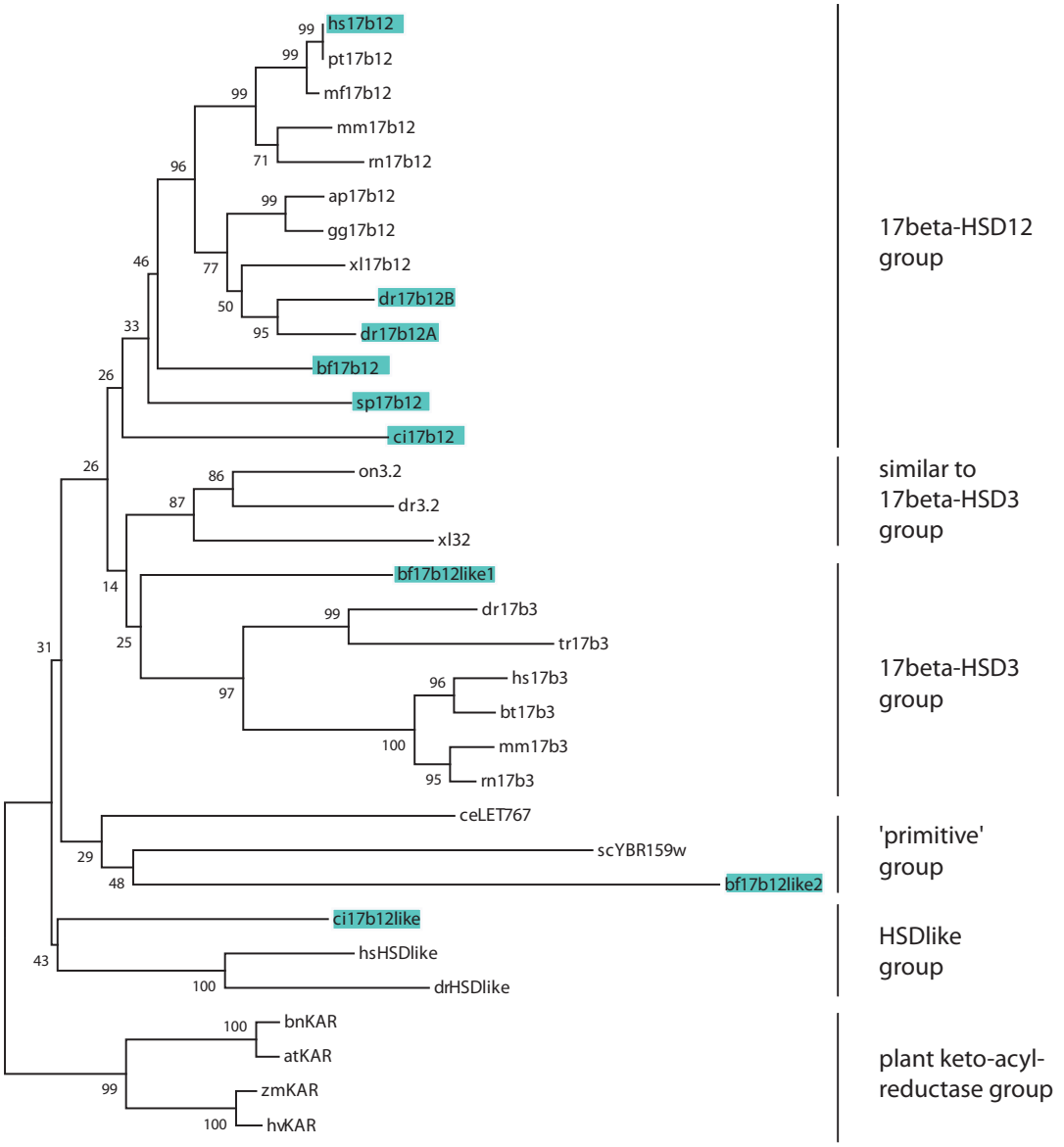

Figure 3.5.: Evolution of 17beta-HSD12 homologs.
Phylogenetic tree was calculated by neighbor-joining with bootstraping. Plant 3keto-acyl-CoA reductases were used as outgroup. Abbreviations: hs = *Homo sapiens*, dr = *Danio rerio*, mm = *Mus musculus*, rn = *Rattus norvegicus*, pt = *Pan troglodytes*, mf = *Macaca fascicularis*, ap = *Anas platyrhynchos*, gg = *Gallus gallus*, xl = *Xenopus laevis*, ci = *Ciona intestinalis*, bf = *Branchiostoma floridae*, sp = *Strongylocentrotus purpuratus*, bt = *Bos taurus*, ce = *Cenorhabditis elegans*, sc = *Saccharomyces cerevisiae*, bn = *Brassica napus*, at = *Arabidopsis thaliana*, zm = *Zea mays*, hv = *Hordeum vulgare*. Sequences investigated in this work are shown in turquoise.

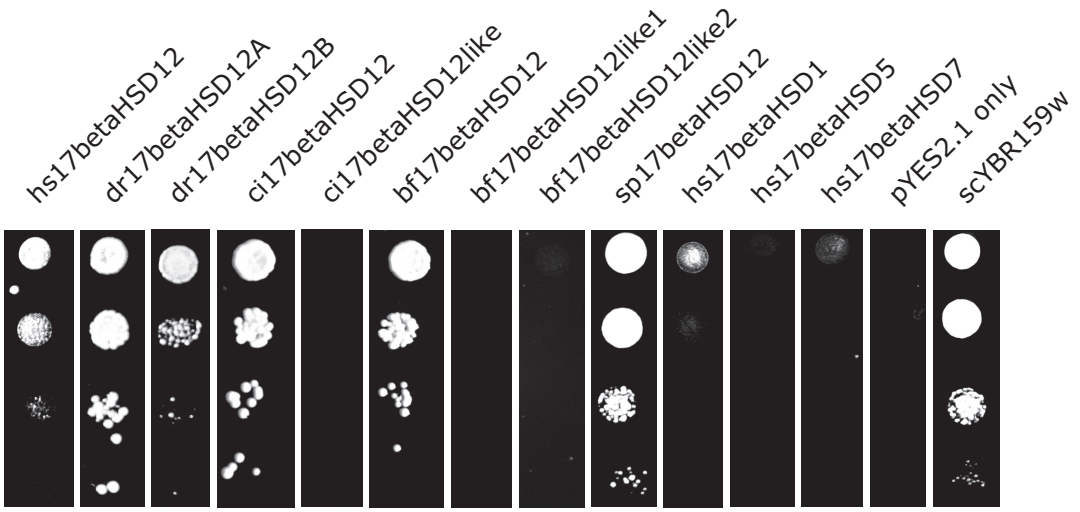

Figure 3.6.: Yeast complementation assay.
YBR159w knock-out yeasts were transfected with candidate 17beta-HSD12 sequences and grown on complementation plates. Human 17beta-HSDs 1, 5, and 7 were chosen as negative and YBR159w as positive control. Abbreviations: hs = *Homo sapiens*, dr = *Danio rerio*, ci = *Ciona intestinalis*, bf = *Branchiostoma floridae*, sp = *Strongylocentrotus purpuratus*, sc = *Saccharomyces cerevisiae*.

3.2.3. Interaction partners of 17beta-HSD12 are involved in fatty acid metabolism

The yeast homolog of 17beta-HSD12, YBR159p has been shown to interact with Elo3p and Tsc13p at protein level [78]. While Elo3p is an elongase that catalyzes the first step in fatty acid elongation, Tsc13p is a trans-2,3 enoyl reductase that catalyzes the final step in the fatty acid elongation cycle. By BLAST searches and literature research several elongases could be identified in humans: Ssc1, Cig30, ELOVL4, and LCE. For Tsc13 only TER could be identified as a homolog. Human 17beta-HSD12 was cloned into a vector coding for a C-terminal myc-tag while the potential interaction partners were cloned into another vector coding for a C-terminal FLAG-tag. Tagged 17beta-HSD12 was immunoprecipitated with anti-myc antibodies and subjected to SDS-PAGE/Western blotting. Co-immunoprecipitated 17beta-HSD12 interactants were detected with anti-FLAG antibodies.

In a preliminary experiment 17beta-HSD12 was immunoprecipitated in a special buffer containing the detergent dodecyl-β-D-maltoside (see Figure 3.7 A). In a subsequent co-immunoprecipitation interaction of 17beta-HSD12 with the proteins ELOVL4 and TER could be shown (see Figures 3.7 B and C, respectively; for mock-transfected cells no interaction was detectable). Unfortunately, this experiment was successfully performed only one time and could not be repeated due to time constraints. The co-IP results presented here therefore still need verification.

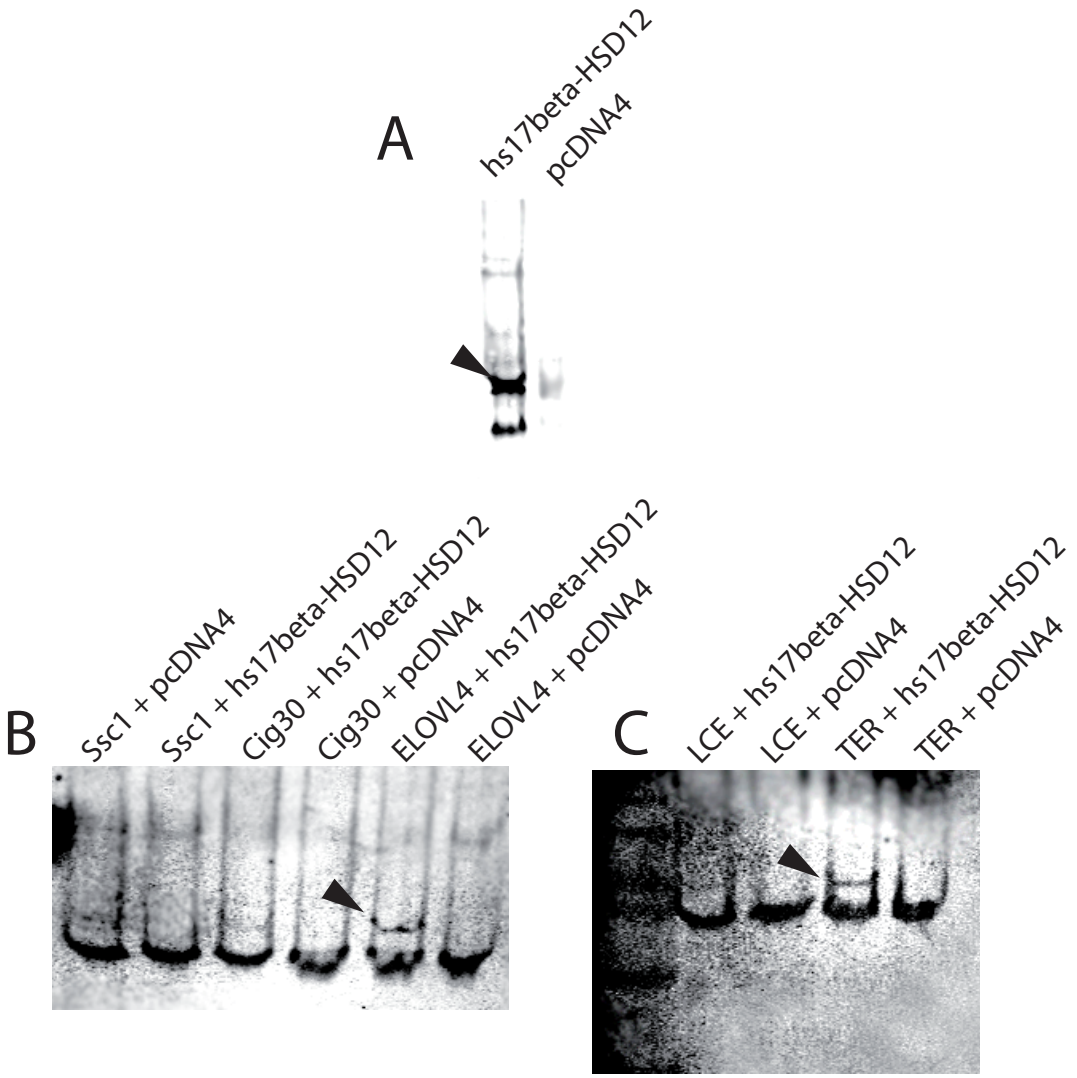

Figure 3.7.: Immunoprecipitation and co-immunoprecipitation of 17beta-HSD12 and its interactants.
HEK293 cells transfected with constructs coding for myc-tagged human 17beta-HSD12 served as 'bait' while mock-transfected HEK293 cells were used as negative controls. The 'bait' constructs coded for potential interaction partners with a C-terminal FLAG-tag. A) Immunoprecipitation of human 17beta-HSD12 (arrowhead). B) Co-immunoprecipitation of human 17beta-HSD12 with Ssc1, Cig30, and ELOVL4. C) Co-immunoprecipitation of human 17beta-HSD12 with LCE and TER. Immunoprecipitated proteins were detected for ELOVL4 and TER (arrowheads).

3.2.4. Substrate assays show that estrogen conversion is not a characteristic of 17beta-HSD12

A time course for the conversion of estrone to estradiol catalyzed by different 17beta-HSD12 homologs was measured (see Figure 3.8). Several of the investigated proteins like the *Ciona intestinalis* and *Strongylocentrotus purpuratus* 17beta-HSD12 homologs did not show estrone conversion above the background level. While one of the *Branchiostoma floridae* proteins showed only background levels of estrone conversion, for the other protein catalysis was slightly above the background.

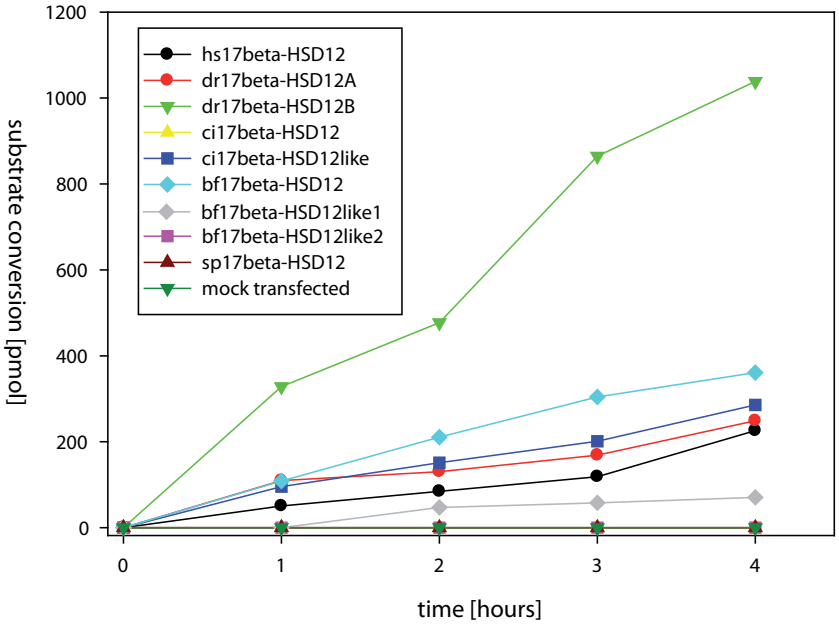

Figure 3.8.: Time dependent conversion of estrone to estradiol catalyzed by 17beta-HSD12 homologs.
$1{\cdot}10^6$ transfected cells were incubated at 37 °C with a final estrone concentration of 10 μM; the enzymes investigated were 17beta-HSD12 from human (=hs), zebrafish (=dr), *Ciona intestinalis* (=ci), *Branchiostoma floridae* (=bf), and *Strongylocentrotus purpuratus* (=sp). As a negative control mock-transfected cells were assayed for their activity.

All vertebrate 17beta-HSD12 homologs catalyzed the reduction of estrone, with dr17beta-HSD12B being the most effective enzyme in this regard. Furthermore, 17beta-HSD12 from *Branchiostoma floridae* showed a distinct catalysis of this reaction. While the 17beta-HSD12 from *Ciona intestinalis* did not have any influence on the reduction, the other protein derived from this organism was able to catalyze estrone conversion.

Generally the extremely long reaction times are of interest. While noticeable substrate conversion occurred within a few minutes for 17beta-HSD1 (see Chapter 3.1.4.1) the reaction time increased to several hours in case of 17beta-HSD12. In addition to the slow progression of this reaction all 17beta-HSDs 12 seem to have a rather low affinity for the substrate. Preliminary experiments suggest a sigmoidal shape of the curve with

low substrate concentrations being not reduced while with higher estrone concentrations progression of the reaction was observed (data not shown).

Another problem in investigating enzymatic activity of 17beta-HSD12 was the high amount of protein needed per reaction. As it would be cost prohibitive to produce enough protein for a full-fledged kinetic measurement (at least when using a mammalian expression system) only the select data presented here was measured.

3.3. Promiscuity in 17beta-HSD3: a new function specific to rodents

3.3.1. Preliminary experiments show a retinoid converting activity in rodent 17beta-HSD3

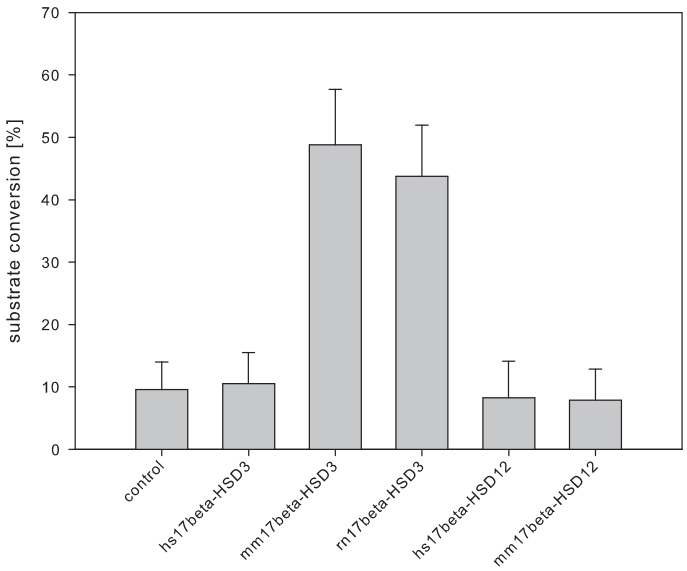

Figure 3.9.: Preliminary experiments to determine the retinoid converting abilities of 17beta-HSDs.
$5{\cdot}10^6$ cells transfected with respective plasmids (empty vector for control) were incubated with NADPH and all-trans retinal for 30 minutes. Measurements were performed in duplicate. Human = hs, mouse = mm, and rn= rat enzymes

Substrate screening experiments with 17beta-HSD3 were performed to learn more about the substrate spectrum of this enzyme. An ability to convert all-trans retinal to all-trans retinol was found in 17beta-HSD3 of rat and mouse (see Figure 3.9). Interestingly, this multifunctionality was not observed in human and zebrafish homologs (data not shown). Additionally, human and mouse 17beta-HSDs type 12 were investigated for

their all-trans retinal reducing activity. For these enzymes no difference to background conversion levels were observable.

3.3.2. Mutagenesis as a tool to investigate the origins of the retinoid converting activity

Multiple alignments of human, mouse and rat 17beta-HSD3 show a high sequence identity of 85 % between the two rodent homologs. The sequence identity of these two enzymes to human 17beta-HSD3 is lower (73 - 74 %). Based on this information a mutagenesis screen was started with the aim to identify the residues that allow for retinal conversion by the rodent enzymes. This screen was performed together with Evi Stahl [79] as part of her Bachelor's Thesis.

Several sequence motifs and singular amino acids have been found to be different between rodent and human 17beta-HSD3 (see Figure 3.10). In human 17beta-HSD3 these motifs were then replaced for the corresponding rodent sequences. Amino acid differences N-terminal to the cofactor binding region and the C-terminal signal sequences were not included in the mutagenesis screen as no influence of these residues on substrate specificity was expected.

3.3.3. Investigation of substrate conversion by 17beta-HSD3 mutants gives inconclusive results

Additional experiments were performed to better establish the relative substrate conversion potentials of human, rat, and mouse 17beta-HSD3. All-trans retinal reduction was monitored in a time-dependent manner yielding a different result compared to preliminary experiments (compare Figures 3.9 and 3.11A). Mouse 17beta-HSD3 showed a much higher potential to catalyze the conversion of all-trans retinal than its human and rat homologs. While an intermediate conversion rate was found for rat 17beta-HSD3, the human enzyme showed the lowest substrate conversion (preliminary experiments and later experiments suggest that this observed conversion is identical to the background conversion observed for mock-transfected cells).

Different mutants were assayed for their ability to reduce all-trans retinal to all-trans retinol (see Figures 3.11B). Judging from the available data the NLL137SFF, A207T, and EV219GI mutants of human 17beta-HSD3 seemed to have the biggest influence on substrate conversion rates. The maximum observed conversion was about 17 % for the EV219GI mutant compared to nearly 50 % conversion observed for mouse 17beta-HSD3 under similar conditions. Generally, the effects of these mutations were rather small so no single sequence motif was identified that had the potential to dramatically increase the all-trans retinal reduction ability of human 17beta-HSD3.

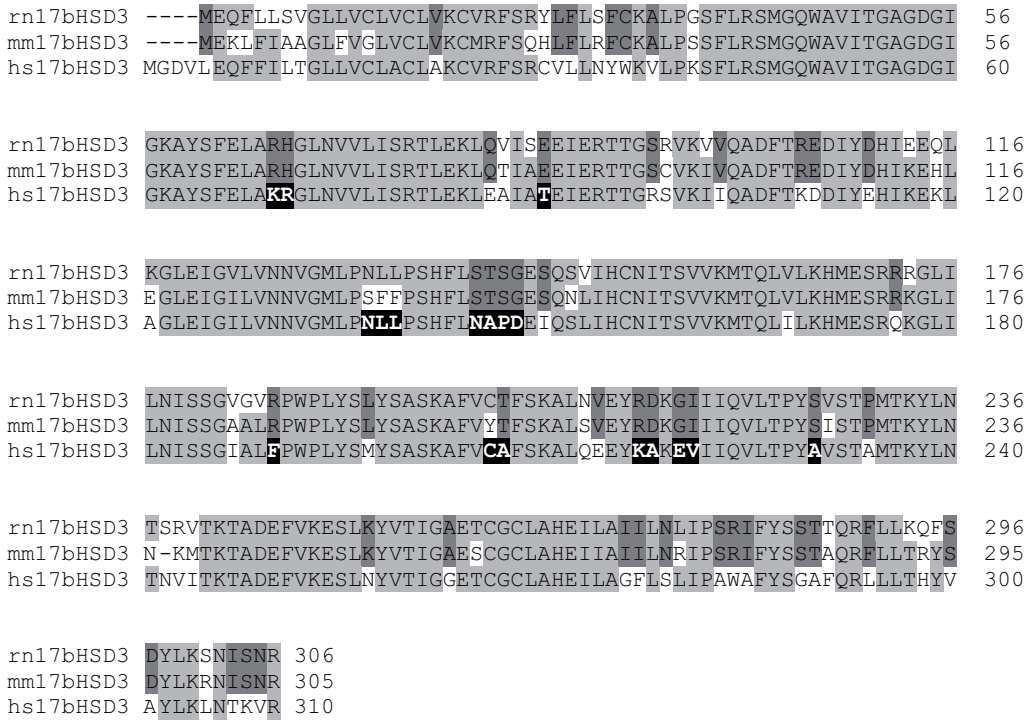

Figure 3.10.: Alignment of 17beta-HSD3 amino acid sequences from human, rat, and mouse.
Residues identical in all three sequences are shown in light grey, residues identical in the two rodent sequences are shown in dark grey, amino acids that were candidates for the insertion of mutations are shown in white on black background)

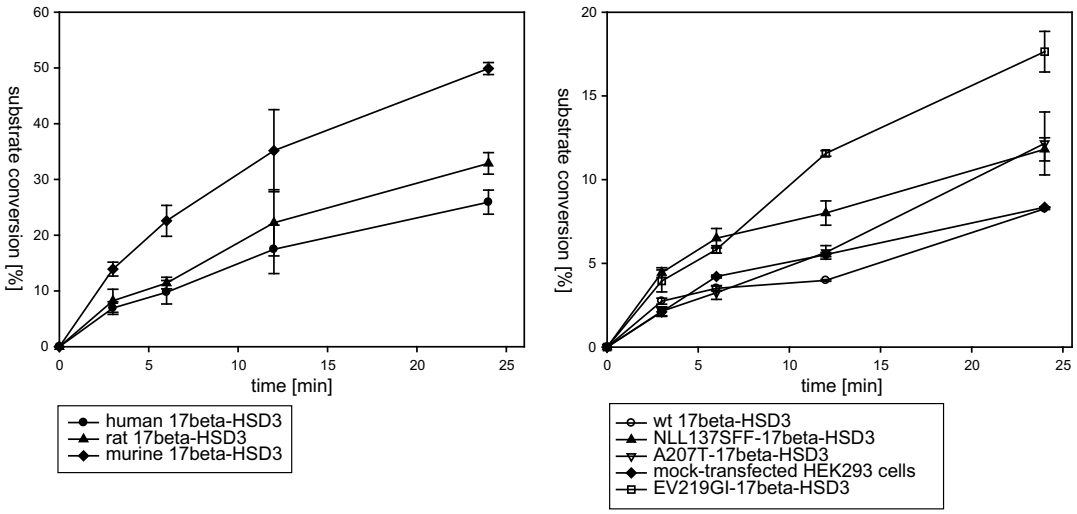

Figure 3.11.: Comparison of enzyme activity of 17beta-HSD3 from different organisms and different 17beta-HSD3 mutants.
Final concentrations of all-trans retinal were 3 μM. Cell lysates with a total protein amount of 50 μg per assay were used. (A) Comparison of human, rat, and murine 17beta-HSD3; (B) Comparison of human wild type 17beta-HSD3 with different mutants of human 17beta-HSD3.

3.3.4. Kinetics of murine 17beta-HSD3 reveal a potential substrate inhibition

Determination of kinetics in a concentration range of 0.5 to 32 μM showed an increase in initial reaction rates up to a substrate concentration of about 20 μM (see Figure 3.12A). Further increases in substrate concentration resulted in a decline in initial reaction rates indicative of substrate inhibition. In this case classical Michaelis-Menten kinetics are supplemented by a term that integrates an inhibitory constant K_i. Using this modified equation for a curve fit yielded values that showed huge variations. Despite a definitive substrate inhibition this phenomenon could not be accurately described by mathematical methods.

After repeating the experiments in a concentration range of 0.5 to 16 μM it was possible to calculate regular Michaelis-Menten kinetics (see Figure 3.12B). These showed a K_M of 10.7 μM and V_{max} of 0.0123 μmol/min/mg total protein). The variability in the values calculated from the data measured in the low concentration range were acceptable.

3.4. Development of a LC-MS/MS method to profile hormones in human and animal plasma

Steroid measurements in blood pose a challenging analytical problem as the concentrations of molecules that have such a high morphogenic potential are usually kept quite low in the body. Furthermore, many steroids are relatively non-polar substances, making

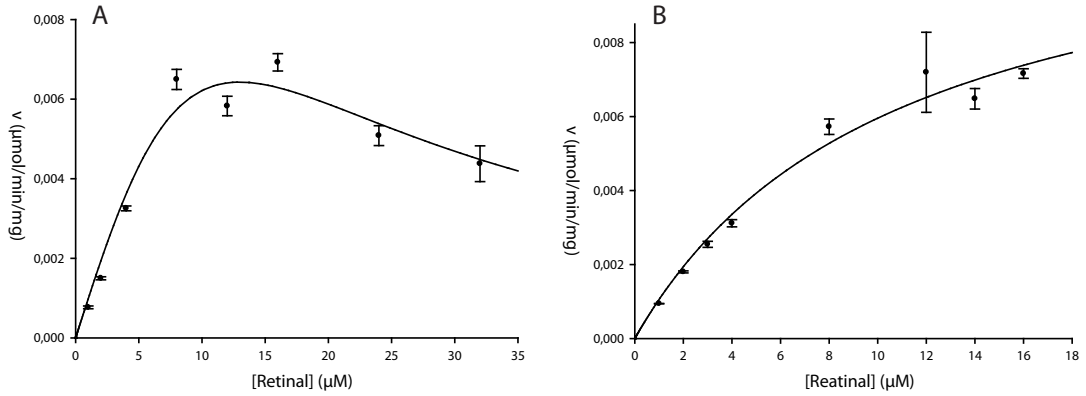

Figure 3.12.: Michaelis-Menten kintics of mouse 17beta-HSD3 using all-trans retinal as substrate (7 minutes incubation at 37 °C using 20 μg total protein).
(A) as a distinct substrate inhibition was visible for murine 17beta-HSD3 a non-linear fit of Michaelis-Menten kinetics including non-competitive substrate inhibition was used. (B) The experiment was repeated in a more narrow concentration range. After fitting using classical Michaelis-Menten the following parameters were calculated: K_M = 10.7 μM and V_{max} = 0.0123 μmol/min/mg total protein)

GC-MS the method of choice for their analysis. Despite several advantages of GC-MS in steroid analytics this method is extremely time-consuming and not applicable in high-throughput analyses. In this work an online-SPE-LC-MS/MS method for the analysis of steroids was developed, validated and used to measure studies in human and mouse plasma (see Chapters 3.4.8 and 3.4.9).

3.4.1. Determination of mass transitions for multiple reaction monitoring (MRM)

The goal in optimizing the ion optics parameters was to achieve the highest possible sensitivity in the analysis of the respective steroids. A further requirement was compatibility to upstream HPLC separations. Therefore optimizations were performed using solvents that were intended to be used in HPLC runs. Analytes were directly injected into the mass spectrometer using a syringe pump at a flow rate of 10 μL/s. The optimized ion optics parameters are listed in table 3.5.

3.4.2. Determination of parameters for the electrospray ion source

Optimization of ion source parameters is a compromise as the optimal settings for each analyte that is measured may be different. In this work the ion source parameters were chosen to have the highest possible sensitivity with the analytes that are most difficult to analyze while still retaining an acceptable sensitivity for other analytes in the mixture. First all parameters were optimized separately for each analyte using flow injection

Substance	Q1 mass	Q3 mass	DP	EP	CE	CXP
Androstenedione	287.2	97.2	81	10	35	6
Testosterone	289.2	97.2	81	10	33	6
Cortisone	361.2	163.2	76	10	33	10
Cortisol	363.2	121.1	86	10	33	6
Corticosterone	347.2	121.1	76	10	33	8
Progesterone	315.2	109.1	51	10	37	8
17OH-progesterone	331.2	97.1	50	10	41	6

Table 3.5.: Ion Optics Parameters of steroids.
Ion optics parameters were determined using the automatic compound optimization of the Analyst 1.4.2 software. Subsequently, a manual fine tuning of these parameters was performed to get the final values. DP = declustering potential, EP = entrance potential, CE = collision energy, CXP = cell exit potential.

analysis (FIA). In the next step all analytes were mixed and the parameters optimized to find a compromise in which all substances can be measured with the highest possible sensitivity. Optimized ion source parameters can be found in Table 3.6.

Parameter	Value
Curtain Gas (CUR)	20
Collision gas (CAD)	6
Ion spray voltage (IS)	4500
Source temperature (TEM)	600
Nebulizer gas (GS1)	40
Turbo gas (GS2)	55

Table 3.6.: Ion Source Parameters: Parameters were optimized to gain the highest sensitivity for 17-hydroxy progesterone while retaining sufficient sensitivity for the other analytes. The value for cutain gas was set to 20 to reduce contamination in Q1.

3.4.3. Development of a chromatographic method for the separation of steroids and coupling to online-SPE

High throughput analyses require a minimization of hands-on time for laboratory personnel while still maintaining a high reproducibility of analysis results. Extraction of analytes from a given matrix can be a time consuming task but is an important prerequisite for mass spectrometry. Modern HPLC systems allow for an automation of this step as enrichment on solid phase extraction (SPE) columns can be combined with high resolution separations on an analytical column by using switching valves. After precipitation of proteins from the plasma sample, it is applied to the SPE column using a high flow rate. For analysis of the sample the valve is switched and analytes are eluted in backflush from the online SPE column. After a separation step on the analytical column

(for steroid analysis an Allure Biphenyl column was used) the compounds are detected by tandem mass spectrometry.

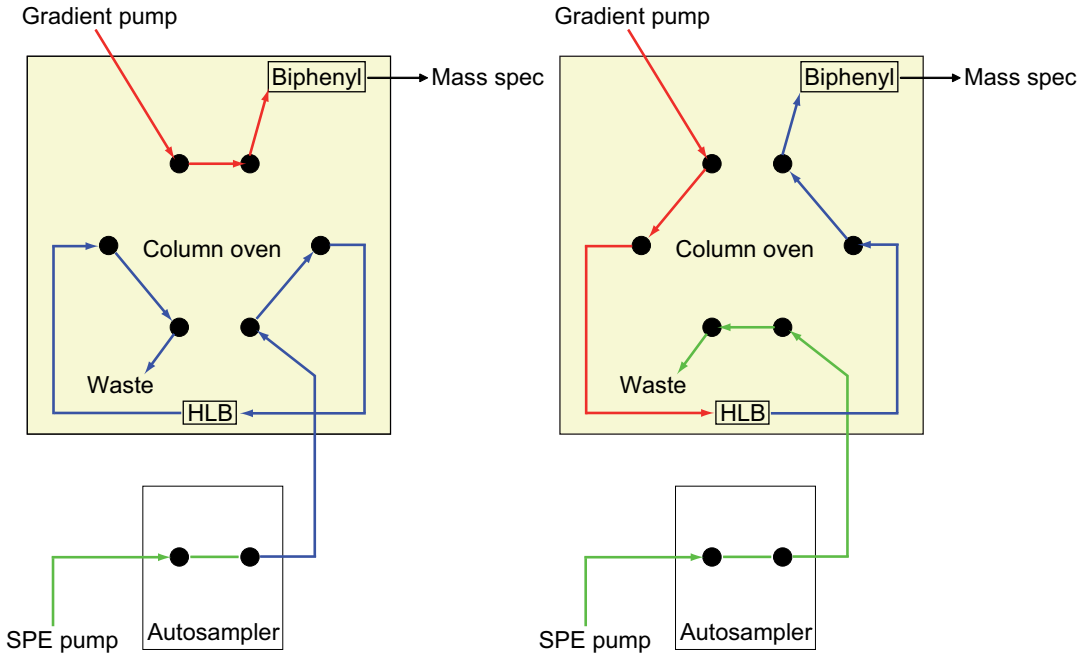

Figure 3.13.: Setup of the online SPE system.
Flow of the online SPE solvent is depicted in green, flow of the analytical gradient solvent is shown in red, flow containing the sample is shown in blue. (A) In the load position the sample is applied to the online SPE column, while the analytical column is flushed with the gradient solvent. (B) After switching to the inject position the online SPE solvent is diverted directly to the waste, while the sample is eluted in backflush from the online SPE column, applied to the analytical column and finally infused into the mass spectrometer.

In this work a system for the online-SPE of analytes was developed (for the setup of the online SPE system see Figure 3.13). The chromatographic conditions for enrichment and analytical separation had to be developed in concert. The parameters specifying the entire gradient run and valve switches can be found in Table 2.4.

3.4.4. Development of a method for the analysis of human plasma

3.4.4.1. Optimization of the online-SPE-LC-MS/MS method

In positive mode 7 different steroids (androstenedione, testosterone, cortisone, cortisol, corticosterone, progesterone, 17-hydroxy-progesterone) were readily measurable in human plasma (for a chromatogram see Figure 3.14). It was not possible to include the analysis of estrogens into this method as these steroids either need to be measured in negative mode or after derivatization.

Due to an update of the Analyst software during method development it was possible to implement scheduled MRMs (sMRMs) into the analysis methods. By using sMRMs it was possible to significantly increase the sensitivity of the analysis method.

3.4.4.2. Determination of selectivity

To have a sufficient selectivity a method needs to be able to simultaneously detect different substances without interfering with each other. In LC-MS/MS selectivity can be achieved in different ways: either by chromatographic separation of the substances of interest or by using different mass transitions. A chromatogram of a human plasma sample (see Figure 3.14) shows separation of the seven steroids investigated. In slightly overlapping peaks selectivity is ensured by using distinct mass transitions.

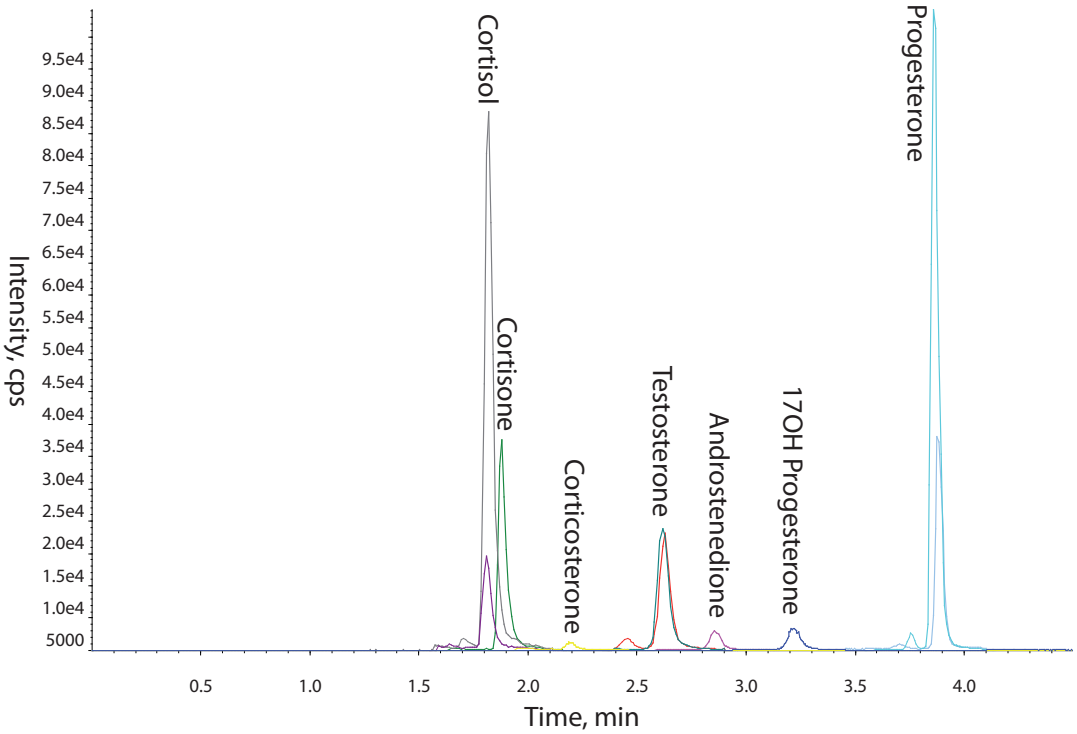

Figure 3.14.: Chromatogram of a human plasma sample.
Retention times were: 3.22 min for androstenedione, 2.62 min for testosterone, 1.88 min for cortisone, 1.82 min for cortisol, 2.18 min for corticosterone, 3.88 for progesterone, and 2.86 min for 17-hydroxy progesterone

3.4.4.3. Determination of linearity

For the determination of linearity a series of nine dilutions was prepared in triplicate. The linear ranges as well as the Pearson correlation coefficient of the linear regression are given in Table 3.7.

Analyte	Linear range	r	LOD	LOQ
Androstenedione	0.3 - 25 μg/L	0.9998	0.109 μg/L	0.296 μg/L
Testosterone	0.2 - 25 μg/L	0.9996	0.063 μg/L	0.155 μg/L
Cortisone	2 - 500 μg/L	0.9991	0.849 μg/L	2.004 μg/L
Cortisol	2 - 500 μg/L	0.9991	0.850 μg/L	2.003 μg/L
Corticosterone	0.8 - 25 μg/L	0.9999	0.287 μg/L	0.787 μg/L
Progesterone	0.3 - 25 μg/L	0.9995	0.044 μg/L	0.107 μg/L
17OH Progesterone	0.1 - 25 μg/L	0.9997	0.138 μg/L	0.293 μg/L

Table 3.7.: Linearity of the method and limits of detection and quantification in human plasma

3.4.4.4. Determination of limits of detection and quantification

The limit of detection (LOD) and limit of quantification (LOQ) were determined as described in Chapter 2.1.9.3. LODs and LOQs for the investigated steroids are depicted in Table 3.7.

3.4.4.5. Determination of intra-day, inter-day and intermediate variability

To determine these parameters a plasma sample was distributed to 15 different test tubes. To measure the intra-day variability 5 aliquots were immediately subjected to the sample preparation procedure. Coefficients of variation (CVs) were calculated and are presented in Table 3.8.

Analyte	intra-day CV	inter-day CV	intermediate CV
Androstenedione	4.65 %	4.38 %	5.11 %
Testosterone	3.92 %	4.34 %	4.18 %
Cortisone	1.54 %	4.79 %	7.09 %
Cortisol	3.74 %	3.97 %	5.62 %
Corticosterone	5.61 %	8.02 %	9.58 %
Progesterone	4.42 %	8.29 %	6.17 %
17OH Progesterone	4.24 %	3.17 %	5.97 %

Table 3.8.: Intra-day, inter-day and intermediate variability

For the determination of inter-day variability 5 samples was prepared and measured on the next day. CVs are also presented in Table 3.8.

For intermediate variability 5 samples were prepared by another experimentator (T. Halex). After measurement CVs were calculated and are also shown in Table 3.8.

3.4.4.6. Recovery

During the recovery experiments a strong matrix effect was observed. The isotonic sodium chloride solution that was used for initial experiments proved to be unsuitable

for these experiments. Instead 'steroid free' plasma was prepared (see Chapter 2.1.8.5) to have a matrix for comparison. This plasma was then used for the calculation of recovery using the following formula:

$$recovery = \frac{S1 - S2}{S3}$$

With S1 being the signal of normal plasma spiked with different amounts of steroid standards, S2 being normal plasma without spiking and S3 being steroid-free plasma spiked with the same amount of steroid standards as used for S1. Recovery was calculated using two different concentrations of spiking solutions (see Table 3.9).

Analyte	recovery conc. 1	recovery conc. 2
Androstenedione	93.79 %	86.84 %
Testosterone	97.61 %	89.55 %
Cortisone	91.65 %	86.62 %
Cortisol	91.42 %	92.75 %
Corticosterone	93.79 %	84.00 %
Progesterone	92.40 %	93.67 %
17OH Progesterone	80.30 %	83.45 %

Table 3.9.: Recovery of investigated steroids from human plasma. Calculated recovery after spiking with two different concentrations.

3.4.4.7. Optimization of the online-SPE-LC-MS/MS method for steroid analysis in murine plasma

The development of the mouse plasma analysis method posed a more difficult challenge. The sample volume had to be adjusted to a smaller amount and the high viscosity of the plasma complicated exact pipetting. Furthermore, several analytes had to be excluded from the analysis for various reasons:

a) In mouse plasma 11-dehydro-corticosterone is only present in small amounts. Measurement of this steroid is further complicated by a co-eluting peak (see Figure 3.15). To achieve a base-line separation of 11-dehydrocorticosterone and the interfering substance the gradient was flattened in this portion of the chromatogram. After these optimization steps the method was more than 15 minutes in length, which made it too long for the intended high-throughput format. For this reason this analyte was not included in the final method.

b) In female mouse plasma a prominent peak was observed for the mass transition 363.2 → 121.1 (see Figure 3.16). Although the MRM is the same as for cortisol, differences in retention times clearly showed that it is a distinct substance. As this substance was unknown, it was not included in the final method.

c) Another critical analyte that was investigated was progesterone. Between the internal standard d9-progesterone and the chromatogram for m/z 315.2 → 109.1 a slight discrepancy was observed: while d9-progesterone eluted at 3.55 minutes, the peak for m/z 315.2

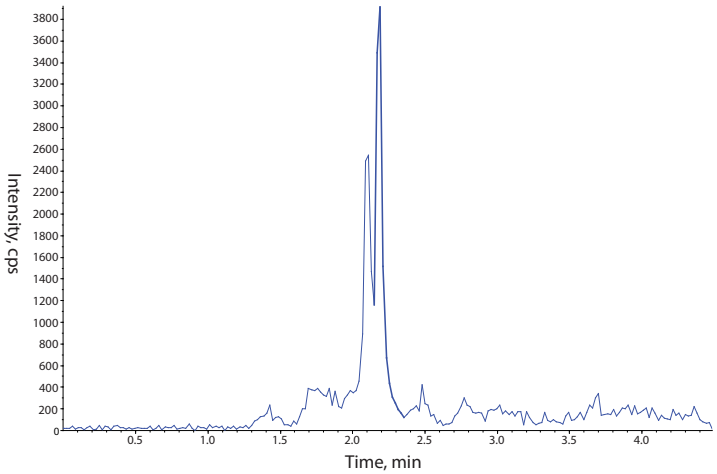

Figure 3.15.: Chromatogram of m/z 345.2 → 121.1.
11-dehyro-corticosterone eluted after 2.21 minutes, the interfering compound after 2.29 minutes. No baseline separation was achieved.

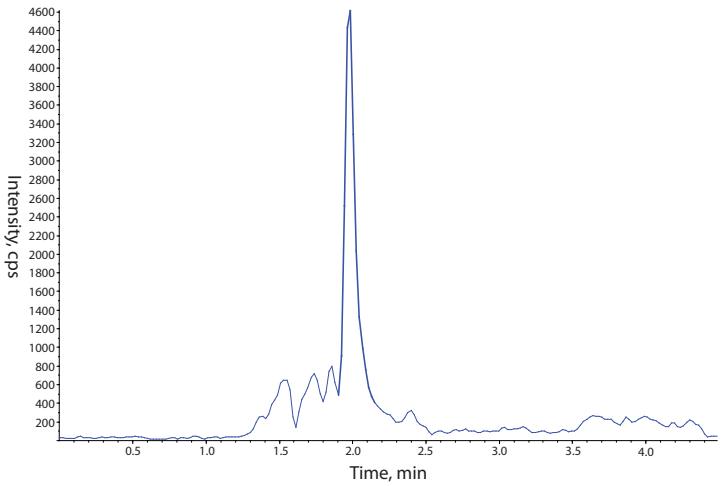

Figure 3.16.: Chromatogram of m/z 363.2 → 121.1.
An unknown substance elutes after 2.08 minutes. While the mass transition is identical to that of cortisol, it is distinguished from cortisol by its retention time.

→ 109.1 eluted at 3.59 minutes (see Figure 3.17). Slight differences in retention times are not unusual between different runs, but the differences were also observed when analyte and internal standard were measured in one run. As the substance seems to be similar to progesterone but obviously is not the same, this analyte was not included in the final method.

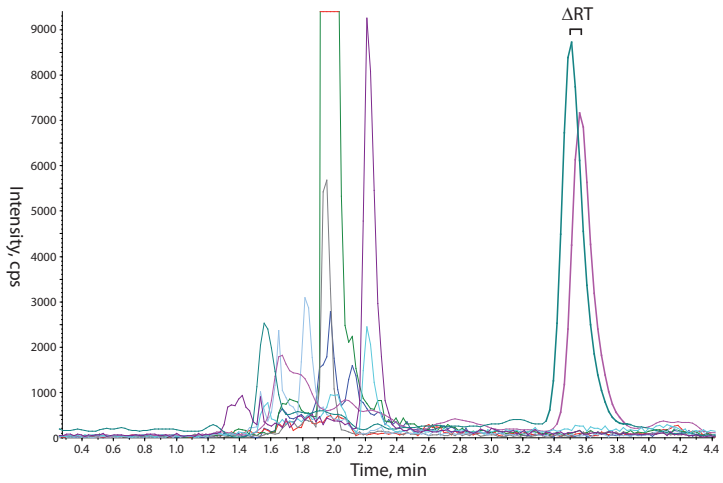

Figure 3.17.: Chromatogram of m/z 315.2 → 109.1 and d9-progesterone.
Progesterone and d9-progesterone (internal standard) elute after 3.55 minutes. The peak observed in this chromatogram is clearly different in retention time and therefore constitutes another substance.

The final method included three different steroids: androstenedione, testosterone, and corticosterone. Due to this very limited set of analytes the method was shortened to 3.5 minutes in total. Furthermore, the method was optimized to get a good separation between the steroids in order to fully benefit from the inclusion of scheduled MRMs.

3.4.5. Validation of a method for the analysis of steroids in mouse plasma

3.4.5.1. Selectivity

Selectivity in mouse plasma analysis was achieved like for human samples: all analytes need to be resolved independently. A chromatogram of a murine plasma sample (see Figure 3.18) shows separation of the three steroids investigated.

3.4.5.2. Linearity, limits of detection, and limits of quantification

For the determination of linearity a series of nine dilutions was prepared in triplicate. The linear ranges as well as the Pearson correlation coefficient of the linear regression are given in Table 3.10.

The limits of detection and quantification were determined as described for human plasma (see 3.4.4.4). Corresponding values for mouse plasma are shown in Table 3.10

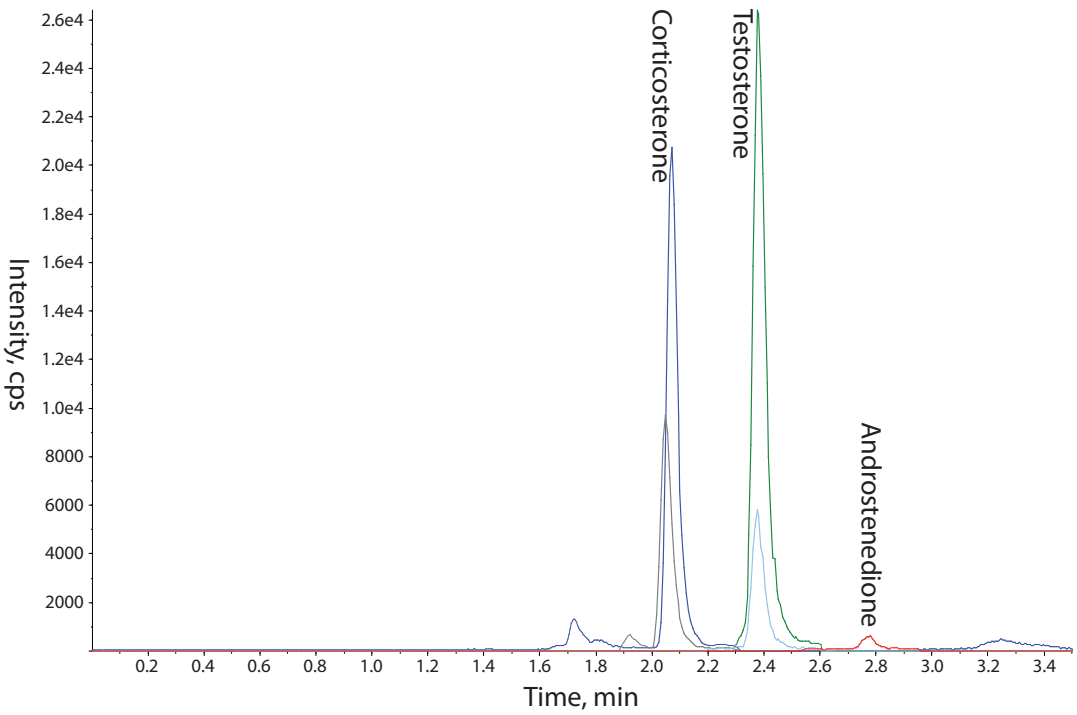

Figure 3.18.: Chromatogram of a murine plasma sample.
Retention times were: 2.78 min for androstenedione, 2.37 min for testosterone, and 2.08 min for corticosterone

Analyte	Linear range	r	LOD	LOQ
Androstenedione	0.1 - 25 μg/L	0.9998	0.008 μg/L	0.1 μg/L
Testosterone	0.1 - 25 μg/L	0.9996	0.045 μg/L	0.1 μg/L
Corticosterone	1 - 500 μg/L	0.9999	0.49 μg/L	1 μg/L

Table 3.10.: Linearity of the method and limits of detection and quantification in mouse plasma

3.4.5.3. Intra-day and inter-day variability

Intra-day and inter-day variabilities in mouse plasma were determined as was already described for human plasma. Intermediate variability was not measured for mouse plasma. Coefficients of variation (CVs) were calculated and are presented in Table 3.11.

Analyte	intra-day CV	inter-day CV
Androstenedione	8.79 %	7.06 %
Testosterone	7.66 %	6.59 %
Corticosterone	5.37 %	10.05 %

Table 3.11.: Intra-day and inter-day variability determined for mouse plasma

The observed coefficients of variation were acceptable with the possible exception of the inter-day variability of corticosterone. By omitting only one value (possibly an outlier) this could be reduced to below 10 %. The inter-day variability was therefore deemed acceptable.

3.4.5.4. Recovery

Recovery was determined as described for human plasma and also calculated by using two different concentrations of spiking solutions (see Table 3.12).

Analyte	recovery conc. 1	recovery conc. 2
Androstenedione	92.3 %	83.8 %
Testosterone	95.8 %	116.7 %
Corticosterone	99.9 %	101.4 %

Table 3.12.: Recovery of investigated steroids from mouse plasma. Calculated recovery after spiking with two different concentrations.

3.4.6. Expansion of the analyte portfolio of the LC-MS/MS method developed for steroid analysis

It was attempted to include the measurement of triiodothyronine (T3), thyroxine (T4) as well as the retinoids retinol and retinoic acid into the LC-MS/MS method for steroid analysis. The inclusion of these substances constitutes a major challenge for analysis as the analytes cover a rather broad range of the polarity spectrum. Especially retinoids are rather non-polar, while thyroid hormones as well as steroids are more polar molecules.

One challenge concerning the analysis of these molecules is detection. Preliminary experiments showed that the use of electrospray ionization did not yield optimal results. Therefore, atmospheric pressure chemical ionization (APCI) was used. Initial experiments using the protein precipitation method developed for steroids did not result in

sufficient recoveries of T3, T4 and retinoic acid. Only retinol gave a signal high enough to be amenable to quantification (see Figure 3.19A).

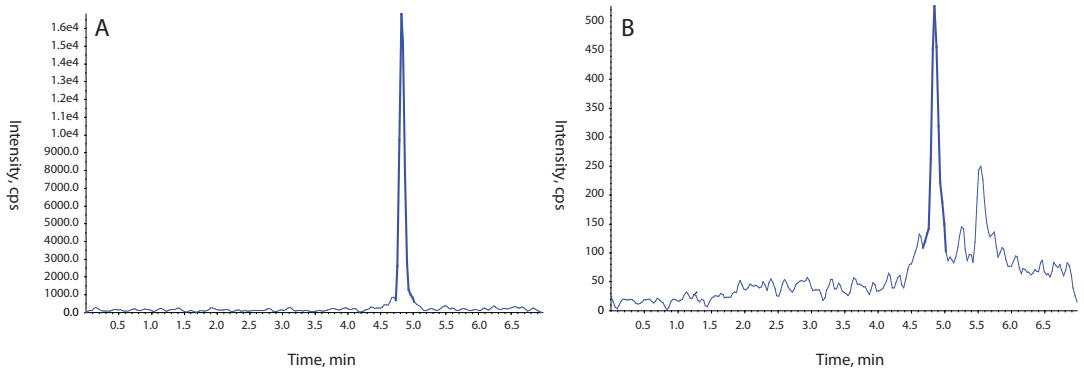

Figure 3.19.: Extracted ion chromatograms of a human plasma sample.
A) Chromatogram of all-trans retinol; B) chromatogram of retinoic acid

To investigate the influence of different protein precipitation solutions on the relative recoveries several different combinations of solvent mixtures were tested (see Figure 3.21). Unfortunately, no solution gave an acceptable extraction efficiency for all three of these analytes. Furthermore, even when the optimal protein precipitation solution for a respective analyte was used it often was not possible to detect signals above the limit of quantification (see Figures 3.19B as well as 3.20).

As simple protein precipitation was obviously not enough to quantify the analytes of interest, several experiments concerning the extraction of plasma were performed. For these experiments liquid-liquid extraction with different solvents was combined with reduction *in vacuo*. This procedure was not successful which may either be attributed to the choice of the wrong solvents or to decomposition of the analytes in the vacuum concentrator (the concentrator was running at temperatures well above 40 °C). It was not possible to further optimize this method due to time constraints.

3.4.7. Development of a method to measure CoA conjugated fatty acids in *in vitro* enzyme assays

Acyl-CoAs are intermediates of fatty acid metabolism. One of the aims in this work was to monitor the conversion of 3-ketopalmitoyl-CoA to 3-hydroxypalmitoyl-CoA catalyzed

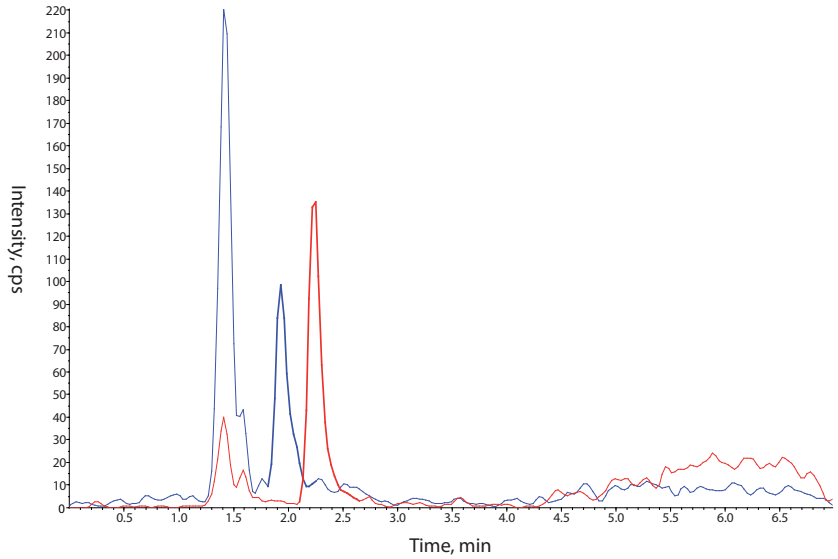

Figure 3.20.: Extracted ion chromatograms of a human plasma sample.
While the peak for thyroxine (red) is high enough to be slightly above a S/N ratio of 10 and is therefore amenable for quantification, the peak for triiodothyronine (blue) is below this limit.

by the enzyme 17beta-HSD12. As 3-ketopalmitoyl-CoA is not commercially available, this molecule had to be synthesized (cooperation with S. Gobec). Ion optics parameters were determined (see Chapter 2.1.8.6) and a LC-MS/MS method was set-up. The method included an online-SPE on an Oasis HLB column using a mixture of formic acid in water and acetonitrile. For the analytical separation a pH-stable C18 column was used with a gradient of ammonium hydroxide and acetonitrile. During chromatography on the C18 column the SPE column was flushed with a mixture of ammonium hydroxide and acetonitrile to ensure complete conditioning of the SPE column.

Using this method it was possible to measure 3-ketopalmitoyl-CoA in a concentration of 10 μM (see Figure 3.22) in phosphate buffer. The product of the reaction of interest, 3-hydroxypalmitoyl-CoA, was neiter available from the cooperation partner nor commercially. The ion optics parameters were therefore infered from the parameters determined for 3-ketopalmitoyl-CoA. To test whether 3-hydroxypalmitoyl-CoA can be synthesized in the reaction catalyzed by 17beta-HSD12, lysates of cells that overexpressed this enzyme were incubated with the substrate. Unfortunately, even short incubation times lead to a rapid degradation of the substrate. Furthermore, it was not possible to detect any specific conversion of substrate to product. Despite the rapid degradation of the product it was attempted to optimize the chromatographic conditions to effect a separation of the 3-keto-substrate from the 3-hydroxy-product.

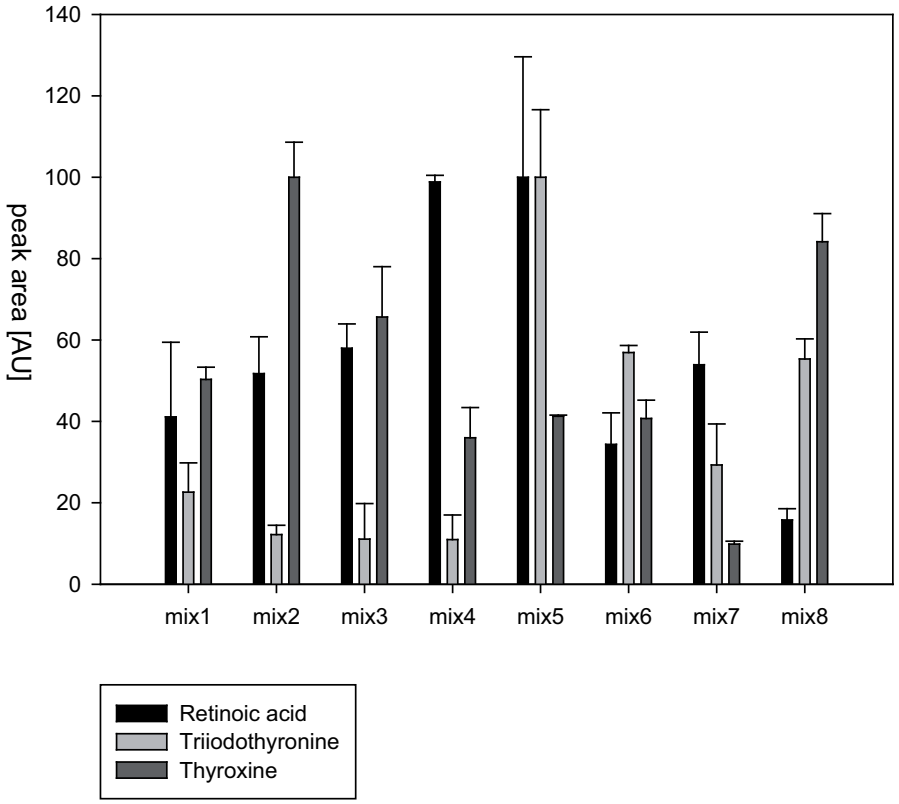

Figure 3.21.: Optimization of protein precipitation solution for retinoic acid, T3, and T4.
Mix 1 = $ZnSO_4$:ACN (1:3); mix 2 = $ZnSO_4$:MeOH:ACN (1:3:4); mix 3 = $ZnSO_4$:MeOH:ACN (1:1:4); mix 4 = $ZnSO_4$:MeOH:ACN (1:1:2); mix 5 = $ZnSO_4$:ACN (1:1); mix 6 = $ZnSO_4$:ACN (3:1); mix 7 = $ZnSO_4$:MeOH:ACN (2:1:1); mix 8 = $ZnSO_4$:MeOH:ACN (3:1:1)

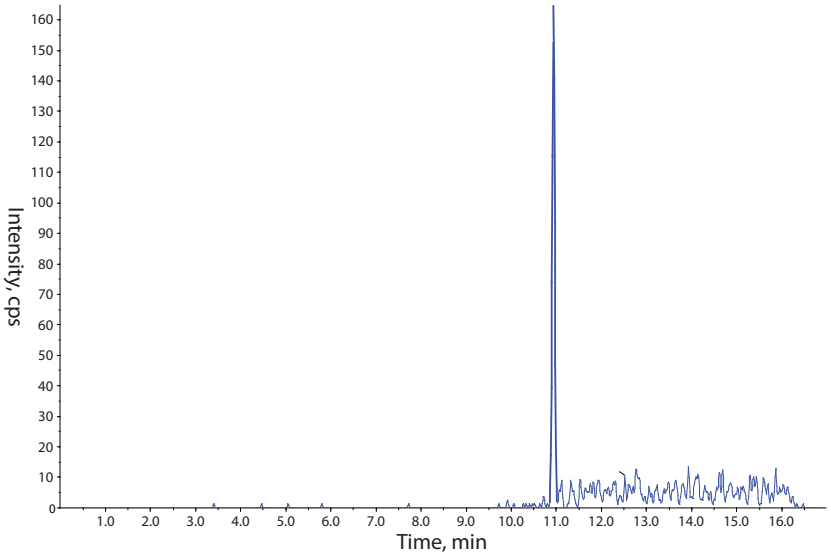

Figure 3.22.: Chromatogram of 3keto-palmitoyl-CoA.
Retention time was 10.91 min for 3-ketopalmitoyl-CoA.

3.4.8. Feasibility study to establish steroid reference values in mouse plasma

The aim of this study was to show that the method developed for the analysis of steroids in mouse plasma can be routinely applied to a large set of samples. Blood samples of three different mouse strains were taken at four different time points (roughly every 4 - 7 weeks), plasma was isolated, and steroid concentrations were measured. Generally, corticosterone was detectable in all strains and genders in easily quantifiable amounts. Testosterone could, with very few exceptions, only be measured in male mice. Androstenedione was not detectable in a reliable manner: in all strains some mice showed quantifiable androstenedione concentrations while others did not. Consequently, a considerable amount of data points was missing for this steroid and the results are not shown in this work.

Generally, the three different mouse strains investigated had very different levels of corticosterone. While C3H-HeB-FeJ mice showed relatively high concentrations in the range of 100 to 200 ng/mL (some mice had even higher concentrations), the concentrations in Bl6J and Balb-cJ strains were lower (around 100 ng/mL and 50 ng/mL respectively; see Figure 3.23)

A more detailed analysis of corticosterone concentrations in these mouse strains revealed remarkable differences between male and female mice as well as age dependent differences in the levels of this steroid. In C3H-HeB-FeJ mice corticosterone levels are lower in males at all ages (see Figure 3.24). Especially young females of this strain show a large margin of deviation with an extremely high median concentration of about 400 ng/mL. For older mice the concentrations show much lower variations and corticosterone

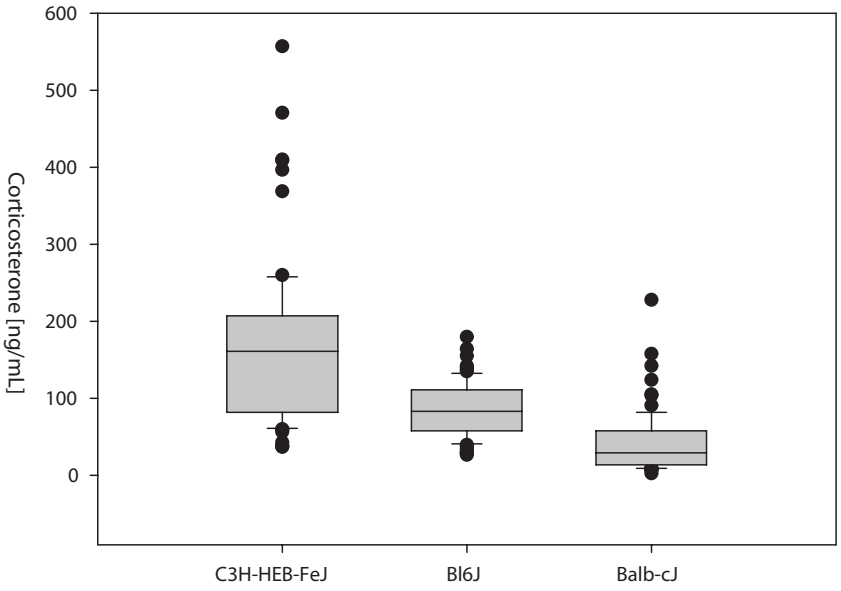

Figure 3.23.: Concentrations of corticosterone in the mouse strains C3H-HeB-FeJ, Bl6J, and Balb-cJ.
Concentrations were measured by LC-MS/MS and all measurements were included in one box plot per strain.

concentrations in males and females are much more similar.

In Bl6J mice the variability of the concentrations measured is much lower (see Figure 3.25). But also for this strain a clear sexual dimorphism can be observed: female mice generally show a higher corticosterone concentration in all age groups (ranging from 80 - 120 ng/mL for females and 40 - 90 ng/mL for male mice). Age did not seem to have a significant influence on corticosterone concentrations.

Blood sampling for the Balb-cJ strain was performed at a much later time point compared to the other two strains. For some time points this resulted in a relatively high variability while at other time points the variability was exceptionally low. For theses mice no remarkable sex differences were observed (see Figure 3.26). Furthermore, corticosterone concentrations did not vary significantly with age.

3.4.9. Measurement of steroids in fasting human subjects (Ramadan study)

Blood samples of fasting male human subjects were taken during and after the month of Ramadan. Samples were taken before (timepoints 1 and 3) and after dinner (timepoints 2 and 4). While samples 1 and 2 were taken in the beginning of the fasting month, samples 3 and 4 were taken two weeks into the month of Ramadan. Samples for time point 5 were taken after the end of the fasting month. Plasma concentrations of steroids were measured with the method described in Chapter 2.1.8.3. The concentrations measured for corticosterone were below LOQ for a considerable number of subjects and those

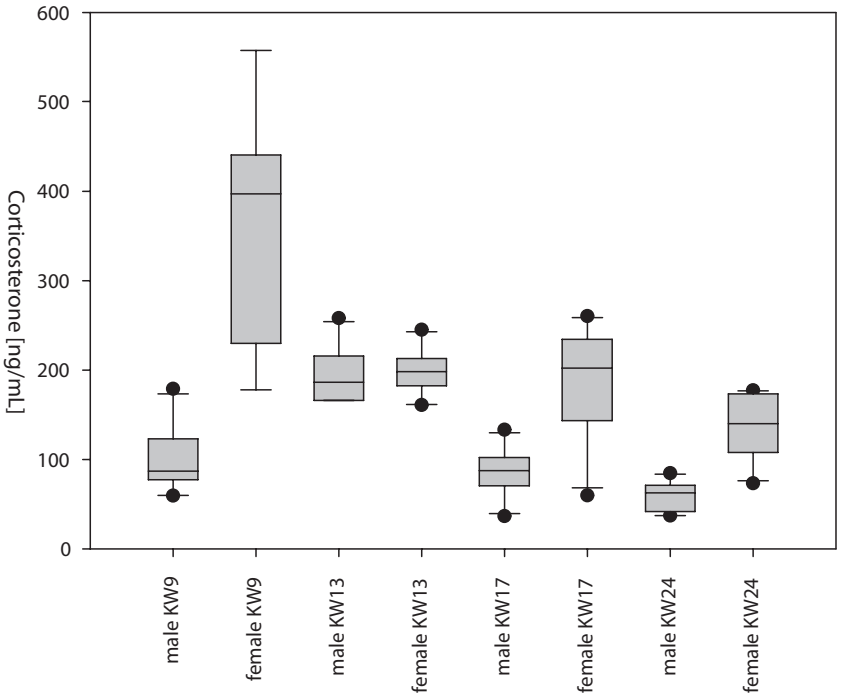

Figure 3.24.: Concentrations of corticosterone in the mouse strain C3H-HeB-FeJ. Concentrations were measured by LC-MS/MS and are shown at different time points separated by sex.

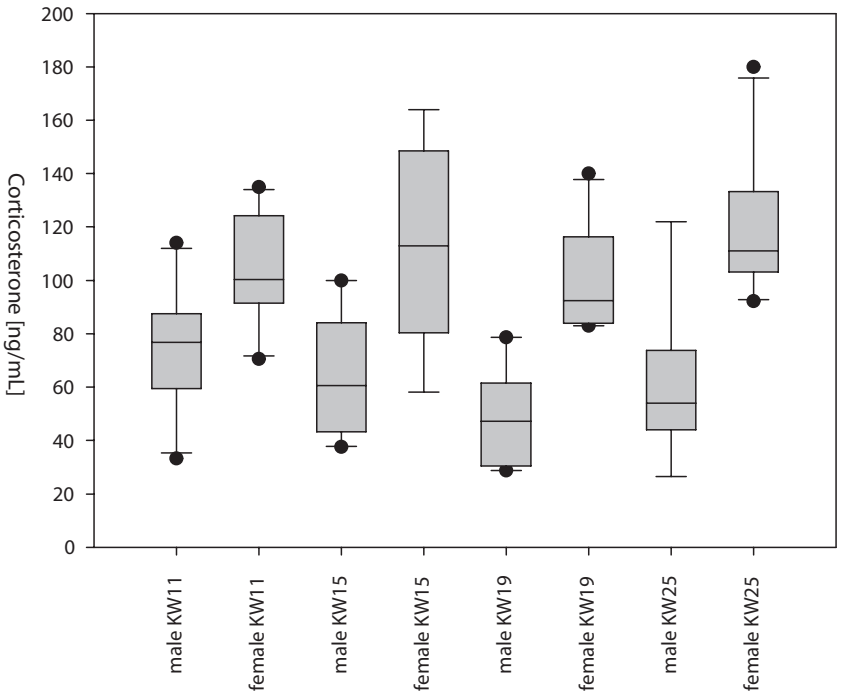

Figure 3.25.: Concentrations of corticosterone in the mouse strain Bl6J. Concentrations were measured by LC-MS/MS and are shown at different time points separated by sex.

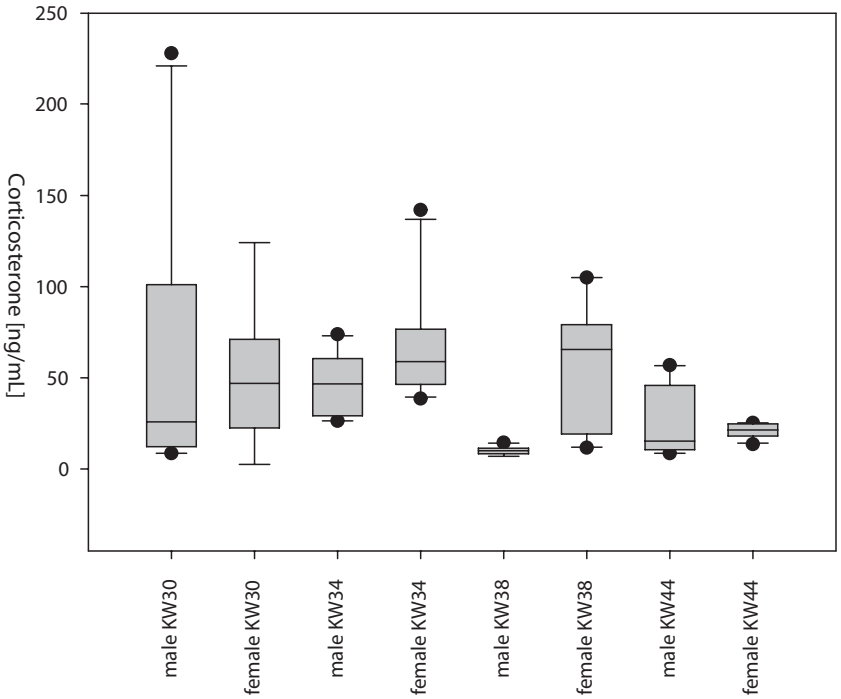

Figure 3.26.: Concentrations of corticosterone in the mouse strain Balb-cJ. Concentrations were measured by LC-MS/MS and are shown at different time points separated by sex.

results are therefore not shown.

Generally the variation in steroid concentrations between the subjects was considerable. As these concentrations were only measured in ten subjects and several data points were missing (not all subjects were available for sampling at the different timepoints) no significant differences were observed. Nevertheless, a few notable tendencies became apparent.

Androstenedione concentrations were lower before dinner on a fasting day but seemed to rise after food intake. This tendency was replicated at the later timepoint. When the subjects were not fasting the androstenedione level is as high as for the samples measured after ingestion. Similar results were obtained for progesterone and cortisone. For cortisone the differences between steroid concentrations before and after dinner were the most pronounced. In case of 17-hydroxy-progesterone, the levels also seem to be higher after ingestion but concentrations of this steroid were higher after the end of the fasting period. The levels of testosterone and cortisol only increased from timepoint 1 to timepoint 2, while the concentrations remained roughly at the same level when comparing timepoint 3 and 4.

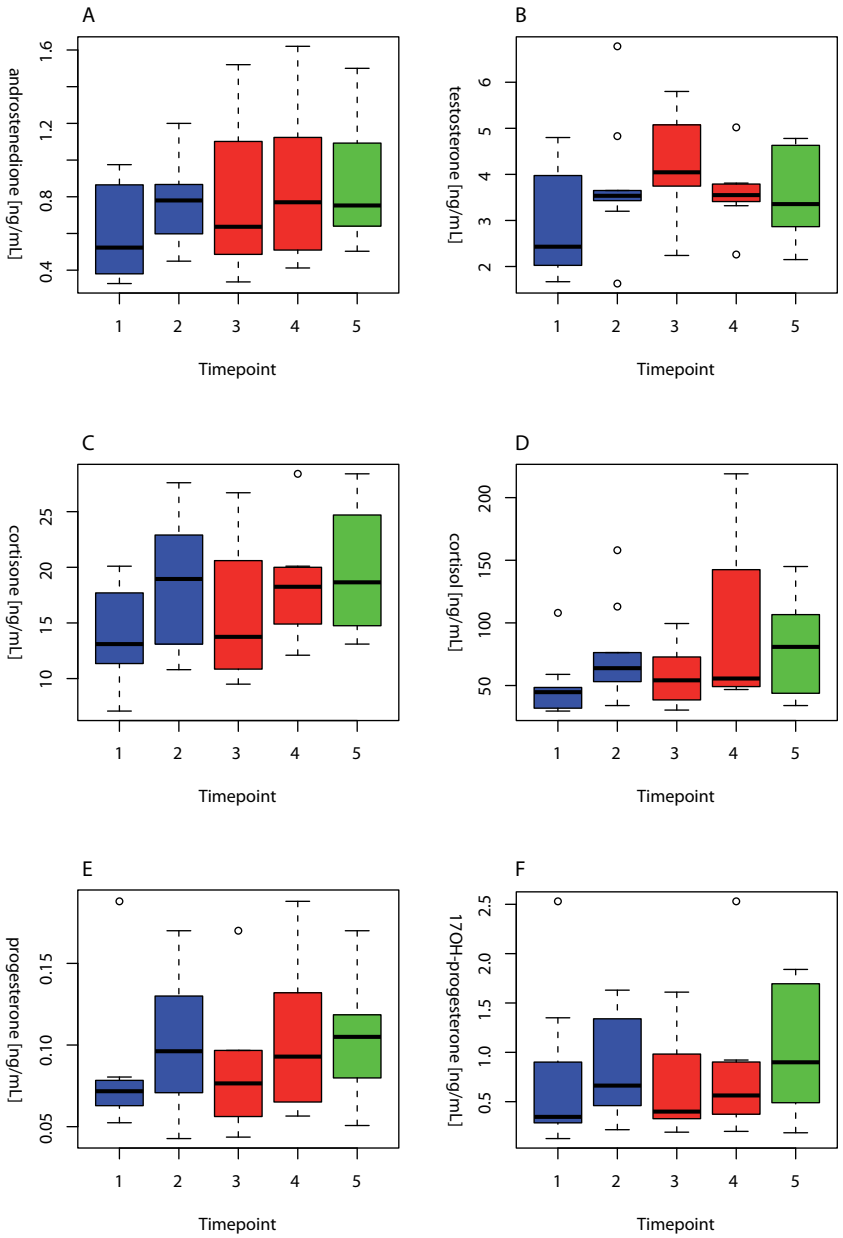

Figure 3.27.: Concentrations of of steroids in fasting human subjects.
Concentrations were measured by LC-MS/MS and are shown at different time points: samples for timepoints 1 and 3 were taken in the evening after a day of fasting but before dinner; samples for timepoint 2 and 4 were taken on the same day but after dinner; samples for timepoints 3 and 4 were taken two weeks after those taken for timepoints 1 and 2; samples for timepoint 5 were taken during a time in which the subjects did not fast; concentrations of A) androstenedione, B) testosterone, C) cortisone, D) cortisol, E) progesterone, and F) 17OH-progesterone are shown in ng/mL

4. Discussion

The analysis of substrate preferences of 17beta-HSDs has an impact on translational research. For many steroid-related disorders like prostate cancer or osteoporosis, 17beta-HSDs are target molecules for future therapies. A copious knowledge of substrates that are accepted by these enzymes may be important in the development of new drugs as well as for investigating adverse effects of drugs already used in treatment of steroid-related diseases.

4.1. New insights into 17beta-HSD1 functionality

4.1.1. A single amino acid has a major influence on the substrate specificities of 17beta-HSD1 and prRDH

To assess possible differences between 17beta-HSD1 and prRDH mutants when compared to their respective wild types, the kinetic parameters of these enzymes were measured. For a better comparability of the kinetic data the enzymes were normalized by quantitative infrared fluorescence Western blotting after expression in cell culture. Particularly an enzyme specific amino acid is of great interest when comparing the kinetics data. While 17beta-HSD1 has a glycine residue in this position, prRDH contains a methionine. In the course of this work the tremendous influence of these conserved amino acids could be shown: Amino acid exchanges between the two functionally different enzymes altered their substrate specificities. After exchanging the glycine to methionine in human 17beta-HSD1 a loss of catalytic efficiency for both substrates was observed. Initially, this exchange was expected to enhance the enzyme's potential for all-trans retinal reduction as the Gly to Met mutation makes the 17beta-HSD1 more similar to prRDH. Molecular modeling studies pinpointed to the reason for this observation: the bulky methionine cannot be inserted into the active site in an extended conformation. The insertion of this amino acid forces surrounding residues, including the catalytic tyrosine, to adopt different conformations to make room for the methionine. For the mutant of zebrafish 17beta-HSD1 the expected increase in the catalytic efficiency of all-trans retinal reduction could be detected. In the zebrafish enzyme the residues in vicinity of the inserted methionine are less bulky when compared to human 17beta-HSD1. Therefore, the Gly143Met mutation can more easily be accommodated.

In the prRDH enzymes (human prRDH and zebrafish prRDH1 and prRDH2) the rather large methionine was exchanged for the smallest amino acid, glycine. In models of prRDH enzymes two amino acids can be seen that form a 'clamp' that breaks the planarity of the conjugated system of all-trans retinal. This distortion may be instrumental

in the catalysis of retinal reduction as it has the potential to lower the energy barrier for this reaction. A similar catalytic strategy has already been described for the binding of retinal to bacteriorhodopsin [80]. Upon insertion of the Met to Gly mutation the 'clamp' would be loosened, therefore reducing catalytic efficiency. This prediction was impressively confirmed by kinetics data as the amino acid exchange indeed decreased the catalytic efficiency for retinal reduction in all three prRDHs.

But not only the reduction of all-trans retinal was investigated. All candidate enzymes were also assayed using estrone as substrate. It has already been mentioned that the methionine did not readily fit into the active site of the human 17beta-HSD1 mutant. Modeling showed that the C18 methyl group of estrone clashes with the methionine in this mutant. Obviously this steric hinderance prevents the steroid to bind in a catalytically favorable pose, which is reflected in the dramatic decrease of catalytic efficiency for estrone. For zebrafish 17beta-HSD1 the same effect could be observed: the active site is distorted in a way that impairs substrate binding and therefore decreases catalytical efficiency.

A gain of function was observed in prRDH mutant enzymes when estrone was used as substrate: while the wild type enzymes did not catalyze the conversion of estrone to estradiol, the Met to Gly mutants catalyzed the reduction of this steroid. The V_{max} value observed for human prRDH was quite low and only non-saturable kinetics were measurable for zebrafish prRDH1 and prRDH2. Nevertheless, these results highlight the importance of this residue for substrate specificity. Molecular modeling showed that estrone can bind to these enzymes in a pose that is similar (with a small shift) to that observed in 17beta-HSD1.

Jensen proposed that today's enzymes evolved from primitive more multifunctional enzymes [3]. Further research revealed that enzyme promiscuity may even be a crucial driving force of protein evolution [4, 5, 6, 81]. In a changing environment an organism needs to rapidly adapt to new challenges. On a molecular level this translates into gaining new functionalities by inserting a minimum number of mutations. In this work, a single amino acid exchange had a very significant effect on substrate specificity, an observation that is relatively rare, but not unheard of. For example, Jez and Penning converted a 5beta-reductase into a 3alpha-HSD by exchanging a single highly conserved amino acid [82].

Although the mutations inserted in 17beta-HSD1 and prRDH had a significant effect on substrate specificity, protein models showed that several other amino acid exchanges would be necessary to turn a prRDH into an effective 17beta-HSD. Especially the part of the active site that interacts with the C3-hydroxy group of estrone would have to be altered to accommodate this functional group. While 17beta-HSD1 integrates the hydroxy group into a hydrogen-bond network, prRDHs possess lipophilic residues in this area that only poorly interact with the hydroxy group. This is consistent with existing theories of protein evolution that state that an enzyme needs to be 'generalized' before 'specializing' to perform a new reaction [4].

Of course this raises the question in which order the investigated proteins evolved. As multifunctionality seems to precede specialization, the common ancestor of 17beta-HSD1 and prRDH was most likely closer to 17beta-HSD1, containing a glycine in the inves-

tigated position and catalyzing the conversion of both, steroids and retinoids. There is no functional information on 17beta-HSD1 or prRDH homologs from evolutionarily older species, but in *Nematostella vectensis* two highly similar sequences have been reported [83]. One contains a glycine (XP001637773.1) and the other one a leucine (XP001634839.1) in the respective position. In the genome of *Strongylocentrotus purpuratus* more than a dozen related proteins can be found. Of those, three contain a glycine and one of them a methionine in this position. But although the methionine/glycine residue obviously distinguishes prRDH from 17beta-HSD1, these amino acids occur as well in the respective position in other closely related but functionally dissimilar enzymes. Therefore, the determination of substrate specificity of more distantly related homologs would be necessary to clearly establish the evolutionary development of steroid/retinoid discrimination in these enzymes.

An interesting observation about 17beta-HSD1 was its ability to accept substrates of very different structure. Especially in comparison to other multifunctional enzymes that mostly accept only one class of substrates this is quite unusual. Several members of the SDR protein superfamiliy have also been shown to catalyze the reactions of steroids and retinoids. The RoDH-like group of SDRs [26] such as RoDH1 [84, 85], RoDH4 [86, 87], RDH5 [88], CRAD1 [89], and CRAD2 [90] have been described to convert not only retinoids but also steroids. What is special about 17beta-HSD1 is the direction of the catalyzed reaction: while all members of the RoDH-like group are oxidative enzymes, 17beta-HSD1 is a reductive enzyme. Furthermore, RoDH-like enzymes accept only androgens as steroid substrates, while 17beta-HSD1 is the only known SDR enzyme to accept retinoids as well as estrogens.

4.1.2. Physiological implications of novel human 17beta-HSD1 properties

17beta-HSD1 was the first 17beta-HSD to be discovered and therefore probably the best characterized member of this group. The discovery of a new functionality in this enzyme was quite surprising and may have implications for human and animal physiology that were not thought of before.

Several knock-out mice have been produced to gain an insight into the role of different retinol dehydrogenases in the conversion of all-trans retinal to all-trans retinol in the retina. Although various combinations of knock-outs were generated none of these mouse lines showed a loss of eyesight [22, 23, 24].

Tissue expression analysis suggests that 17beta-HSD1 is also present in the eye. Therefore, it might be one of the so far unidentified enzymes that harbor a reductive activity towards all-trans retinal. As such it may be able to rescue the loss of any of the specialized retinol dehydrogenases involved in vision. Furthermore, the wide-spread expression of 17beta-HSD1 could hint at a cross-talk between retinoid and steroid pathways, a possibility that warrants further research. However, it certainly cannot be ruled out that the observed *in vitro* activity constitutes an evolutionary remnant that has no significance *in vivo*.

4.1.3. Importance of steroid / retinoid discrimination in drug development

In addition to characterizing potentially new physiological functions of 17beta-HSD1 the effects of a selective inhibitor of 17beta-HSD1 were investigated [48]. These inhibitor studies showed that 2-phenethyl-D-homo-estrone was effective in inhibiting the reduction of estrone. This was not only observed in the human enzyme for which the inhibitor was developed but also for the zebrafish homolog. The influence of the Gly to Met mutations on the effectiveness of the inhibitors was very consistent. In human 17beta-HSD1 the affinity (i.e. K_M) was very similar for wild type and mutant. In concert also the observed IC_{50} values did not differ significantly. In contrast K_M values for zebrafish wild type and mutant differed by the factor of 10. For their IC_{50} values the differences were up to the factor 100.

Interestingly, the inhibition of all-trans retinal reduction was nowhere near as effective. This may be, at least in part, explained by the concentration ranges in which the inhibitors were tested. Another possible explanation for this observation could be that the binding mode of all-trans retinal differs very much from that of 2-phenethyl-D-homo-estrone. Nevertheless, the high affinity of the inhibitor to the enzyme should theoretically result in the observation of a much more effective inhibition.

When comparing the inhibitory effects (assuming competitive inhibition) of 2-phenethyl-D-homo-estrone on 17beta-HSDs 1 and prRDHs a rather unexpected pattern can be observed. As the Met to Gly mutation should make prRDHs more similar to 17beta-HSD1 a better inhibition of these mutants might have been expected. In reality only zebrafish prRDH2M showed this behavior (i.e. a decrease in IC_{50}), while for zebrafish prRDH1 and human prRDH an opposite effect was observed (the IC_{50} values even increased). This discrepancy suggests that the binding of the inhibitor to the enzyme is governed by more than just the investigated amino acid. For the 17beta-HSD1 enzymes and their respective mutants the effects of the inhibitor are much easier to explain. Insertion of the Gly to Met mutation in human 17beta-HSD1 dramatically increased the IC_{50} value as the active site is disturbed by this amino acid exchange and hence the inhibitor is not readily bound any more. In zebrafish 17beta-HSD1 the IC_{50} values are not affected by the mutation. This may be explained by the much more flexible amino acids surrounding the inserted methionine. The binding of the inhibitor is therefore not impaired as much as seen in human 17beta-HSD1.

On a more general perspective it can be stated that the investigated inhibitor has a very good selectivity. It is quite obvious that this substance inhibits prRDHs (which are the most closely related enzymes) only in very high concentrations and treatment with this compounds probably will not cause adverse effects in the human eye. At the same time it binds to 17beta-HSD1 with very high affinity. But as 2-phenethyl-D-homo-estrone is not the only compound that may be used for cancer treatment (a variety of different inhibitors have been developed [91, 92]) it may be necessary to also test other inhibitors for their cross-reactivity with prRDHs. Another point to be thought about in inhibitor development is the possible involvement of 17beta-HSD1 in metabolic pathways apart from steroid metabolism. Therefore, inhibitors targeting this enzyme

may have adverse effects that have not been considered yet. Potential adverse effects observed during clinical testing of these substance may be attributable to impaired retinoid metabolism, requiring an according adjustment of therapeutic strategies.

4.1.4. Conclusion

The enzymes 17beta-HSD1 and prRDH were analyzed to gain insights into their ability to catalyze the conversion of estrone and all-trans retinal. An amino acid important for steroid/retinoid discrimination was identified and its significance was highlighted by results from molecular modeling studies done in collaboration with Saarland University. The substrate promiscuity observed for 17beta-HSD1 does not only illustrate the functioning of an important evolutionary mechanism, but (especially in the light of its wide-spread basal expression) may represent a new physiological function for this enzyme that may also be important in drug development.

4.2. Multifunctionality in 17beta-HSD12: steroid or fatty acid metabolism

Concerning the primary function of 17beta-HSD12 there has been a long debate in the scientific community. In recent year evidence for a major role of this enzyme in fatty acid metabolism has been building up. As all approaches up to now were not directly focused on clarifying this issue, the work at hand was intended to provide some definitive answers.

4.2.1. An evolutionary approach to investigate 17beta-HSD function

For the functional characterization of 17beta-HSD12 a rather unique approach was used as several invertebrate enzymes were included in the study. The invertebrates from which the enzymes were derived represent the three closest evolutionary relatives of vertebrates: tunicates, cephalochordates, and echinoderms [93, 94]. In this work it was of major interest to see whether these enzymes were capable of catalyzing the conversion of steroids and fatty acids, and if so to get an impression about the importance of 17beta-HSD12 in steroid and fatty acid metabolism. Furthermore, the investigation of the emergence of steroid metabolism in invertebrates may help us to better understand the evolution of the endocrine system.

A major challenge in finding candidates for 17beta-HSD12 homologs in such distantly related species is the relatively low sequence identity among the enzymes. This problem becomes very obvious when examining the phylogenetic tree for 17beta-HSD12 (see Figure 3.5). Only low to mid range bootstrap values support the phylogeny depicted here, necessitating functional proof for these enzymes' classification as 17beta-HSD12.

4.2.2. The defining characteristics of a ketoacyl reductase: does 17beta-HSD12 meet them?

The defining property of a ketoacyl reductase is certainly its substrate specificity. But aside from that other information may be necessary to make a definitive statement. In this respect interaction partners may give helpful hints at an enzyme's function. Seemingly (although it could not be shown conclusively as mentioned in Chapter 3.2.3) human 17beta-HSD12 interacts with TER (2,3-transenoyl reductase) and ELOVL4 (elongation of very long chain fatty acids 4) a situation that closely resembles that seen in yeast [78]. In *S. cerevisiae* the 17beta-HSD12 homolog YBR159p interacts with Elo3p (an elongase) and Tsc13p (a transenoyl reductase). A close association of enzymes that are part of the same metabolic pathway is very common [95] and from available data the same may be hypothesized for the human very long chain fatty acid elongation system. In a first step ELOVL4 [1] catalyzes the condensation of malonyl-CoA to a CoA-conjugated long chain fatty acid. Subsequently, the keto-product of this reaction is reduced by 17beta-HSD12 and dehydratized by a so far unknown dehydratase (potential homologs of this enzyme have been identified in yeast [97] and *Arabidopsis thaliana* [98]). In the final step a saturated very long chain fatty acid is generated in a reaction catalyzed by TER [56].

The complementation studies done with the different 17beta-HSD12 homologs are much closer to the goal of determining the substrate specificity of this enzyme. These experiments have the advantage that they represent *in vivo* data and are therefore very closely linked to the physiological function of the enzyme. The disadvantage is that a lot of unknown factors are involved and the results are hardly quantitative. Nevertheless, this method has already been used to investigate the elongation of VLCFAs. In this way homologs of YBR159 (and therefore also of 17beta-HSD12) have been identified in *Cenorhabditis elegans* [66] and *Gossypium hirsutum* [99].

Several interesting observations could be made in these experiments. It was possible to identify functional analogs of YBR159 from all investigated organisms. Interestingly, these results fitted very well with those obtained from the phylogenetic tree described above: all these functional analogs clustered within the 17beta-HSD12 group. The other two homologs LET767 and YBR159 are obviously too far removed from the other sequences to cluster with them (divergence of *S.cerevisiae* and *C.elegans* more than 1 billion years ago while divergence between the other investigated organisms occurred hundreds of million years later [93]).

One noteworthy result of the yeast complementation assay was the observation that the enzyme designated as *Ciona intestinalis* 17beta-HSD12 in this work complemented the ΔYBR159 phenotype. The sequence has already been cloned and partially characterized [77]. Judging from the results of this work the annotation of this sequence as *Ciona intestinalis* 17beta-HSD3 is erroneous as the enzyme clearly is a functional analog of 17beta-HSD12 and does not convert androstenedione [100]. A close examination of the multiple alignment shown in this paper reveals that the authors used sequences of

[1] humans possess several other ER-localized elongases that may be involved in this step but were not tested for their interaction (for a review on elongases see Jakobsson *et al.* [96])

human and mouse 17beta-HSD12 for their alignments. In their final experiment the authors show that the enzyme is expressed in testis, which can not only be expected for 17beta-HSD3 but also for the ubiquitously expressed 17beta-HSD12 [56]. In summary, it was warranted to rename this enzyme to *Ciona intestinalis* 17beta-HSD12.

Although the results of this complementation assay strongly suggest that the main role of 17beta-HSD12 is related to fatty acid metabolism, the only definite proof is to quantitatively evaluate the catalysis of 3-ketoacyl-CoA reduction. For this purpose a LC-MS/MS method of Magnes *et al.* [75] was adapted to measure 3-ketopalmitoyl-CoA. As already mentioned this molecule is relatively instable and assumably prone to spontaneous decarboxylation [101]. While this molecule is already short-lived in a buffer solution the situation is aggravated in cell lysates. Being an activated molecule (by its energy rich thioester bond) 3-ketopalmitoyl-CoA is potentially degenerated by various proteins present in a crude cellular lysate. It therefore seems impossible to monitor this reaction without prior purification of the enzyme. Although some experiments showed that dodecyl-β-D-maltoside does not negatively affect the enzymatic activity of human 17beta-HSD12 (data not shown), it was not possible to establish a purification protocol. The low expression of the enzyme from cultured cells made it cost-prohibitive to attempt a large scale purification of protein derived from a mammalian expression system and the protein could not be solubilized when expressed in bacterial systems.

As it was not possible to characterize the fatty acid converting potential of 17beta-HSD12 in the course of this work, only activity assays using estrone as substrate were performed. These assays showed that the 17beta-HSDs 12 of the two vertebrates (human and zebrafish) catalyzed the reduction of estrone. Furthermore, the enzyme identified as *Branchiostoma floridae* 17beta-HSD12 in the yeast complementation assay also catalyzed this reaction. Interestingly, *Ciona intestinalis* 17beta-HSD12 did not catalyze the conversion of estrogens but the enzyme that was annotated as *Ciona intestinalis* 17beta-HSD12like in this work was active. All other enzymes, especially *Strongylocentrotus purpuratus* 17beta-HSD12, were did not catalyze the reduction of estrone. The inability of *Ciona intestinalis* and *Strongylocentrotus purpuratus* 17beta-HSD12 to convert estrogens indicates that these enzymes have no role in this metabolic pathway. This notion is further corroborated by the fact that the observed conversion rates are exceptionally low. Another observation in preliminary experiments was that estrone reduction was low at low concentrations and only increased with higher substrate concentrations (data not shown), which may hint at a sigmoidal kinetics curve. Although this needs to be ascertained in further experiments it seems improbable that an enzyme that converts substrates that occur in low concentrations (i.e. steroids) shows sigmoidal kinetics with a presumably high K_m. The proposal of Luu-The *et al.* that 17beta-HSD12 is a major estrogen supplying enzyme is therefore invalid [59].

4.2.3. Does 17beta-HSD12 represent the transition from fatty acid to steroid metabolism?

A steroid converting potential of 17beta-HSD12 has been shown in many different organisms including humans [59], mice [61], monkeys [60], and *C.elegans* [62]. Furthermore, a major role for this enzyme in steroid dependent tumorigenesis has been proposed [63]. The importance of these observations for clarifying the *in vivo* function of 17beta-HSD12 has always been doubtful. Two studies showed that 17beta-HSD12 has no significance in hormone dependent cancers [64, 65], with the latter even claiming that the enzyme does not convert estrone. This observation may be attributable to the low activity (see Chapter 4.2.2) and a suboptimal experimental setup. A recent study may reconcile the aforementioned observations as a role of 17beta-HSD12 in breast cancer was described but the molecular cause of this influence was located in fatty acid metabolism [102]. Several other publications cast doubt on the enzymes function in steroid metabolism and indicate a role in fatty acid metabolism. An ubiquitous enzyme expression [103] and expressional regulation by SREBP-1 [104] are properties of a fatty acid metabolizing enzyme.

4.3. Discovery of multifunctionality in rodent 17beta-HSDs type 3

It was attempted to investigate the molecular basis of steroid / retinoid multifunctionality in rodent 17beta-HSD3. Therefore, the retinoid converting ability of mouse 17beta-HSD3 was characterized (the catalytic activity towards retinoids in rat 17beta-HSD3 was much lower and could not be characterized properly) and a mutagenesis screen was performed to find amino acids important for substrate discrimination.

4.3.1. Characterization of retinoid conversion catalyzed by murine 17beta-HSD3

Steady-state kinetics measured for murine 17beta-HSD3 showed that increasing substrate concentrations did not result in a saturation, but a decline in reaction rates. This curve is indicative for substrate inhibition, a well known phenomenon that has been observed for several other enzymes [105, 106]. Although the curve for murine 17beta-HSD3 seems to accurately fit to the data points and is similar to those published for other enzymes, the calculated values had dramatic errors. This may be explained by the relatively slow decline of reaction rates for higher concentrations. A possible way to reduce the errors would have been to increase the investigated substrate range to get more data on curve progression for higher substrate concentrations. A broader data base would have allowed for a more accurate mathematical description of the observed substrate inhibition.

To determine K_M and V_{max} murine 17beta-HSD3 kinetics were measured in the lower substrate concentration range up to 16 μM. As retinoids naturally occur concentrations

much less than 16 μM this may be a viable approach. But as in classical Michaelis-Menten kinetics a saturation is assumed the calculated values of 10.7 μM for K_M and 12.3 nmol/min/mg total protein) for V_{max} are only approximations. Nevertheless, a comparison to the values measured for human 17beta-HSD1 is possible as the conditions for these measurements were quite similar. Generally, all-trans retinol reduction by human 17beta-HSD1 seems to be much more efficient (about 16 times) than that of murine 17beta-HSD3. Judging from the evolutionary background of 17beta-HSD1 with a close relationship to retinol dehydrogenases this observation is not surprising. But on the other hand the fact that for 17beta-HSD3 a common ancestry with retinol dehydrogenases is much further away, makes this result much more surprising than the retinal converting ability discovered in 17beta-HSD1.

4.3.2. Application of a mutagenesis strategy to gain insights into 17beta-HSD3 multifunctionality

Single amino acids or short amino acid motifs in human 17beta-HSD3 were exchanged to corresponding residues of the rodent enzymes. Of the investigated exchanges in the human 17beta-HSD3 sequence many had no effect on substrate specificity. Even those mutations that influenced enzyme activity only had a minor impact on all-trans retinol reduction. In the course of this study up to 7 different mutations were inserted into one construct, but not even this combination of exchanges was enough to significantly alter the retinal reducing activity in human 17beta-HSD3.

The NLL137SFF, A207T, and EV219GI mutations had the most significant effect on retinal reduction catalyzed by human 17beta-HSD3. To really establish the influence of these residues on substrate specificity it would have been necessary to mutate the corresponding sequence of murine 17beta-HSD3 to the human sequences. If differences in retinal reduction were observed in these mutants a role of these residues would have been corroborated. In contrast to 17beta-HSD1 no single amino acid governing the substrate spectrum could be found in 17beta-HSD3.

4.3.3. Implications of rodent 17beta-HSD3 multifunctionality

The ability to catalyze the conversion of retinoids seems to be quite common in the SDR protein-superfamily. Even within the subgroup of 17beta-HSDs this trait is quite common. For 17beta-HSD9 a retinoid converting ability has been known for quite some time [107] and in the course of this work an all-trans retinal reducing function has been discovered for 17beta-HSD1. The *in vivo* significance of these findings is uncertain as retinoids within cells are often bound to cellular retinol binding proteins (CRBPs). Nevertheless, the assumption that these enzymes catalyze the conversion of retinoids could be deduced from their evolutionary relationships to retinol dehydrogenases. As no such relationships are known for 17beta-HSD3 this newly discovered retinoid converting function is all the more surprising. But at the same time the importance of this function *in vivo* is certainly much less likely. The dependance of spermatogenesis on retinoids

has been recognized for decades [108, 109, 110]. Additionally, retinoids seem to have direct influence on testosterone levels [111]. As spermatogenesis is localized in testicles, the very tissue in which the highest expression of murine 17beta-HSD3 has been shown, a cross-talk between steroid and retinoid pathways may be imaginable in this tissue.

While it is uncertain whether the multifunctionality observed in rodent type 3 17beta-HSDs is of significance *in vivo* striking differences between steroid metabolism in humans and rodents have once more been uncovered. Right from the beginning of research on 17beta-HSDs significant differences in rodent and human enzymes could be observed. Multifunctionality concerning estrogens and androgens has been observed in rodent 17beta-HSD1 [34]. But also when comparing 17beta-HSDs3 derived from human and mouse this multifunctionality was observable: while the substrate spectrum of human 17beta-HSD3 is restricted to androgens, murine 17beta-HSD3 catalyzes the conversion of estrone to estradiol in addition to the conversion of androstenedione to testosterone [112].

These results cast serious doubts on the suitability of rodent enzymes for predictions about endocrinology in humans. The consequences are that testing endocrine-modulating drugs on rodents may in many cases not induce a reaction that is comparable to the drug's effect in humans. Therefore, a thorough characterization of steroid metabolizing enzymes in humans as well as in rodents acting as model organisms is a prerequisite to generating meaningful data in studies with steroid-affecting drugs in laboratory animals.

4.4. Challenges and opportunities in LC-MS/MS method development

Several different online-SPE coupled LC-MS/MS methods were developed in the course of this work. The application of the online-SPE system set up in this work allowed for high sample through-put while minimizing the hands-on time for the experimentator. For many analytes investigated in this work the method proved to be sensitive enough to measure blood plasma samples. In summary the goals set in the beginning of this work were achieved.

4.4.1. Tailor-made methods - what is to be expected from steroid measurements?

In recent years a lot of different methods for the measurement of steroids have been described. Some of them focused only on one analyte or a class of analytes. So methods for the analysis of corticosteroids [113, 114, 115, 116], androgens [117, 118, 119], and estrogens [120, 121, 122] have been described. Although several publications covered a broader spectrum of steroid classes most of these studies lacked in their suitability for high-through-put analyses [123, 124] as these methods use complicated extraction steps and lengthy gradient runs. Only recently another method by Ceglarek *et al.*

was published that achieved similar, or an even better performance [125]. The main differences between these two methods are the steroids measured: while Ceglarek *et al.* included DHEA-S, 11-deoxycortisol, aldosterone, and estradiol (the latter two were measured in a separate run in negative ion mode) the method developed in this work included cortisone and corticosterone. In addition to the measurement of steroids in human plasma the method was also adapted for the measurement of steroids in mouse plasma.

Compared to human plasma, mouse plasma constitutes a rather unique challenge. As the blood volume of mice is very low only 50 μL sample were available for each mouse. Another problem is the high viscosity of mouse plasma which complicates accurate and reproducible pipetting. Furthermore, the concentrations of many steroids are lower than in humans. A very interesting observation during the development of this method for mouse plasma was the discovery of unknown metabolites. Interestingly, these metabolites were defined by their difference in retention time rather than mass transition, highlighting the importance of a chromatographic separation that precedes mass spectrometry. To identify these molecules an approach already used for identification of zebrafish steroids could be employed. In collaboration with Janina Tokarz candidate molecules were characterized by comparing retention times and fragment spectra. In this way the product of an *in vitro* enzymatic assay was identified. This process would be slightly more complicated for identifying the mouse metabolites as the molecule that needs to be identified is not part of a controlled experimental setup but a constituent of a complex biological fluid, i.e. blood. Although it is not even certain that the unknown metabolites are steroids, the mass transitions may be suggestive for this molecule class. Both, cortisol and progesterone are fragmented within the B ring of the steroid backbone (see Figure 4.1), fragments that are rather typical for steroids. At least for the 363.2 → 121.1 transition there are a number of potential candidate molecules described [126].

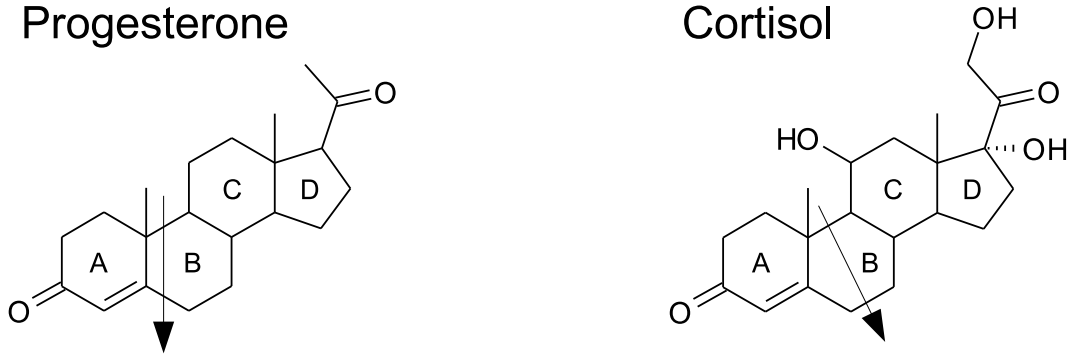

Figure 4.1.: Fragmentation of progesterone and cortisol.
In progesterone bonds in ring B are cleaved to form a fragment of m/z 109.1, while in cortisol cleavage of different bonds in ring B leads to a fragment of m/z 121.1

To see if a method works as intended, its inherent uncertainty needs to be determined [127]. Several different validation guidelines have been published to ascertain that methods are suitable for their purpose [128, 129], most of them apply to the pharmaceutical

industry. In academia no such guidelines apply, nevertheless it is just as necessary to develop methods that are fit for their purpose. For this several validation parameters were chosen to evaluate the methods developed in this work.

Precision is the variation between samples containing the same amount of analyte. In bioanalytics the Food and Drug Adminstration accepts up to 15 % variation (even 20 % at LOQ) [128], values that are undermatched by the method developed in this work.

Accuracy and selectivity of the method were determined as part of recovery experiments, which is a very common way to establish this parameter [130]. For most analytes recovery rates were above 90 % which is comparable to the values obtained by Ceglarek *et al.* [125]. Generally, even a method with recoveries as low as 50 % may be acceptable if it is sensitive enough [131]. Selectivity is ensured by baseline separation of all analytes apart from cortisone and cortisol (these two analytes were distinguished by their unique mass transitions).

For the determination of linearity standard curves were prepared in isotonic sodium chloride solution. Although it is a very common practice to prepare the standards in buffers [125, 114, 132, 133], it is generally preferable to prepare the standards in the matrix [128]. The problem was that the 'steroid-free' plasma prepared in this work still contained small amounts of steroids. Therefore, it might be advisable to further optimize the steroid depletion procedure to get a more realistic standard curve. For the standard curve itself the correlation coefficient 'r' should exceed a value 0.99 [134], which was attained for all analytes.

Stability tests are often performed in the pharmaceutical industry as drugs need a certain shelf life in which they can be applied to a patient. For the purposes of this work this parameter was only determined superficially. Several samples were prepared, measured, stored overnight at 4 °C, and measured again (data not shown). As the samples are measured directly after sample preparation the only time period in which the analytes may degrade is during the time in the autosampler (cooled to 4 °C). As the sample capacity of the equipment used in this work only supported measurements overnight this abbreviated stability test was deemed to be sufficient.

Robustness of a method is determined to evaluate the impact of slight variations in external conditions on the performance of this method. In HPLC the mobile phase (pH, solvent composition), the stationary phase, flow rate or ambient temperature could be varied in increments. Also intermediate precision is often included in the definition of robustness [130]. The latter is the only parameter which was determined in this work to see if the method can routinely be performed by another experimentator. While the regulations on variations in an analytical method are very strict in the pharmaceutical industry there are no such restrictions in academia. To conduct the very time- and cost-intensive procedure of determining the robustness was not deemed necessary.

4.4.2. Extending the steroid method to a hormone screening assay

In the field of metabolomics a larger set of analytes allows for deeper insights into the metabolic state of an organism. To broaden the spectrum of the steroid method developed in this work the inclusion of further hormones was attempted. The thyroid hormones 3,3',5-triiodo-L-thyronine (T3) and thyroxine (T4) are essential for the maintenance of physiological functions and balancing metabolism by regulating gluconeogenesis and lipolysis. Therefore, hypothyroidism leads to lethargy and obesity. The various physiological roles of vitamin A and its derivatives have already been described in other parts of this work. While several methods for single hormone classes like steroids [125, 123, 124], retinoids [135, 136, 137], and thyroid hormones [138, 139] have been described, a combination of these different analytes in one method was never attempted. However, inclusion of as many analytes as possible into one analysis step/method is highly desired, because especially in cohort studies the sample amounts are often a limiting factor (e.g. mouse plasma, human biopsies).

To include these very diverse analytes in one method, chromatographic as well as mass spectrometric parameters had to be adapted. While the HPLC gradient merely needed to be adapted in a few places to achieve an acceptable separation, the ion source needed to be changed on the mass spectrometric side. Although the change from electrospray (ESI) to atmospheric pressure chemical ionization (APCI) resulted in lower sensitivity for androgens and corticosteroids, the gain in sensitivity for the two new substance classes was substantial. Apart from retinol the sensitivities for the other analytes were rather low. To get higher signal intensities different solvents for the protein precipitation step were tested. Unfortunately, none of the solutions tested gave good results for all analytes. Due to time constraints it was not possible to finalize this method, but the basis for successful measurements was laid.

To get a higher sensitivity for T4 and especially T3 a different approach to sample preparation may be advisable. While some groups also use protein precipitation (which was combined with several extraction steps) [138] the method of choice for thyroid hormone analysis seems to be direct equilibrium dialysis [139]. Although this procedure includes an overnight incubation step, the hands-on time is not much higher than for protein precipitation. The experimental setup should also work for all other analytes and may allow a successful establishment of screening assay for a variety of hormones.

4.5. Challenges in evaluating steroid reference values measured in mouse plasma

Measurements of corticosterone concentrations showed clear differences between the different strains investigated. Furthermore, for some of these mice a distinct sexual dimorphism was observable. On the downside are the, at least in part, huge variations within the sample groups. A part of this variability is clearly attributable to the fact that the study deals with complex organisms that cannot be expected to show only minor

differences in their metabolic compositions. But another part of these inhomogeneities results from sampling issues.

For humans it is known that the major corticosteroid, cortisol, is subject to a significant variability depending on the time of day [140]. These changes are especially pronounced in the morning. This circadian rhythm of corticosterone concentrations can also be observed in mice although major concentration changes occur in the afternoon/evening [141]. The influences of this factors are probably only minor as most of the blood sampling was done in the morning but still there are some exceptions where the blood was taken in the early afternoon.

Corticosteroids are stress hormones that are distributed in the body when an organism perceives an external threat. As the blood sampling procedure involves several steps that potentially cause stress for the animals (catching the mice, anesthetizing the mice, sometimes blood sampling is done without anesthesia and the mice are fixated) this can also have an effect on corticosterone concentrations. How individual mice react to this treatment may account for additional variability. To circumvent this problem, blood sampling could be done using blood-sucking bugs, although it is doubtful whether this technique could be used on a routine basis [142].

A further complication in interpreting the available data is the fact that the data sets are incomplete. On the one hand blood sampling was not performed at all time points and on the other hand some animals died during the course of this investigation. Also the times of blood sampling varied between the different strains making the available data hard to compare.

In case of testosterone only male mice showed levels of this steroid that were sufficiently high for quantification. For nearly all female mice this steroid was below the limit of detection. Within the group of male mice the variability of this steroid's concentration was even higher than for corticosterone. Possible explanations for this observation may be circadian as well as seasonal variations of this steroid which have already been described in male humans [143, 144, 145]. Furthermore, sexual activity seems to have an influence on serum levels of testosterone [146].

Although the setup of this study has several minor faults (e.g. heterogeneity of sampling times) the biological variation within a mouse population is considerable. It may be possible to obtain more significant data by using more standardized experimental conditions and using a larger population of animals but even then it may only be possible to recognize phenotypes whose steroid concentrations deviate extraordinarily from the norm.

4.6. Exploring uncharted waters: interpretation of metabolomics data from fasting subjects

The number of subjects investigated in this study was quite low (only 11 probands), which may be one reason why no significant changes in steroid concentrations were observed. Although it would be necessary to investigate a much larger cohort to obtain

definitive answers, the observed tendencies will be interpreted in this section.

Progesterone concentrations suggest that the levels of this steroid are reduced during fasting but can be restored to a normal level by food intake. Progesterone itself is mainly known to be involved in the menstrual cycle [147, 148] and its function as neurosteroid [149]. Furthermore, it has been described to have regional effects on gluteofemoral adipocytes [150] but direct nutrition-related effects of progesterone have not been described. For 17OH-progesterone the situation is quite similar: this steroid has also never been investigated in connection with nutrition. The slight effects observed (more pronounced for progesterone, but less so for 17OH-progesterone) may therefore be attributed to the position of these molecules in the biosynthesis pathway of steroids. Both of these progestins are relatively in the beginning of the pathway (see Figure 4.2) and their concentrations may therefore be regulated in response to increasing needs for downstream steroids.

For androgens more direct references to nutrition are available, although most investigations in this area focused on obesity rather than fasting. It is well known that androgens have effects on body fat distribution and therefore can partially reverse symptoms of the metabolic syndrome [151, 152]. Furthermore, elevated levels of testosterone have been observed after feeding a diet of low protein content to rats [153]. Although these animals were not actually fasting, it has at least been demonstrated that nutrition has a direct effect on androgen levels. The observation that testosterone concentrations are low after the first day of fasting and remain at a relatively constant level afterwards could also hint at a rapid adaptation of the endocrine system to a changing environment although more timepoints would be needed to ascertain this assumption. Another explanation for the relatively constant testosterone concentrations may be due to intracrinology in target tissues [154]. Local reduction of androstenedione to testosterone has already been shown in adipose tissue [155]. Therefore, some effects of fasting on androgen concentrations may not be accessible by measuring plasma concentrations of these steroids.

Corticosteroids like cortisone and cortisol have been known to be associated with energy metabolism for a very long time. These steroids are therefore often called glucocorticoids. Especially in recent years there has been great interest in this class of steroids as they are closely associated with the metabolic syndrome, a disease state that is becoming more and more common in the Western world [156, 157]. Excess cortisol is known to cause the accumulation of abdominal fat, increases in plasma lipid levels, and insulin resistance. Starvation in mice triggers a stress response which causes an increase in cortisol levels by converting inactive cortisone to cortisol [158]. In the present study cortisol levels seem to be lowered compared to the reference level (timepoint 5), an observation in stark contrast to the expectations (due to the high variability of cortisol concentrations it is not certain if this assertion can be made). There are possible explanations for this higher cortisol level in controls. Long-term stress (such as a whole month of fasting) leads to the accumulation of stress hormones like cortisol [148, 159]. It may therefore be necessary to take samples before and a longer time after the month of fasting to get better reference values. The rise in cortisone levels observed after a meal may be explained by a reduced state of stress when food becomes available. But,

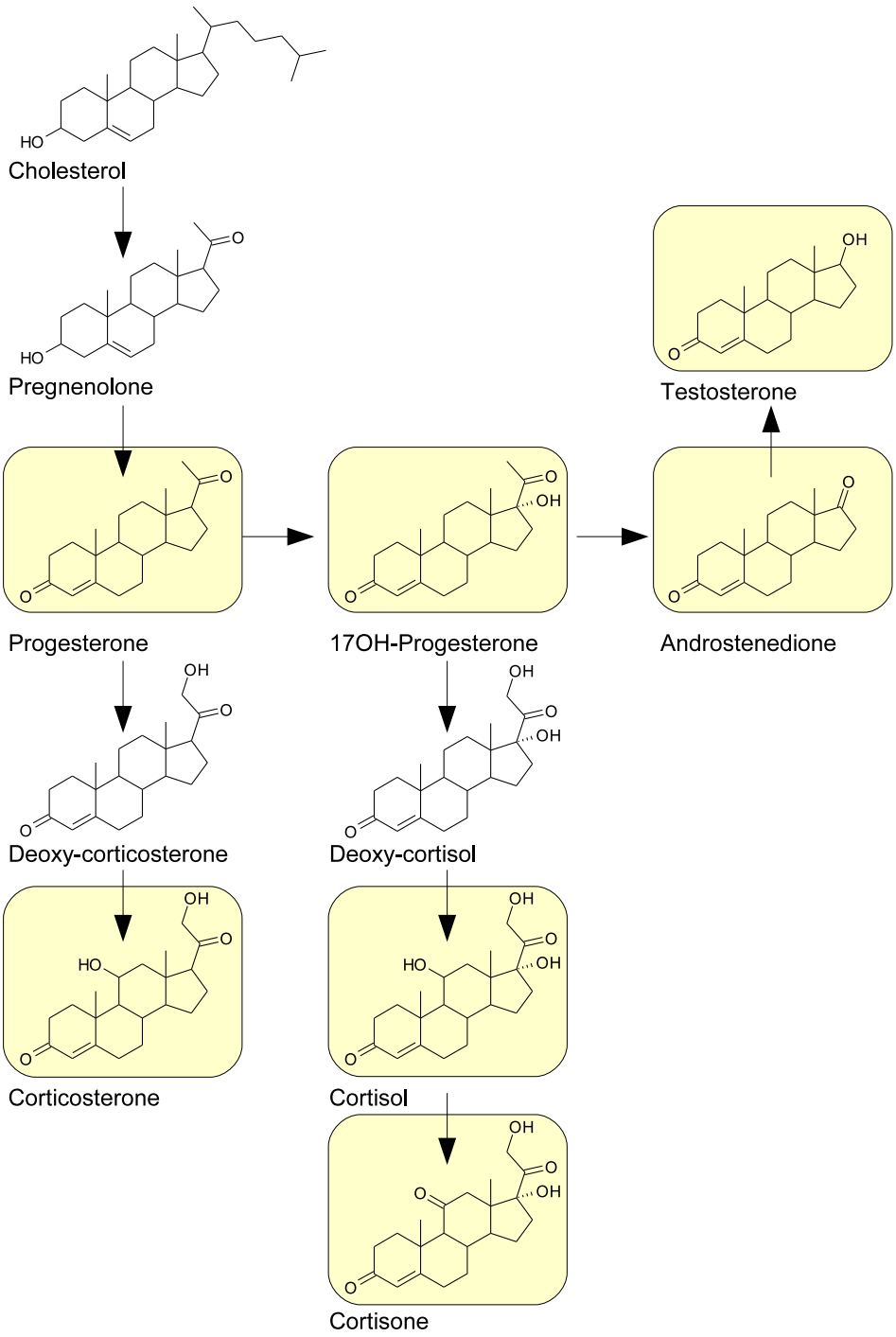

Figure 4.2.: Synthesis of steroid hormones starting from cholesterol.
Scheme of different steroid synthesis pathways; progesterone and 17OH-progesterone are precursors to different other steroids; steroids measured with the method developed in this work are shaded in light yellow.

as cortisone is generated by inactivation of cortisol a concomitant decrease in cortisol would be expected, which could not be observed.

Of course it is also possible that all the effects observed in this study are merely secondary. Circadian rhythms affecting steroid concentrations have already been mentioned above (see Chapter 4.5) and are especially pronounced in corticosteroid concentrations. Another problem may have been blood sampling, as there is no information whether it was performed at comparable timepoints. It is also possible that the sudden availability of food causes an increase in anabolic metabolism. This may be an explanation why all steroid concentrations seem to rise to some degree after food intake. To better differentiate between the direct effects of fasting from secondary effects the study design needs to be adapted. By including an outgroup without food restriction it may be possible to get more meaningful results. Further means to improve the study would be to dramatically increase the number of subjects as at the moment the relatively large variability in steroid concentrations (which of course is not unexpected in a small population of study subjects) may obscure significant effects attributable to fasting.

Bibliography

[1] Peter J. Bowler. Darwin's originality. *Science*, 323:223–226, 2009.

[2] Patrick J. O'Brien and Daniel Herschlag. Catalytic promiscuity and the evolution of new enzymatic activities. *Chem. Biol.*, 6(4):R91–R105, 1999.

[3] Roy A. Jensen. Enzyme recruitment in evolution of new function. *Ann. Rev. Microbiol.*, 30:409–425, 1976.

[4] Olga Khersonsky, Cintia Roodveldt, and Dan S. Tawfik. Enzyme promiscuity: evolutionary and mechanistic aspects. *Curr. Opin. Chem. Biol.*, 10:498–508, 2006.

[5] Sergio G. Peisajovich and Daniel S. Tawfik. Protein engineers turned evolutionists. *Nature Methods*, 4(12):991–994, 2007.

[6] Amir Aharoni, Leonid Gaidukov, Olga Khersonsky, Stephen McQ Gould, Cintia Roodveldt, and Daniel S. Tawfik. The 'evolvability' of promiscuous protein functions. *Nature Genetics*, 37(1):73–76, 2005.

[7] D.H. Fong and A.M. Berghuis. Substrate promiscuity of an aminoglycoside antibiotic resistance enzyme via target mimicry. *EMBO J.*, 21(10):2323–2331, 2002.

[8] M.S. Hanes, K.M. Jude, J.M. Berger, R.A. Bonomo, and T.M. Handel. Structural and biochemical characterization of the interaction between KPC-2 beta-lactamase and beta-lactamase inhibitor protein. *Biochemistry*, 48(39):9185–9193, 2009.

[9] Udo Oppermann, Charlotta Filling, Malin Hult, Naeem Shafqat, Xiaoqiu Wu, Monica Lindh, Jawed Shafqat, Erik Nordling, Yvonne Kallberg, Bengt Persson, and Hans Jörnvall. Short-chain dehydrogenases/reductases (SDR): the 2002 update. *Chem. Biol. Interact.*, 143-144:247–253, 2003.

[10] James E. Bray, Brian D. Marsden, and Udo Oppermann. The human short-chain dehydrogenase/reductase (SDR) superfamily: A bioinformatics summary. *Chem.-Biol. Interact.*, 178(1-3):99–109, 2009.

[11] J. Adamski, B. Husen, F. Marks, and P.W. Jungblut. Purification and properties of oestradiol 17beta-dehydrogenase extracted from cytoplasmic vesicles of porcine endometrial cells. *Biochem. J.*, 288:375–381, 1992.

[12] E.G. van Grunsven, E. van Berkel, L. Ijlst, P. Vreken, J.B. de Klerk, J. Adamski, H. Lemonde, P.T. Clayton, D.A. Cuebas, and R.J. Wanders. Peroxisomal D-hydroxyacyl-CoA dehydrogenase deficiency: resolution of the enzyme defect and its molecular basis in bifunctional protein deficiency. *Proc. Natl. Acad. Sci.*, 95:2128–2133, 1998.

[13] Frauke Leenders, Jacob G. Tesdorpf, Monika Markus, Thomas Engel, Udo Seedorf, and Jerzy Adamski. Porcine 80-kDa protein reveals intrinsic 17beta-hydroxysteroid dehydrogenase, fatty acyl-CoA-hydratase/dehydrogenase, and sterol transfer activities. *J. Biol. Chem.*, 271:5438–5442, 1996.

[14] G. Wolf. Multiple functions of vitamin A. *Physiol. Rev.*, 64:873–937, 1984.

[15] G.M. Morriss-Kay and S.J. Ward. Retinoids and mammalian development. *Int. Rev. Cytol.*, 188:73–131, 1999.

[16] G. Wolf. The visual cycle of the cone photoreceptors of the retina. *Nutr. Rev.*, 62:283–286, 2004.

[17] Martin Liden and Ulf Eriksson. Understanding retinol metabolism: structure and function of retinol dehydrogenases. *J. Biol. Chem.*, 281:13001–13004, 2006.

[18] H. Joernvall, B. Persson, M. Krook, S. Atrian, R. Gonzalez-Duarte, J. Jeffery, and D. Ghosh. Short-chain dehydrogenases/reductases (SDR). *Biochemistry*, 34(18):6003–6013, 1995.

[19] Gregg Duester. Families of retinoid dehydrogenases regulating vitamin A function. *Eur. J. Biochem.*, 267:4315–4324, 2000.

[20] R.R. Rando. The biochemistry of the visual cycle. *Chem. Rev.*, 101:1881–1896, 2001.

[21] A. Rattner, P.M. Smallwood, and J. Nathans. Identification and characterization of all-trans-retinol dehydrogenase from photoreceptor outer segments, the visual cycle enzyme that reduces all-trans-retinal to all-trans-retinol. *J. Biol. Chem.*, 275:11034–11043, 2000.

[22] A. Maeda, T. Maeda, Y. Imanishi, V. Kuksa, A. Alekseev, and J.D. Bronson. Role of photoreceptor-specific retinol dehydrogenase in the retinoid cycle *in vivo*. *J. Biol. Chem.*, 280:18822–18832, 2005.

[23] A. Maeda, T. Maeda, W. Sun, H. Zhang, W. Baehr, and K. Palczewski. Redundant and unique roles of retinol dehydrogenases in the mouse retina. *Proc. Natl. Acad. Sci.*, 104:19565–19570, 2007.

[24] A. Maeda, T. Maeda, M. Golczak, and K. Palczewski. Retinopathy in mice induced by disrupted all-trans-retinal clearance. *J. Biol. Chem.*, 283:26684–26693, 2008.

[25] Michael E. Baker. Evolution of 17beta-hydroxysteroid dehydrogenases and their role in androgen, estrogen and retinoid action. *Mol. Cell. Endocrinol.*, 171:211–215, 2001.

[26] O.V. Belyaeva and N.Y. Kedishvili. Comparative genomic and phylogenetic analysis of short-chain dehydrogenases/reductases with dual retinol/sterol substrate specificity. *Genomics*, 88:820–830, 2006.

[27] Gabriele Moeller and Jerzy Adamski. Multifunctionality of human 17beta-hydroxysteroid dehydrogenases. *Mol. Cell. Endocrinol.*, 248:47–55, 2006.

[28] P. Lukacik, K.L. Kavanagh, and U. Oppermann. Structure and function of human 17beta-hydroxysteroid dehydrogenases. *Mol. Cell. Endocrinol.*, 248:61–71, 2006.

[29] G. Moeller and J. Adamski. Integrated view on 17beta-hydroxysteroid dehydrogenases. *Mol. Cell. Endocrinol.*, 301:7–19, 2009.

[30] P.W. Jungblut, J. Gaues, L. Gorlich, A. Hughes, E. Kallweit, J. Kielhorn, M. Little, I. Maschler, S. McCann, F. Parl, G.C. Rosenfeld, W. Sierralta, G. Stone, P.I. Szendro, C. Teran, A.J. Truitt, and R.K. Wagner. Intracellular actions of gonadal steroids. *Exp. Brain Res.*, 3:37–60, 1981.

[31] Zrinka Marijanovic, Daniela Laubner, Gabriele Moeller, Christian Gege, Bettina Husen, Jerzy Adamski, and Rainer Breitling. Closing the gap: Identification of human 3-ketosteroid reductase, the last unknown enzyme of mammalian cholesterol biosynthesis. *Mol. Endocrinol.*, 17(9):1715–1725, 2003.

[32] S. Andersson and N. Moghrabi. Physiology and molecular genetics of 17 beta-hydroxysteroid dehydrogenases. *Steroids*, 62(1):143–147, 1997.

[33] N. Khan, K.K. Sharma, S. Andersson, and R.J. Auchus. Human 17beta-hydroxysteroid dehydrogenases types 1, 2, and 3 catalyze bi-directional equilibrium reactions, rather than unidirectional metabolism, in HEK-293 cells. *Arch. Biochem. Biophys.*, 429(1):50–59, 2004.

[34] Terhi Puranen, Matti Poutanen, Debashis Ghosh, Reijo Vihko, and Pirkko Vihko. Origin of substrate specificity of human and rat 17beta-hydroxysteroid dehydrogenase type 1, using chimeric enzymes and site-directed substitutions. *Endocrinology*, 138:3532–3539, 1997.

[35] Rebekka Mindnich, Dominga Deluca, and Jerzy Adamski. Identification and characterization of 17beta-hydroxysteroid dehydrogenases in the zebrafish, *Danio rerio*. *Mol. Cell. Endocrinol.*, 215:19–30, 2004.

[36] S.A. Ghersevich, M.H. Poutanen, H.K. Martikainen, and R.K. Vihko. Expression of 17beta-hydroxysteroid dehydrogenease in human granulosa cells: correlation with follicular size, cytochrome P-450 aromatase activity and oestradiol production. *J. Endocrinol.*, 143:139–150, 1994.

[37] O. Maentausta, H. Peltoketo, V. Isomaa, P. Jouppila, and R. Vihko. Immunological measurement of human 17beta-hydroxysteroid dehydrogenase. *J. Steroid Biochem.*, 36:673–680, 1990.

[38] C. Sawetawan, L. Milewich, R.A. Word, B.R. Cam, and W.E. Rainey. Compartmentalization of type I 17beta-hydroxysteroid oxidoreductase in the human ovary. *Mol. Cell. Endocrinol.*, 99:161–168, 1994.

[39] V. Luu-The, C. Labrie, J. Simard, Y. Lachance, H.F. Zhao, J. Couet, G. Leblanc, and F. Labrie. Structure of two in tandem human 17 beta-hydroxysteroid dehydrogenase genes. *Mol. Endocrinol.*, 4:268–275, 1990.

[40] C. Martel, E. Rheaume, M. Takahashi, C. Trudel, J. Couet, V. Luu-The, J. Simard, and F. Labrie. Distribution of 17beta-hydroxysteroid dehydrogenase gene expression and activity in rat and human tissues. *J. Steroid Biochem. Mol. Biol.*, 41:597–603, 1992.

[41] P. Vihko, P. Harkonen, O. Oduwole, S. Torn, R. Kurkela, K. Porvari, A. Pulkka, and V. Isomaa. 17beta-hydroxysteroid dehydrogenases and cancers. *J. Steroid Biochem. Mol. Biol.*, 83:119–122, 2002.

[42] Joanna M Day, Helena J Tutill, Atul Purohit, and Michael J Reed. Design and validation of specific inhibitors of 17beta-hydroxysteroid dehydrogenases for therapeutic application in breast and prostate cancer, and in endometriosis. *Endo. Rel. Cancer*, 15:665–692, 2008.

[43] D. Ghosh, V.Z. Pletnev, D.W. Zhu, Z. Wawrzak, W.L. Duax, W. Pangborn, F. Labrie, and S.X. Lin. Structure of human estrogenic 17beta-hydroxysteroid dehydrogenase at 2.20 A resolution. *Structure*, 3:503–513, 1995.

[44] R. Breton, D. Housset, C. Mazza, and J.C. Fontecilla-Camps. The structure of a complex of human 17beta-hydroxysteroid dehydrogenase with estradiol and NADP+ identifies two principal targets for the design of inhibitors. *Structure*, 4:905–915, 1996.

[45] G.M. Allan, N. Vicker, H.R. Lawrence, H.J. Tutill, J.M. Day, M. Huchet, E. Ferrandis, M.J. Reed, A. Purohit, and B.V. Potter. Novel inhibitors of 17beta-hydroxysteroid dehydrogenase type 1: templates for design. *Bioorg. Med. Chem.*, 16(8):4438–4456, 2008.

[46] E. Bey, S. Marchais-Oberwinkler, M. Negri, P. Kruchten, A. Oster, T. Klein, A. Spadaro, R. Werth, M. Frotscher, B. Birk, and R.W. Hartmann. New insights into the SAR and binding modes of bis(hydroxyphenyl)thiophenes and -benzenes: influence of additional substituents on 17beta-hydroxysteroid dehydrogenase type 1 (17beta-HSD1) inhibitory activity and selectivity. *J. Med. Chem.*, 52(21):6724–6743, 2009.

[47] S. Marchais-Oberwinkler, P. Kruchten, M. Frotscher, E. Ziegler, A. Neugebauer, U. Bhoga, E. Bey, U. Mueller-Vieira, J. Messinger, H. Thole, and R.W. Hartmann. Substituted 6-phenyl-2-naphthols. Potent and selective nonsteroidal inhibitors of 17beta-hydroxysteroid dehydrogenase type 1 (17beta-HSD1): design, synthesis, biological evaluation, and pharmacokinetics. *J. Med. Chem.*, 51(15):4685–4698, 2008.

[48] G. Moeller, D. Deluca, C. Gege, A. Rosinus, D. Kowalik, O. Peters, P. Droescher, W. Elger, J. Adamski, and A. Hillisch. Structure-based design, synthesis and *in vitro* characterization of potent 17beta-hydroxysteroid dehydrogenase type 1 inhibitors based on 2-substitutions of estrone and D-homo-estrone. *Bioorg. Med. Chem. Lett.*, 19(23):6740–6744, 2009.

[49] Wayne M. Geissler, Daphne L. Davis, Ling Wu, Karen D. Bradshaw, Sushma Patel, Bernice B. Mendonca, Keith O. Elliston, Jean D. Wilson, David W. Russel, and Stefan Andersson. Male pseudohermaphroditism caused by mutations of testicular 17beta-hydroxysteroid dehydrogenase 3. *Nature Genetics*, 7:34–39, 1994.

[50] K. Margiotti, E. Kim, C.L. Pearce, E. Spera, G. Novelli, and J.K. Reichardt. Association of the G289S single nucleotide polymorphism in the HSD17B3 gene with prostate cancer in Italian men. *Prostate*, 53:65–68, 2002.

[51] Rebekka Mindnich, Ferdinand Haller, Felix Halbach, Martin Hrabe de Angelis, and Jerzy Adamski. Androgen metabolism via 17beta-hydroxysteroid dehydrogenase type 3 in mammalian and non-mammalian vertebrates: comparison of the human and the zebrafish enzyme. *J. Mol. Endocrinol.*, 35(2):305–316, 2005.

[52] Chon Hwa Tsai-Morris, Azra Khanum, Pei-Zhong Tang, and Maria L. Dufau. The rat 17beta-hydroxysteroid dehydrogenase type III: Molecular cloning and gonadotropin regulation. *Endocrinology*, 140:3534–3542, 1999.

[53] J.A. Sha, K. Dudley, W.R. Rajapaksha, and P.J. O'Shaughnessy. Sequence of mouse 17beta-hydroxysteroid dehydrogenase type 3 cDNA and tissue distribution of the type 1 and type 3 isoform mRNAs. *J. Steroid Biochem. Mol. Biol.*, 60:19–24, 1997.

[54] A.M. Corbould, S.J. Judd, and R.J. Rodgers. Expression of types 1, 2, and 3 17beta-hydroxysteroid dehydrogenease in subcutaneous abdominal and intra-abdominal adipose tissue of women. *J. Clin. Endocrinol. Metab.*, 83(1):187–194, 1998.

[55] Dmitri V. Gnatenko, Lisa D. Cupit, Emily C. Huang, Anilkumar Dhundale, Peter L. Perrotta, and Wadie F. Bahou. Platelets express steroidogenic 17beta-hydroxysteroid dehydrogenases. *Thromb. Haemost.*, 94:412–421, 2005.

[56] Young-Ah Moon and Jay D. Horton. Identification of two mammalian reductases involved in the two-carbon fatty acyl elongation cascade. *J. Biol. Chem.*, 2778(9):7335–7343, 2003.

[57] Dominick L. Cinti, Lynda Cook, Mahmoud N. Nagi, and Sanoj K. Suneja. The fatty acid chain elongation system of mammalian endoplasmic reticulum. *Prog. Lipid Res.*, 312(1):1–51, 1992.

[58] Frederic Beaudoin, Ken Gable, Olga Sayanova, Teresa Dunn, and Johnathan A. Napier. A *Saccharomyces cerevisiae* gene required for heterologous fatty acid elongase activity encodes a microsomal beta-keto-reductase. *J. Biol. Chem.*, 2778(13):11481–11488, 2002.

[59] Van Luu-The, Philippe Tremblay, and Fernand Labrie. Characterization of type 12 17beta-hydroxysteroid dehydrogenase, an isoform of type 3 17beta-hydroxysteroid dehydrogenase responsible for estradiol formation in women. *Mol. Endocrinol.*, 20(2):437–443, 2006.

[60] Hong Liu, ShuFang Zheng, Veronique Bellemare, Georges Pelletier, Fernand Labrie, and Van Luu-The. Expression and localization of estrogenic type 12 17beta-hydroxysteroid dehydrogenase in the cynomolgus monkey. *BMC Biochemistry*, 8(2):doi:10.1186/1471–2091–8–2, 2007.

[61] Pierre-Gilles Blanchard and Van Luu-The. Differential androgen and estrogen substrates specificity in the mouse and primates type 12 17beta-hydroxysteroid dehydrogenase. *J. Endocrinol.*, 194:449–455, 2007.

[62] Serge Desnoyers, Pierre-Gilles Blanchard, Jean-Francois St-Laurent, Steve N. Gagnon, David L. Baillie, and Van Luu-The. *Caenorhabditis elegans* LET-767 is able to metabolize androgens and estrogens and likely shares common ancestor with human types 3 and 12 17beta-hydroxysteroid dehydrogenases. *J. Endocrinol.*, 195:271–279, 2007.

[63] D. Song, G. Liu, V. Luu-The, D. Zhaoc, L. Wanga, H. Zhang, G. Xueling, S. Li, L. Desy, F. Labrie, and G. Pelletier. Expression of aromatase and 17beta-hydroxysteroid dehydrogenase types 1, 7 and 12 in breast cancer An immunocytochemical study. *J. Steroid Biochem. Mol. Biol.*, 101:136–144, 2006.

[64] Agneta K. Jansson, Cecilia Gunnarsson, Maja Cohen, Tove Sivik, and Olle Stal. 17beta-hydroxysteroid dehydrogenase 14 affects estradiol levels in breast cancer cells and is a prognostic marker in estrogen receptor-positive breast cancer. *Cancer Res.*, 66(23):11471–11477, 2006.

[65] Joanna M. Day, Paul A. Foster, Helena J. Tutill, Michael F.C. Parsons, Simon P. Newman, Surinder K. Chander, Gillian M. Allan, Harshani R. Lawrence,

Nigel Vicker, Barry V.L. Potter, Michael J. Reed, and Atul Purohit. 17beta-hydroxysteroid dehydrogenase type 1, and not type 12, is a target for endocrine therapy of hormone-dependent breast cancer. *Int. J. Cancer*, 122:1931–1940, 2008.

[66] Eugeni V. Entchev, Dominik Schwudke, Vyacheslav Zagoriy, Vitali Matyash, Aliona Bogdanova, Bianca Habermann, Lin Zhu, Andrej Shevchenko, and Teymuras V. Kurzchalia. LET-767 is required for the production of branched chain and long chain fatty acids in *Caenorhabditis elegans*. *J. Biol. Chem.*, 283(25):17550–17560, 2008.

[67] J.L. Griffin. The cinderella story of metabolic profiling: does metabolomics get to go to the functional genomics ball? *Philos. Trans. R. Soc. Lond. B Biol. Sci.*, 361:147–161, 2006.

[68] S.G. Villas-Boas, U. Roessner, M. Hansen, J. Smedsgaard, and J. Nielsen. *Metabolome Analysis: An introduction*. John Wiley & Sons, Hoboken, N.J., 2007.

[69] E.C. Horning, C.J. Brooks, and W.J. Vanden Heuvel. Gas phase analytical methods for the study of steroids. *Adv. Lipid Res.*, 6:273–392, 1968.

[70] K. Sjövall, J. Sjövall, K. Maddock, and E.C. Horning. Estimation of dehydroepiandrosterone sulfate in human serum by gas-liquid chromatography. *Anal. Biochem.*, 14(3):337–346, 1966.

[71] U. Ceglarek, C. Shackleton, F.Z. Stanczyk, and J. Adamski. Steroid profiling and analytics: going towards sterome. *J. Steroid Biochem. Mol. Biol.*, 121(3-5):479–480, 2010.

[72] C. Porte, G. Janer, L.C. Lorusso, M. Ortiz-Zarragoitia, M.P. Cajaraville, M.C. Fossi, and L. Canesi. Endocrine disruptors in marine organisms: approaches and perspectives. *Comp. Biochem. Physiol. C Toxicol. Pharmacol.*, 143(3):303–315, 2006.

[73] E. Oberdörster and A.O. Cheek. Gender benders at the beach: endocrine disruption in marine and estuarine organisms. *Environ. Toxicol. Chem.*, 20(1):23–36, 2001.

[74] M. Alasandro, D. Wiesler, and M. Novotny. Effects of starvation and refeeding on the excretion of urinary steroid metabolites in mice with different genetic background. *J. Chromatogr.*, 308:1–9, 1984.

[75] Christoph Magnes, Maria Suppan, Thomas R. Pieber, Tarek Moustafa, Michael Trauner, Guenter Haemmerle, and Frank M. Sinner. Validated comprehensive analytical method for quantification of coenzyme A activated compounds in biological tissues by online solid-phase extraction LC/MS/MS. *Anal. Chem.*, 80:5736–5742, 2008.

[76] K. Tamura, J. Dudley, M. Nei, and S. Kumar. MEGA4: Molecular evolutionary genetics analysis (MEGA) software version 4.0. *Mol. Biol. Evol.*, 24(8):1596–1599, 2007.

[77] Kang Hee Kho and Kazuo Inaba. Expression of 17beta-hydroxysteroid dehydrogenease in testis of the ascidian *Ciona intestinalis*. *Mol. Cells*, 18(2):171–176, 2004.

[78] Gongshe Han, Ken Gable, Sepp D. Kohlwein, Frederic Beaudoin, Johnathan A. Napier, and Teresa M. Dunn. The *Saccharomyces cerevisiae* YBR159w gene encodes the 3-ketoreductase of the microsomal fatty acid elongase. *J. Biol. Chem.*, 277(38):35440–35449, 2002.

[79] Evi Stahl. Substrate specificity of 17beta-hydroxysteroid-dehydrogenase type III: a comparison between human and murine homologues. Bachelor's thesis, TU München, 2009.

[80] E. Tajkhorshid, J. Baudry, K. Schulten, and S. Suhai. Molecular dynamics study of the nature and origin of retinal's twisted structure in bacteriorhodopsin. *Biophys. J.*, 78:683–693, 2000.

[81] Irene Nobeli, Angelo Favia, and Janet M. Thornton. Protein promiscuity and its implications for biotechnology. *Nat. Biotechnol.*, 27:157–167, 2009.

[82] Joseph M. Jez and Trevor M. Penning. Engineering steroid 5beta-reductase activity into rat liver 3alpha-hydroxysteroid dehydrogenase. *Biochemistry*, 37:9695–9703, 1998.

[83] A.M. Tarrant, A.M. Reitzel, C.H. Blomquist, F. Haller, J. Tokarz, and J. Adamski. Steroid metabolism in cnidarians: insights from *Nematostella vectensis*. *Mol. Cell. Endocrinol.*, 301:27–36, 2009.

[84] Manja H.E.M. Boerman and Joseph L. Napoli. Characterization of a microsomal retinol dehydrogenase: A short-chain alcohol dehydrogenase with integral and peripheral membrane forms that interacts with holo-CRBP (type I). *Biochemistry*, 34:7027–7037, 1995.

[85] M.G. Biswas and D.W. Russell. Expression cloning and characterization of oxidative 17beta- and 3alpha-hydroxysteroid dehydrogenases from rat and human prostate. *J. Biol. Chem.*, 272:15959–15966, 1997.

[86] W.H. Gough, S. VanOoteghem, T. Sint, and N.Y. Kedishvili. cdna cloning and characterization of a new human microsomal NAD+-dependent dehydrogenase that oxidizes all-trans-retinol and 3alpha-hydroxysteroids. *J. Biol. Chem.*, 273:19778–19785, 1998.

[87] V. Jurukovski, N.G. Markova, N. Karaman-Jurukovska, R.K. Randolph, J. Su, J.L. Napoli, and M. Simon. Cloning and characterization of retinol dehydrogenase transcripts expressed in human epidermal keratinocytes. *Mol. Genet. Metab.*, 67:62–73, 1999.

[88] J. Wang, X. Chai, U. Eriksson, and J.L. Napoli. Activity of human 11-cis-retinol dehydrogenase (Rdh5) with steroids and retinoids and expression of its mRNA in extraocular human tissue. *Biochem. J.*, 338:23–27, 1999.

[89] X. Chai, Y. Zhai, and J.L. Napoli. cdna cloning and characterization of a cis-retinol/3alpha-hydroxysterol short-chain dehydrogenase. *J. Biol. Chem.*, 272:33125–33131, 1997.

[90] J. Su, X. Chai, B. Kahn, and J.L. Napoli. cDNA cloning, tissue distribution, and substrate characteristics of a cis-retinol/3alpha-hydroxysterol short-chain dehydrogenase isozyme. *J. Biol. Chem.*, 273:17910–17916, 1998.

[91] Gabriele Moeller, Bettina Husen, Dorota Kowalik, Leena Hirvelae, Dariusz Plewczynski, Leszek Rychlewski, Josef Messinger, Hubert Thole, and Jerzy Adamski. Species used for drug testing reveal different inhibition susceptibility for 17beta-hydroxysteroid dehydrogenase type 1. *PLoS ONE*, 5:e10969, 2010.

[92] Donald Poirier. 17beta-hydroxysteroid dehydrogenase inhibitors: a patent review. *Expert Opin. Ther. Pat*, page doi:10.1517/13543776.2010.505604, 2010.

[93] Jamie E. Blair and S. Blair Hedges. Molecular phylogeny and divergence times of deuterostome animals. *Mol. Biol. Evol.*, 22(11):2275–2284, 2005.

[94] Frederic Delsuc, Henner Brinkmann, Daniel Chourrout, and Herve Phillipe. Tunicates and not cephalochordates are the closest living relatives of vertebrates. *Nature*, 439:965–968, 2006.

[95] Bruce Alberts, Alexander Johnson, Julian Lewis, Martin Raff, Keith Roberts, and Peter Walter. *Molecular Biology of the Cell*. Garland Science, 4th edition edition, 2002.

[96] Andreas Jakobsson, Rolf Westerberg, and Anders Jacobsson. Fatty acid elongases in mammals: Their regulation and roles in metabolism. *Prog. Lipid Res.*, 45(3):237–249, 2006.

[97] A. Kihara, H. Sakuraba, M. Ikeda, A. Denpoh, and Y. Igarashi. Membrane topology and essential amino acid residues of Phs1, a 3-hydroxyacyl-CoA dehydratase involved in very long-chain fatty acid elongation. *J. Biol. Chem.*, 283(17):11199–11209, 2008.

[98] L. Bach, L.V. Michaelson, R. Haslam, Y. Bellec, L. Gissot, J. Marion, M. Da Costa, J.P. Boutin, M. Miquel, F. Tellier, F. Domergue, J.E. Markham, F. Beaudoin, J.A.

Napier, and J.D. Faure. The very-long-chain hydroxy fatty acyl-CoA dehydratase PASTICCINO2 is essential and limiting for plant development. *Proc. Natl. Acad. Sci.*, 105(38):14727–14731, 2008.

[99] Yong Mei Qin, Francois Ma Pujol, Yong Hui Shi, Jian Xun Feng, Yi Ming Liu, Alexander J. Kastaniotis, J. Kalervo Hiltunen, and Yu Xian Zhu. Cloning and functional characterization of two cDNAs encoding NADPH-dependent 3-ketoacyl-CoA reductased from developing cotton fibers. *Cell Res.*, 15(6):465–473, 2005.

[100] Ferdinand Haller. The origins of hydroxysteroid-dehydrogenases: Identification and characterization of new HSDs from several invertebrates. Master's thesis, TU München, 2006.

[101] Francis Carey. *Organic Chemistry*. McGraw-Hill, 7th edition edition, 2007.

[102] Shuji Nagasaki, Takashi Suzuki, Yasuhiro Miki, Jun ichi Akahira, Kunio Kitada, Takanori Ishida, Hiroshi Handa, Noriaki Ohuchi, and Hironobu Sasano. 17beta-hydroxysteroid dehydrogenase type 12 in human breast carcinoma: a prognostic factor via potential regulation of fatty acid synthesis. *Cancer Res.*, 69(4):1392–1399, 2009.

[103] Nobuyuki Sakurai, Yasuhiro Miki, Takashi Suzuki, Keiko Watanabe, Takashi Narita, Kozue Ando, Tetsu M.C. Yung, Daisuke Aoki, Hironobu Sasano, and Hirosji Handa. Systemic distribution and tissue localizations of human 17beta-hydroxysteroid dehydrogenase type 12. *J. Steroid Biochem. Mol. Biol.*, 99:174–181, 2006.

[104] S. Nagasaki, Y. Miki, J. Akahira, T. Suzuki, and H. Sasano. Transcriptional regulation of 17beta-hydroxysteroid dehydrogenase type 12 by SREBP-1. *Mol. Cell. Endocrinol.*, 307(1-2):163–168, 2009.

[105] L. DiConstanzo, J.E. Drury, T.M. Penning, and D.W. Christianson. Crystal structure of human liver Δ^4-3-ketosteroid 5beta-reductase (AKR1D1) and implications for substrate binding and catalysis. *J. Biol. Chem.*, 283(24):16830–16839, 2008.

[106] S. Steckelbroeck, Y. Jin, B. Oyesanmi, H.J. Kloosterboer, and T.M. Penning. Tibolone is metabolized by the 3alpha/3beta-hydroxysteroid dehydrogenase activities of the four human isozymes of the aldo-keto reductase 1C subfamily: inversion of stereospecificity with a $\Delta^{5(10)}$-3-ketosteroid. *Mol. Pharmacol.*, 66:1702–1711, 2004.

[107] Jian Su, Min Lin, and Joseph L. Napoli. Complementary deoxyribonucleic acid cloning and enzymatic characterization of a novel 17beta/3alpha-hydroxysteroid/retinoid short chain dehydrogenase/reductase. *Endocrinology*, 140(11):5275–5284, 1999.

[108] S.B. Wolbach and P.R. Howe. Tissue changes following deprivation of fat-soluble A vitamin. *J. Exp. Med.*, 42:753–777, 1925.

[109] J.M. Howell, J.N. Thompson, and G.A.J. Pitt. Histology of the lesions produced in the reproductive tract of animals fed a diet deficient in vitamin a alcohol but containing vitamin a acid. *J. Reprod. Fertil.*, 5:159–167, 1963.

[110] A.I. Packer and D.J. Wolgemuth. *Genetic and molecular approaches to understanding the role of retinoids in mammalian spermatogenesis*, pages 347–368. Springer-Verlag, Berlin, 1999.

[111] L.R. Chaudhary and D.M. Stocco. An *in vitro* cell model system to study the action of retinoids on Leydig cell steroidogenesis. *Biochem. Int.*, 21(6):1033–1042, 1990.

[112] Fabian Ströhle. Funktionelle Analyse der 17β-Hydroxysteroiddehydrogenase Typ 3. Bachelor's thesis, TU München, 2005.

[113] Valdemir Melechco Carvalho, Odete Hirata Nakamura, and Jose Gilberto Henriques Vieira. Simultaneous quantitation of seven endogenous c-21 adrenal steroids by liquid chromatography tandem mass spectrometry in human serum. *J. Chromatogr. B*, 872:154–161, 2008.

[114] Ilias Perogamvros, Laura J. Owen, John Newell-Price, David W. Ray, Peter J. Trainer, and Brian G. Keevil. Simultaneous measurement of cortisol and cortisone in human saliva using liquid chromatography-tandem mass spectrometry: Application in basal and stimulated conditions. *J. Chromatogr. B*, 877:3771–3775, 2009.

[115] Robert L. Taylor, Dwaine Machacek, and Ravinder J. Singh. Validation of a high-throughput liquid chromatography-tandem mass spectrometry method for urinary cortisol and cortisone. *Clin. Chem.*, 48(9):1511–1519, 2002.

[116] Michael Vogeser, Josef Briegel, and Karl Jacob. Determination of serum cortisol by isotope-dilution liquid-chromatography electrospray ionization tandem mass spectrometry with on-line extraction. *Clin. Chem. Lab. Med.*, 39(10):944–947, 2001.

[117] Ravinder J. Singh. Validation of a high throughput method for serum/plasma testosterone using liquid chromatography tandem mass spectrometry (LC-MS/MS). *Steroids*, 73:1339–1344, 2008.

[118] Linda M. Thienpont, Katleen Van Uytfanghe, Stuart Blincko, Carol S. Ramsay, Hui Xie, Robert C. Doss, Brian G. Keevil, Laura J. Owen, Alan L. Rockwood, Mark M. Kushnir, Kelly Y. Chun, Donald W. Chandler, Helen P. Field, and Patrick M. Sluss. State-of-the-art of serum testosterone measurement by isotope dilution-liquid chromatography-tandem mass spectrometry. *Clin. Chem.*, 54(8):1290–1297, 2008.

[119] Christina Wang, Steve Shiraishi, Andrew Leung, Sima Baravarian, and Laura Hull. Validation of a testosterone and dihydrotestosterone liquid chromatography tandem mass spectrometry assay: Interference and comparison with established methods. *Steroids*, 73:1345–1352, 2008.

[120] Xia Xu, Larry K. Keefer, David J. Waterhouse, Joseph E. Saavedra, Timothy D. Veenstra, and Regina G. Ziegler. Measuring seven endogenous ketolic estrogens simultaneously in human urine by high-performance liquid chromatography-mass spectrometry. *Anal. Chem.*, 76(19):5829–5836, 2004.

[121] Xia Xu, Larry K. Keefer, Regina G. Ziegler, and Timothy D. Veenstra. A liquid chromatography-mass spectrometry method for the quantitative analysis of urinary endogenous estrogen metabolites. *Nat. Protocols*, 2(6):1350–1355, 2007.

[122] Mark M. Kushnir, Alan L. Rockwood, Jonas Bergquist, Marina Varshavsky, William L. Roberts, Bingfang Yue, Ashley M. Bunker, and A. Wayne Meikle. High-sensitivity tandem mass spectrometry assay for serum estrone and estradiol. *Am. J. Clin. Pathol.*, 129:530–539, 2008.

[123] Anel M. Flores-Valverde and Elizabeth M. Hill. Methodology for profiling the steroid metabolome in animal tissues using ultraperformance liquid chromatography electrospray-time-of-flight mass spectrometry. *Anal. Chem.*, 80(22):8771–8779, 2008.

[124] P. Regal, B.I. Vazquez, C.M. Franco, A. Cepeda, and C. Fente. Quantitative LC-MS/MS method for the sensitive and simultaneous determination of natural hormones in bovine serum. *J. Chromatogr. B*, 877:2457–2464, 2009.

[125] Uta Ceglarek, Linda Kortz, Alexander Leichtle, Georg M. Fiedler, Juergen Kratzsch, and Joachim Thiery. Rapid quantification of steroid patterns in human serum by on-line solid phase extraction combined with liquid chromatography-triple quadrupole linear ion trap mass spectrometry. *Clin. Chim. Acta*, 401(1-2):114–118, 2009.

[126] C.H.L. Shackleton, B.A. Hughes, G.G. Lavery, E.A. Walker, and P.M. Steward. The corticosteroid metabolic profile of the mouse. *Steroids*, 73(11):1066–1076, 2008.

[127] A. Williams, S. Ellison, M. Berglund, W. Haesselbarth, K. Hedegaard, R. Kaarls, M. Mansson, M. Roesslein, R. Stephany, A. van der Veen, W. Wegscheider, H. van de Wiel, and R. Wood. *Quantifying Uncertainty in Analytical Measurement*. EURACHEM/CITAC Working group, 2nd edition edition, 2000.

[128] U.S. Department of Health and Human Services Food and Drug Administration. *Guidance for Industry Bioanalytical Method Validation*, 2001.

[129] INTERNATIONAL CONFERENCE ON HARMONISATION OF TECHNICAL REQUIREMENTS FOR REGISTRATION OF PHARMACEUTICALS FOR HUMAN USE. *Validation of analytical procedures: text and methodology Q2(R1)*, step 4 version edition, 1994-2005.

[130] Stavros Kromidas. *Validierung in der Analytik*. Wiley-VCH, 1999.

[131] Roger Causon. Validation of chromatographic methods in biomedical analysis viewpoint and discussion. *J. Chromatogr. B*, 689:175–180, 1997.

[132] Ilse Becue, Christof Van Poucke, Jeroen C. W. Rijk, Toine F. H. Bovee, Michel Nielen, and Carlos Van Peteghem. Investigation of urinary steroid metabolites in calf urine after oral and intramuscular administration of dhea. *Anal. Bioanal. Chem.*, 396:799–808, 2010.

[133] Lan Gao, William J. Chiou, Heidi S. Camp, David J. Burns, and Xueheng Cheng. Quantitative measurements of corticosteroids in *ex vivo* samples using on-line SPE-LC-MS/MS. *J. Chromatogr. B*, 877:303–310, 2009.

[134] Anthony G. Causey, Howard M. Hill, and Lois J. Phillips. Evaluation of criteria for the acceptance of bioanalytical data. *J. Pharm. Biomed. Anal.*, 8:625–628, 1990.

[135] Maureen A. Kane, Na Chen, Susan Sparks, and Joseph L. Naploi. Quantification of endogenous retinoic acid in limited biological samples by LC/MS/MS. *Biochem. J.*, 388:363–369, 2005.

[136] Maureen A. Kane, Alexandra E. Folias, Chao Wang, and Joseph L. Napoli. Quantitative profiling of endogenous retinoic acid *in vivo* and *in vitro* by tandem mass spectrometry. *Anal. Chem.*, 80:1702–1708, 2008.

[137] Thomas E. Gundersen, Nasser E. Bastani, and Rune Blomhoff. Quantitative high-throughput determination of endogenous retinoids in human plasma using triple-stage liquid chromatography/tandem mass spectrometry. *Rapid Commun. Mass Spectrom.*, 21:1176–1186, 2007.

[138] Susan S.-C. Tai, David M. Bunk, Edward White V, and Michael J. Welch. Development and evaluation of a reference measurement procedure for the determination of total 3,3',5-triiodothyronine in human serum using isotope-dilution liquid chromatography-tandem mass spectrometry. *Anal. Chem.*, 76:5092–5096, 2004.

[139] Bingfang Yue, Alan L. Rockwood, Tanya Sandrock, Sonia L. La'ulu, Mark M. Kushnir, and A. Wayne Meikle. Free thyroid hormones in serum by direct equilibrium dialysis and online solid-phase extraction-liquid chromatography/tandem mass spectrometry. 54(4):642–651, 2008.

[140] Zi-Yan Zhao, Yi Xie, Yue-Rong Fu, Yu-Yang Li, Andre Bogdan, and Yvan Touitou. Circadian rhythm characteristics of serum cortisol and dehydroepiandrosterone sulfate in healthy chinese men aged 30 to 60 years. A cross-sectional study. *Steroids*, 68:133–138, 2003.

[141] C. Barriga, M.I. Martin, R. Tabla, E. Ortega, and A.B. Rodriguez. Circadian rhythm of melatonin, corticosterone and phagocytosis: effect of stress. *J. Pineal Res.*, 30:180–187, 2001.

[142] Christian C. Voigt, Robert Michener, Gudrun Wibbelt, Thomas H. Kunz, and Otto von Helversen. Blood-sucking bugs as a gentle method for blood-collection in water budget studies using doubly labelled water. *Comp. Biochem. Physiol. A*, 142:318–324, 2005.

[143] C. Lejeune-Lenain, E. Van Cauter, D. Desir, M. Beyloos, and J.R. Franckson. Control of circadian and episodic variations of adrenal androgens secretion in man. *J. Endocrinol. Invest.*, 10(3):267–276, 1987.

[144] G.Y. Nicolau, E. Haus, D.J. Lakatua, C. Bogdan, L. Sackett-Lundeen, M. Popescu, H. Berg, E. Petrescu, and E. Robu. Circadian and circannual variations of FSH, LH, testosterone, dehydroepiandrosterone-sulfate (DHEA-S) and 17-hydroxy progesterone (17 OH-Prog) in elderly men and women. *Endocrinologie*, 23(4):223–246, 1985.

[145] A. Reinberg and M. Lagoguey. Circadian and circannual rhythms in sexual activity and plasma hormones (FSH, LH, testosterone) of five human males. *Arch. Sex Behav.*, 7(1):13–30, 1978.

[146] C.A. Fox, A.A. Ismail, D.N. Love, K.E. Kirkham, and J.A. Loraine. Studies on the relationship between plasma testosterone levels and human sexual activity. *J. Endocrinol.*, 52(1):51–58, 1972.

[147] D. Apter, L. Viinikka, and R. Vihko. Hormonal pattern of adolescent menstrual cycles. *J. Clin. Endocrinol. Metab.*, 47(5):944–954, 1978.

[148] P.R. Larsen, H.M. Kronenberg, S. Melmed, K.S. Polonsky, and J.D. Wilson. *Williams Textbook of endocrinology*. Saunders, 10th edition edition, 2002.

[149] E. Baulieu and M. Schumacher. Progesterone as a neuroactive neurosteroid, with special reference to the effect of progesterone on myelination. *Steroids*, 65:605–612, 2000.

[150] M. Rebuffe-Scrive. Steroid hormones and distribution of adipose tissue. *Acta Med. Scand. Suppl.*, 723:143–146, 1988.

[151] Karine Blouin, Ariane Boivin, and Andre Tchernof. Androgens and body fat distribution. *J. Steroid Biochem. Mol. Biol.*, 108:272–280, 2008.

[152] Per Marin and Stefan Arver. Androgens and abdominal obesity. *Bailliere's Clin. Endocrinol. Metab.*, 12(3):441–451, 1998.

[153] C. da F. Ramos, M.A. Babinski, W.S. Costa, and F.J. Sampaio. The prostate of weaned pups is altered by maternal malnutrition during lactation in rats. *Asian J. Androl.*, 12(2):180–185, 2010.

[154] F. Labrie. Intracrinology. *Mol. Cell. Endocrinol.*, 78(3):113–118, 1991.

[155] Marcus Quinkler, Binayak Sinha, Jeremy W. Tomlinson, Iwona J. Bujalska, Paul M. Steward, and Wiebke Arlt. Androgen generation in adipose tissue in women with simple obesity - a site-specific role for 17beta-hydroxysteroid dehydrogenase type 5. *J. Endocrinol.*, 183:331–342, 2004.

[156] N.M. Morton. Obesity and corticosteroids: 11beta-hydroxysteroid type 1 as a cause and therapeutic target in metabolic disease. *Mol. Cell. Endocrinol.*, 316(2):154–164, 2010.

[157] S.P. Thomson, C.S Stump, L.R. Kurukulasuriya, and J.R. Sowers. Adrenal steroids and the metabolic syndrome. *Curr. Hypertens. Rep.*, 9:512–519, 2007.

[158] Yuri Kotelevtsev, Megan C. Holmes, Ann Burchell, Pamela M. Houston, Dieter Schmoll, Pauline Jamieson, Ruth Best, Roger Brown, Christopher R. W. Edwards, Jonathan R. Seckl, and John J. Mullins. 11beta-hydroxysteroid dehydrogenase type 1 knockout mice show attenuated glucocorticoid-inducible responses and resist hyperglycemia on obesity or stress. *Proc. Natl. Acad. Sci.*, 94:14924–14929, 1997.

[159] C. Muhtz, B.C. Zyriax, T. Klahn, E. Windler, and C. Otte. Depressive symptoms and metabolic risk: effects of cortisol and gender. *Psychoneuroendocrinology*, 34(7):1004–1011, 2009.

A. Publications

A.1. Scientific presentations

XV. Lipid Meeting 2007, Leipzig, Germany
Haller F., Adamski J.: *Methods for analyzing the substrate spectrum of 17beta-Hydroxysteroid Dehydrogenases* (oral presentation)

Workshop on pre-receptor steroid metabolism as target for pharmacological treatment, 2008, Greinau, Germany
Haller F., Mindnich R., Kirsch S., Adamski J.: *The physiological role of 17beta-HSD12* (Poster Presentation)

A.2. Scientific papers

Mindnich R., **Haller F.**, Halbach F., Moeller G., Hrabe de Angelis M., Adamski J. (2005) *Androgen metabolism via 17beta-hydroxysteroid dehydrogenase type 3 in mammalian and non-mammalian vertebrates: comparison of the human and the zebrafish.* J. Mol. Endo. **35**, 305 - 316.

Prehn C., Ströhle F., **Haller F.**, Keller B., Hrabe de Angelis M., Adamski J., Mindnich R. (2007) *A comparison of methods for assays of steroidogenic enzymes: New GC/MS versus HPLC and TLC.* Enzymology and Molecular Biology of Carbonyl Metabolism **12**, 277 - 283

Fuchs M., Hermannstädter C., Hutzler P., Häcker G., **Haller F.**, Höfler H., Luber B. (2008) *Deletion of exon 8 increases cisplatin-induced E-cadherin cleavage.* Exp. Cell Res. **314**, 153 - 163

Tarrant A.M., Reitzel A.M., Blomquist C.H., **Haller F.**, Tokarz J., Adamski J. (2009) *Steroid metabolism in cnidarians: insights from Nematostella vectensis.* Mol. Cell. Endo. **301**, 27 - 36

Meier M., Tokarz J., **Haller F.**, Mindnich R., Adamski J. (2009) *Human and zebrafish hydroxysteroid dehydrogenase like 1 (HSDL1) proteins are inactive enzymes but conserved among species.* Chem. Biol. Interact. **178**, 197 - 205

Kowalik D.[1], **Haller F.**[1], Adamski J., Möller G. (2009) *In search for function of two human orphan SDR enzymes: hydroxysteroid dehydrogenase like 2 (HSDL2) and short-chain dehydrogenase/reductase-orphan (SDR-O).* J. Steroid Biochem. Mol. Biol. **117**, 117-124

Haller F., Prehn C., Adamski J. (2010) *Quantification of steroids in human and mouse plasma using online solid phase extraction coupled to liquid chromatography tandem mass spectrometry* Nature Protocols Network 10.1038/nprot.2010.22

Haller F., Moman E., Hartmann R.W., Adamski J., Mindnich R. (2010) *Molecular framework of steroid/retinoid discrimination in 17beta-hydroxysteroid dehydrogenase type 1 and photoreceptor-associated retinol dehydrogenase.* J. Mol. Biol. **399**, 255-267

Brandl M., Seidler B., **Haller F.**, Adamski J., Schmid R.M., Saur D., Schneider G. (2010) *IKKalpha controls canonical TGFbeta-SMAD signaling to regulate SNAIL and SLUG gene expression in a Panc1 cell model of EMT.* J. Cell Sci. *Manuscript accepted*

Haller F., Mindnich R., Mörtl S., Gobec S., Adamski J. (2010) *The evolutionary origins of 17beta-hydroxysteroid dehydrogenase type 12 shed light on its role in human metabolism. Manuscript in preparation*

[1]these authors contributed equally

B. Primers

Gene	Internal No.	Orientation	Application
Ssc1	2159	for	gateway cloning
Ssc1	2160	rev	gateway cloning
Cig30	2161	for	gateway cloning
Cig30	2162	rev	gateway cloning
ELOVL4	2163	for	gateway cloning
ELOVL4	2164	rev	gateway cloning
TER	2165	for	gateway cloning
TER	2166	rev	gateway cloning
LCE	2167	for	gateway cloning
LCE	2168	rev	gateway cloning
hsprRDH	2149	for	qRT-PCR
hsprRDH	2150	rev	qRT-PCR
hs17beta-HSD1	2137	for	qRT-PCR
hs17beta-HSD1	2138	rev	qRT-PCR
mm17beta-HSD3	2090	for	gateway cloning
mm17beta-HSD3	2091	rev	gateway cloning
rn17beta-HSD3	2092	for	gateway cloning
rn17beta-HSD3	2093	rev	gateway cloning
hs17beta-HSD1	2030	for	cloning (EcoRI)
hs17beta-HSD1	2002	rev	cloning (XhoI)
hs17beta-HSD1	2003	for	mutagenesis
hs17beta-HSD1	2004	rev	mutagenesis
hsprRDH	1997	for	cloning (BamHI)
hsprRDH	1998	rev	cloning (XhoI)
hsprRDH	1999	for	mutagenesis
hsprRDH	2000	rev	mutagenesis
hs17beta-HSD3	1995	for	gateway cloning
hs17beta-HSD3	1996	rev	gateway cloning
TER	1983	for	cDNA cloning
TER	1984	rev	cDNA cloning
Cig30	1985	for	cDNA cloning
Cig30	1986	rev	cDNA cloning
Ssc1	1987	for	cDNA cloning
Ssc1	1988	rev	cDNA cloning
ELOVL4	1989	for	cDNA cloning

ELOVL4	1990	rev	cDNA cloning
hELO1	1991	for	cDNA cloning
hELO1	1992	rev	cDNA cloning
LCE	1993	for	cDNA cloning
LCE	1994	rev	cDNA cloning
ci17beta-HSD3	1954	for	TOPO cloning
ci17beta-HSD3	1955	rev	TOPO cloning
bf17beta-HSD3	1958	for	TOPO cloning
bf17beta-HSD3	1959	rev	TOPO cloning
hs17beta-HSD12	1033	for	TOPO cloning
hs17beta-HSD12	1458	rev	TOPO cloning
zf17beta-HSD12A	1027	for	TOPO cloning
zf17beta-HSD12A	1459	rev	TOPO cloning
zf17beta-HSD12B	1029	for	TOPO cloning
zf17beta-HSD12B	1460	rev	TOPO cloning
ci17beta-HSD12	1072	for	TOPO cloning
ci17beta-HSD12	1461	rev	TOPO cloning
bf17beta-HSD12	1174	for	TOPO cloning
bf17beta-HSD12	1462	rev	TOPO cloning
bf17beta-HSD12-2	1177	for	TOPO cloning
bf17beta-HSD12-2	1463	rev	TOPO cloning
sp17beta-HSD12	1078	for	TOPO cloning
sp17beta-HSD12	1464	rev	TOPO cloning

C. Constructs

Gene	Vector	Restriction Sites	Application
hs17beta-HSD12	pYES2.1	n.a. (TOPO)	complementation assay
zf17beta-HSD12A	pYES2.1	n.a. (TOPO)	complementation assay
zf17beta-HSD12B	pYES2.1	n.a. (TOPO)	complementation assay
ci17beta-HSD3	pYES2.1	n.a. (TOPO)	complementation assay
ci17beta-HSD12	pYES2.1	n.a. (TOPO)	complementation assay
bf17beta-HSD3	pYES2.1	n.a. (TOPO)	complementation assay
bf17beta-HSD12	pYES2.1	n.a. (TOPO)	complementation assay
bf17beta-HSD12-2	pYES2.1	n.a. (TOPO)	complementation assay
sp17beta-HSD12-2	pYES2.1	n.a. (TOPO)	complementation assay
Ssc1	pCTAP	n.a. (gateway)	co-immunoprecipitation
Cig30	pCTAP	n.a. (gateway)	co-immunoprecipitation
ELOVL4	pCTAP	n.a. (gateway)	co-immunoprecipitation
LCE	pCTAP	n.a. (gateway)	co-immunoprecipitation
TER	pCTAP	n.a. (gateway)	co-immunoprecipitation
hELO1	pCTAP	n.a. (gateway)	co-immunoprecipitation
hs17beta-HSD1	NFLAG-pcDNA3	EcoRI & XhoI	enzyme activity
hs17beta-HSD1-G145M	NFLAG-pcDNA3	EcoRI & XhoI	enzyme activity
hsprRDH	NFLAG-pcDNA3	BamHI & XhoI	enzyme activity
hsprRDH-M144G	NFLAG-pcDNA3	BamHI & XhoI	enzyme activity
hs17beta-HSD3	p530	n.a. (gateway)	enzyme activity
rn17beta-HSD3	p530	n.a. (gateway)	enzyme activity
mm17beta-HSD3	p530	n.a. (gateway)	enzyme activity

D. Supplementary data

D.1. Enzyme kinetics figures

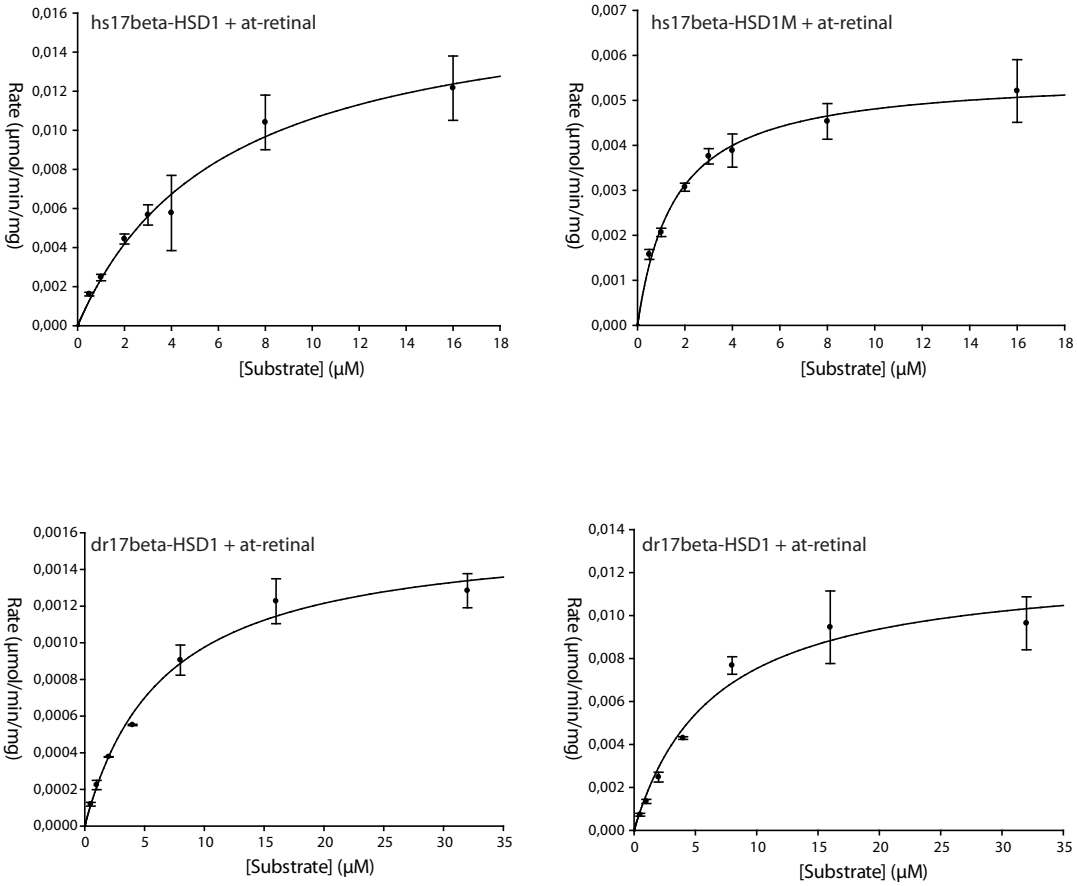

Figure D.1.: Michaelis-Menten kinetics of human and zebrafish 17beta-HSD1 and respective mutants (substrate: all-trans retinal).

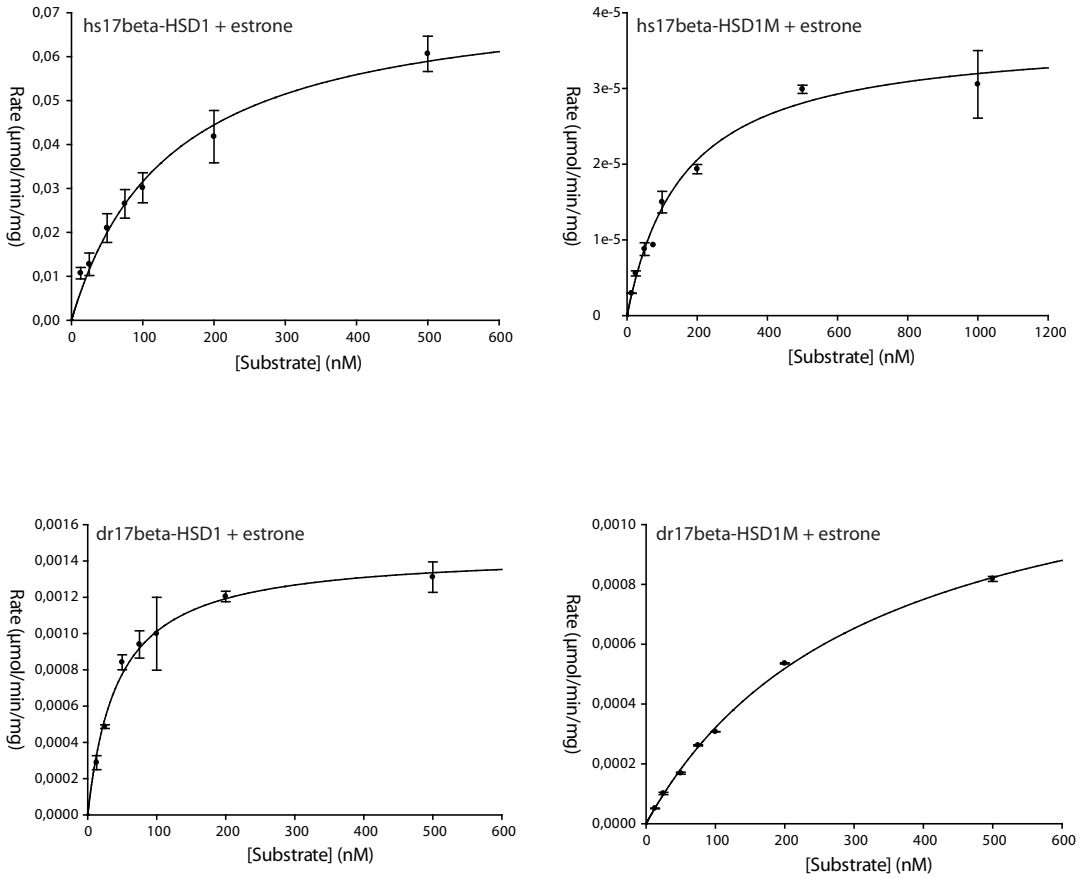

Figure D.2.: Michaelis-Menten kinetics of human and zebrafish 17beta-HSD1 and respective mutants (substrate: estrone).

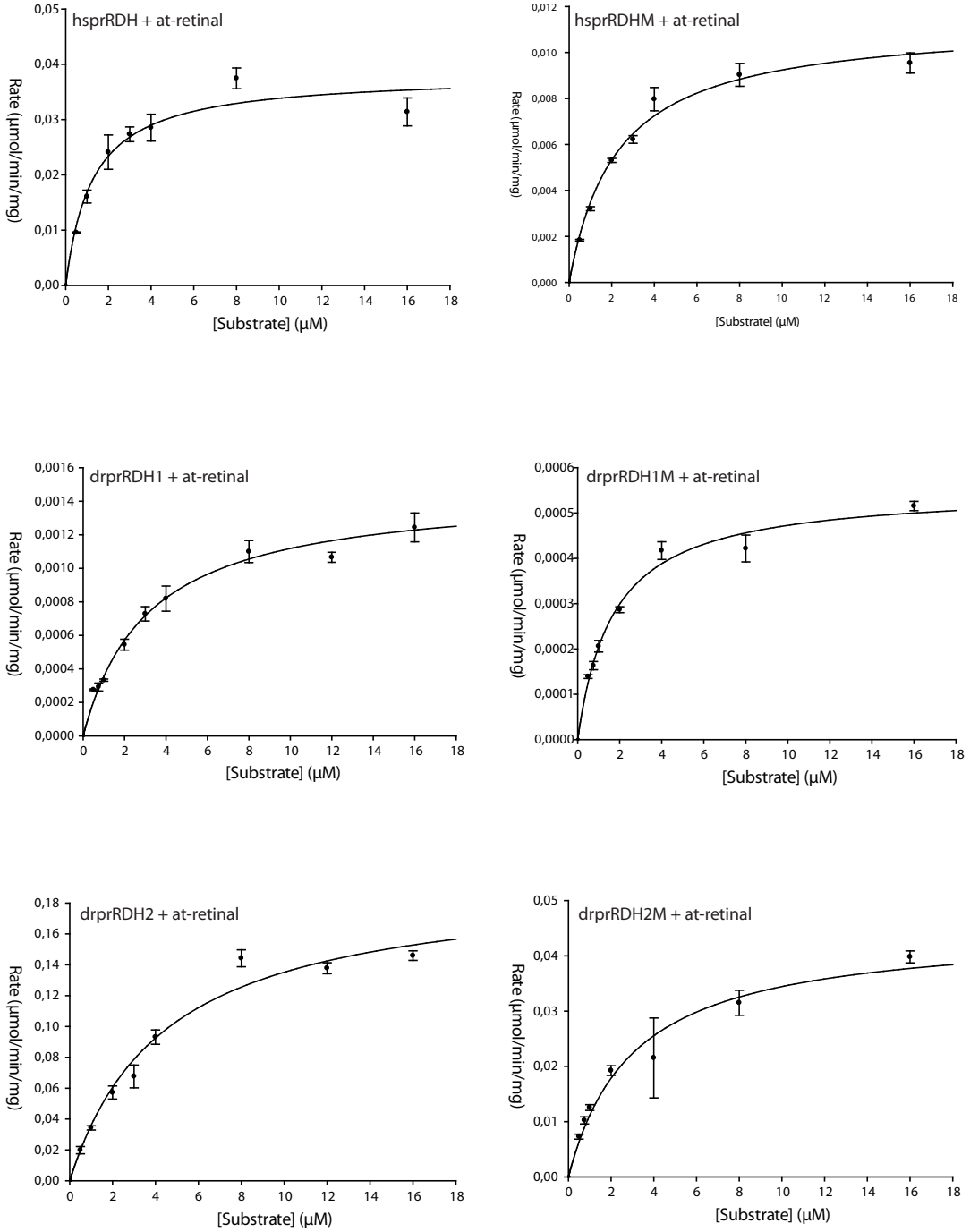

Figure D.3.: Michaelis-Menten kinetics of human and zebrafish prRDH and respective mutants (substrate: all-trans retinal).

hsprRDH + estrone

not determined

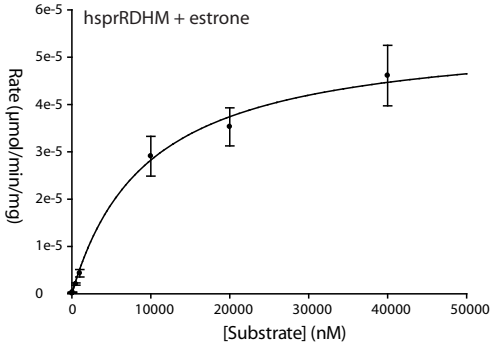

drprRDH1 + estrone

not determined

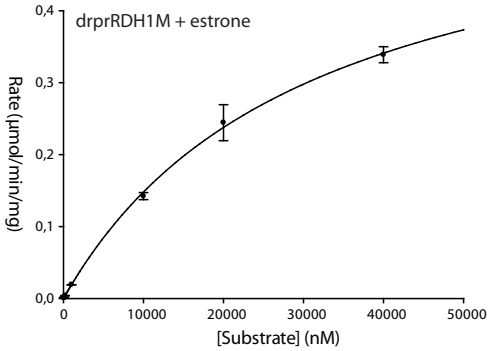

drprRDH2 + estrone

not determined

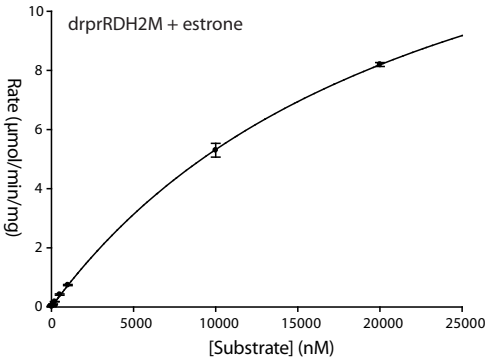

Figure D.4.: Michaelis-Menten kinetics of human and zebrafish prRDH and respective mutants (substrate: estrone).

Acknowledgements

Auch wenn es viele Menschen gibt denen ich am Ende meiner Doktorarbeit danken würde, so gilt mein besonderer Dank Prof. Dr. Jerzy Adamski. Nicht nur dafür, dass er mir dieses Thema überlassen hat sondern auch für seine immerwährende Unterstützung während meiner gesamten Promotionszeit. So viele Freiheiten und so viel Offenheit für meine Ideen hätte ich sonst wohl an keinem Lehrstuhl gefunden. Danke!

An dieser Stelle würde ich auch gerne Dr. Gabriele Möller danken: Für ihre stetige Bereitschaft mir bei wissenschaftlichen Fragen zuzuhören, mir mit guten Ideen zu helfen und nicht zuletzt für ihre Korrekturen an dieser Arbeit. Meinem ehemaligen Doktorandenkollegen Dr. Marc Meier möchte ich für die vielen freudigen Stunden im Labor, für gute Gespräche, das Korrekturlesen dieser Arbeit und seine Freundschaft danken (ohne den Marchetto macht Forschung nur halb so viel Spaß ☺). An dieser Stelle möchte ich auch Dr. Christian 'Spielhauptinho' Spielhaupter für seine wissenschaftlichen und anderweitigen Ratschläge danken. Janina Tokarz, Eva Lattka, Anna Halama und Katja Vouk danke ich für unsere gemeinsame Zeit im Labor und die schöne Arbeitsatmosphäre. Ganz besonders will ich mich auch bei unseren technischen Angestellten bedanken. Insbesondere Gabriele Zieglmeier und Marion Schieweg aber auch Kerstin Schwerdtner und Tamara Halex danke ich nicht nur für ihre Hilfe sondern auch für den schönen Laboralltag.

Dr. Rebekka Mindnich danke ich für die Inspiration von vielen HSD Projekten und auch für ihre Mitarbeit am 17beta-HSD1 / RDH Projekt. In diesem Zusammenhang möchte ich auch Dr. Edelmiro Moman und Prof. Dr. Rolf W. Hartmann für ihre Mitarbeit an diesem Projekt danken.

Dr. Simone Mörtl möchte ich für ihre Hilfe mit den ΔYBR159 Hefen und Prof. Stanislav Gobec für die Synthese von 3-Ketopalmitoyl-CoA danken. Prof. Tea Lanisnik Rizner und Prof. Jonathan Nathans danke ich für die Bereitstellung eines YBR159w bzw. eine hsprRDH Konstruktes.

Meiner Familie und ganz besonders meinen Eltern danke ich für ihre langjährige Unterstützung. Nicht nur dass Ihr mir diese Ausbildung ermöglicht habt (wofür ich Euch nicht dankbar genug sein kann), Ihr habt auch immer an mich geglaubt. Danke!

Meine liebe Martina, mein ☼, wie kann ich dem Menschen danken der mir am Wichtigsten ist? Auch wenn diese Worte nur ansatzweise ausdrücken können was es mir bedeutet hat, so bin ich doch unendlich dankbar, dass Du während meiner Promotionszeit immer für mich da warst.